Molecular genetic and physiological studies on the dual role of purine catabolism in plant growth and stress response

Hiroshi Takagi

Department of Mathematical and Life Sciences

Graduate School of Science

Hiroshima University

2017

DECLARATION OF CO-AUTHORSHIP/PREVIOUS PUBLICATION

I. Co-Authorship Declaration

I hereby declare that this thesis incorporates material from joint research. I certify that I have essentially done all the work and obtained written permission from each of the co-authors to include the above material in my thesis.

I certify that, with the above qualification, this thesis and the work to which it refers are the results of my own efforts.

II. Declaration of Previous Publication

This thesis includes one original paper that has been published in a peer-reviewed journal:

Authors: Takagi, H., Ishiga, Y., Watanabe, S., Konishi, T., Egusa, M., Akiyoshi, N., Matsuura, T., Mori, I.C., Hirayama, T., Kaminaka, H., Shimada, H. and Sakamoto, A.
Article title: Allantoin, a stress-related purine metabolite, can activate jasmonate signaling in a MYC2-regulated and abscisic acid-dependent manner
Journal: Journal of Experimental Botany **67** (8): 2519–2532
Publisher: Oxford University Press
DOI: 10.1093/jxb/erw071
Article first published online: 1 March 2016
Accepted manuscript online: 5 February 2016

I certify that I have obtained a written permission from the copyright owner to use the above-published material in my thesis. It is noted that, where it was necessary, the original text is slightly modified to fit the formatting and structuring style of the thesis. I certify that the above material describes work completed during my registration as graduate student at Hiroshima University.

Contents

Abbreviations

AAH……...…allantoate amidohydrolase
ABA……abscisic acid
ABA-GE…..…….....abscisic acid glucosyl ester
ACT……..…actin
ALN……..…allantoinase
AMP…….….adenosine mono phosphate
ANAC……Arabidopsis NAM/ATAF/CUC
AOC…….allene oxide cyclase
AOS……allene oxide synthase
AS……....allantoin synthase
ATP…….……adenosine triphosphate
BGLU……β-glucosidase
C……carbon
CYP……...……cytochrome P450 monooxygenase
DW……..dry weight
ER ……...endoplasmic reticulum
ERF……ethylene response factor
FAD……..flavin adenine dinucleotide
FW……fresh weight
GA……...gibberellin
GO…….……...gene ontology
GS……..glutamine synthase
HR……...hypersensitive response
IAA……...indole-3-acetic acid
ICS……...isochorismate synthase
IMP…….……inosine monophosphate
iP…….....N^6-(Δ^2-isopentenyl)adenine
JA……...jasmonic acid

JAI/JIN……. ……jasmonate insensitive
JAM……jasmonate-associated MYC2-like
JAR…….….jasmonate resistance
JA-Ile…….….jasmonoyl-L-isoleucine
JAZ…….....jasmonate ZIM-domain
LOX……...13-lipoxygenase
MeJA……methyl jasmonate
MON……...monensin sensitivity
N…….……....nitrogen
NAD^+…….....nicotinamide adenine dinucleotide
$NADP^+$…….....nicotinamide adenine dinucleotide phosphate
NCED…….….9-*cis*-epoxycarotenoid dioxygenase
NUE…….nitrogen use efficiency
OPR……12-oxophytodienoate reductase
ORA……....octadecanoid-responsive Arabidopsis AP2/ERF
PR……....pathogenesis-related
PDF……..…..plant defensin
PTGS……post-transcriptional gene suppression
qPCR…….……quantitative PCR
RBOH…….. respiratory burst oxidase homolog
ROS……reactive oxygen species
SA……salicylic acid
SAG……..senescence-associated gene
SAGT..……..salicylic acid glucosyltransferase
TAIR……..The Arabidopsis Information Resource
T-DNA……...transfer DNA
tZ……*trans*-zeatin
UAH……..ureidoglycolate amidohydrolase
UBC……..ubiquitin conjugating enzyme
UGAH…. ……ureidoglycine aminohydrolase

UOX….. …….urate oxidase
UPS……. ……..ureide permease
URE……...urease
VSP……vegetative storage protein
WAG……..weeks after germination
WT……wild-type
XDH……..xanthine dehydrogenase
XO…….xanthine oxidase

GENERAL INTRODUCTION

Diversity and complexity of plant nitrogen metabolisms

Nitrogen (N) is the most quantitatively required mineral element that plays fundamental roles in plants. It is the essential component of many organic compounds such as amino acids, proteins, chlorophylls and nucleic acids. Plants can assimilate inorganic N absorbed from soils and recycle it from old to young tissues, whereas animals simply take organic N from the diet and excrete excessive N. Thus, N metabolisms and pathways in plants are much more diverse and complex than those in animals.

N transport and assimilation

Plants absorb inorganic N such as nitrate and ammonia from soils, and convert to glutamine using adenosine triphosphate (ATP), an energy currency supplied from photosynthesis. This first organic N is further converted to various other organic N metabolites. Although the amount of available inorganic N in soils is often limited, sessile plants have mechanisms to prevent from N deficiency through the regulation of N transport activity. Plants can monitor N nutritional status in the body, sense the availability of nitrate and ammonia in soils, and control N uptake thorough transcriptional and post-translational regulation of membrane-bound transporters (Nozoa *et al*., 2003; Yuan *et al*., 2007; Rubin *et al.*, 2009; Wang *et al.*, 2009; Krouk *et al.*, 2010; Gojon *et al.*, 2011; Marchive *et al.*, 2013; Sun *et al.*, 2014).

N recycle and remobilization

Transcriptional and post-translational regulations of nitrate and ammonium transporters substantially contribute to good N nutritional status. On the other hand, N recycling and remobilization are required to use N efficiently (Masclaux-Daubresse *et al.*, 2010). In the reproductive stage, plants negatively regulate N uptake from soils, and activate N recycling metabolism. Amino acids such as glutamine and aspargine derived from chloroplastic proteins, particularly ribulose-1,5-bisphosphate carboxylase/oxygenase, are regarded as the main form of remobilized N. After proteolysis and deamination, protein-derived N is released as ammonium, followed by re-assimilation into glutamine by key cytosolic enzymes, glutamine synthetase1 (GS1). *GS1* genes involved in N recycling are induced by natural senescence (Masclaux-Daubresse *et al.*, 2010; Yamaya and Kusano, 2014), supporting its crucial role especially at late growth stages that demand high N amounts. These genes are essential components for plant growth and grain yield (Hirel *et al.*, 2001; Tabuchi *et al.*, 2005; Martin *et al.*, 2006), demonstrating that N recycling and remobilization are fundamental to substantial growth and survive of plants in wild nature.

N metabolism and environmental stress

Environmental stresses have a great impact on metabolic profiles (Cheng and Murata, 2002). These include many N metabolites. Interestingly, N recycling and remobilization are activated by some biotic and abiotic stresses (Pérez-García *et al.*, 1998*a*,*b*; Chaffei *et al.*, 2004; Olea *et al.*, 2004; Pageau *et al.*, 2006). This may be, at least in part, due to the effect of stress-induced senescence, and required to collect available N from damaged tissues.

Apart from efficient N utilization under stress environments, some

stress-associated N metabolites contribute to stress adaptation. For instance, proline and glycinbetaine function as compatible solute, and some alkaloids serve as defense metabolites (Sakamoto and Murata, 2002; Verslues and Sharma, 2010; Mithöfer and Boland, 2012). In many cases, however, physiological function and significance of stress-associated N metabolites still remain elusive.

Plant purine catabolic pathways

Purine rings are N-rich compounds that play vital roles in every organism (Smith and Atkins, 2002). Inosine monophosphate (IMP) is the first purine compound, and provides basic purine ring structures for other purine compounds. The most specific and prominent function of purines is the storage of genetic information. In addition to this, nucleoside triphosphates such as ATP serve as the cellular energy currencies that are required for many biochemical reactions. Purine bases are also precursors to a number of biologically important compounds: B-class vitamins like riboflavin, essential coenzymes like NAD^+, $NADP^+$, FAD and Coenzyme A.

Although purine compounds play ubiquitous and crucial roles in all organisms, its catabolic pathway in plants is very different from that in animals. Animals excrete certain intermediates of purine catabolism as waste products, probably to prevent from release of toxic ammonia by full breakdown of purine compounds. For instance, the excretory N product is uric acid in birds, primates and terrestrial reptiles, while it is generally allantoin in other animals (Vogels and Drift, 1976). On the other hand, plants completely oxidize purine rings and release four molar equivalents of ammonia through long sequential reaction steps (Werner and Witte, 2011; Fig. 1).

Adenine nucleotides constitute the largest purine nucleotides pool and must be reverted to the first purine compound, IMP, to enter purine catabolic steps (Stasolla *et al.*, 2003). IMP is eventually converted to the key compound xanthine for full catabolism. It should be noted that the pathways from XMP to xanthosine and from guanine to xanthine do not exist in plants (Stasolla *et al.*, 2003; Dahncke and Witte, 2013). Xanthine is further oxidized to uric acid by xanthine dehydrogenase (XDH). Although Arabidopsis [*Arabidopsis thaliana* (L.) Heynh.] possesses two orthologous XDH proteins (AtXDH1 and AtXDH2), it is highly likely that AtXDH1 is responsible for major XDH activities in Arabidopsis (Yesbergenova *et al.*, 2005; Hauck *et al.*, 2014). Although XDH has been shown to be localized in the cytosol of cowpea nodules (Datta *et al*., 1991), a recent study showed that AtXDH1 is localized to tonoplast in both epidermal and mesophyll cells (Ma *et al.*, 2016). The subsequent catabolic steps proceed in peroxisomes and endoplasmic reticulum (ER) (reviewed by Werner and Witte, 2011). In the peroxisomes, uric acid is converted by urate oxidase (UOX) to 5-hydroxyisourate from which allantoin is produced by allantoin synthase (AS). Allantoin is then transported into the ER where it is hydrolyzed to allantoate by allantoinase (ALN), and further transformed to ureidoglycine by allantoate amidohydrolase (AAH). Ureidoglycine and its downstream metabolite ureidoglycolate are catabolized by the ER-localizing enzymes, ureidoglycine aminohydrolase (UGAH) and ureidoglycolate amidohydrolase (UAH), respectively. During these catabolic reactions in the ER, allantoin is degraded to glyoxylate and releases four mol ammonium. Alternatively, it is conceivable that ureidoglycine and ureidoglycolate are unstable and spontaneously decayed to urea, which is further degraded by urease (URE), resulting in the release of ammonia (Werner *et al*. 2013).

Purine catabolism in legume plants

Purine catabolic pathways has long attracted plant scientists, since it is essential for storage and utilization of symbiotically fixed atmospheric N in some of agriculturally important legumes of tropical origin and sun-tropical origin such as soybean (*Gycine max*) (Smith and Atkins, 2002). This is also because plant N fixation has been practically exploited for N supplementation to soils. In this type of legume plants, fixed N is stored and translocated as allantoin and allantoate, collectively called as ureides, although ureide biosynthesis is accomplished by the biochemically complex pathways including *de novo* synthesis of purine rings and some purine catabolic steps. Ureides cannot be directly applied for protein biosynthesis like amino acids; however, both allntoin and allantoate are N-rich compounds with a carbon (C):N ratio of 1:1 compared with 2.5 and 2.0 for Gln and Asn, respectively (Smith and Atkins, 2002). This low C:N ratio may allow plants to translocate N at relatively high efficiency and also save photosynthetates during N translocation.

Purine catabolism in non-legume plants

Although plant purine catabolism has been investigated well using some tropical legume plants, this catabolic pathway is ubiquitously present in plants including non-legumes. This fact indicates that the roles of purine catabolism are not necessarily confined to symbiotically fixed N utilization. As its general function, N recycling and remobilization during senescence have been proposed, since the complete breakdown of a purine ring releases four molar

equivalents of ammonia. In fact, Arabidopsis was able to grow on the medium containing allantoin as sole N, indicating that not only legumes but also other plants can utilize ureides as a N source (Desimone *et al*., 2002; Yang and Han, 2004). Moreover, in Arabidopsis, the expression of several upstream enzyme of purine catabolism, such as *XDH1* and *UOX*, were reportedly upregulated during the progression of senescence, suggesting the possible involvement of the pathway in source–sink N remobilization. Still, there has been little experimental evidence to support that purine catabolism substantially contributes to N recycling metabolism (Werner and Witte, 2011). Previously, Nakagawa *et al.* (2007) showed that RNA interference-mediated suppression of AtXDH1 and AtXDH2, the bottleneck enzymes of purine catabolism, led to attenuated plant growth and early leaf senescence in Arabidopsis. The mutant phenotype was recently confirmed in *AtXDH1*-null mutants (Ma *et al*., 2016). Interestingly, these impaired growth phenotypes were largely restored by exogenous uric acid (Nakagawa *et al*., 2007; Ma *et al*., 2016), suggesting the fundamental role of purine catabolism in proper maintenance of plant growth and physiological processes such as leaf senescence. However, loss-of-function of the downstream enzymes, ALN and AAH, has been reported to result in no apparent growth phenotype (Yang and Han, 2004; Todd and Polacco, 2006; Werner *et al*., 2008). Thus, the general role of purine catabolism in plant growth and development remains to be elucidated.

Transport of purine metabolites

If plants utilize purine-derived metabolites as remobilized N, specific transporters may be required for the source–sink N translocation. Ureide permeases (UPSs) constitute a group of membrane-associated transporter

proteins that shows affinity to ureides including allantoin. An Arabidopsis UPS (AtUPS1) is the first characterized member of plant UPS (Desimone *et al.*, 2002), and among five family members of AtUPSs, allantoin-transporting activity were thus far experimentally confirmed for AtUPS1, AtUPS2 and AtUPS5 (Desimone *et al.*, 2002; Schmidt *et al.*, 2004, 2006). Soybean homologs of UPS1, GmUPS1-1 and GmUPS1-2, are an essential component for ureide translocation from nodules to shoots and healthy nodule development (Collier and Tegeder, 2012). In addition to the roles in root nodules, the common bean (*Phaseolus vulgare* L.) UPS1 (PvUPS1) is most likely involved in source–sink ureide transport. Common beans fed with ^{14}C-labeled allatoin at the source leaf or root showed strong label accumulation signals in sink organs, and *PvUPS1* transcripts were detected in shoot endodermis and phloem (Pélissier *et al.*, 2004; Pélissier and Tegeder, 2007). Despite putative functions of PvUPS1 in N recycling and remobilization, Arabidopsis mutants defective in AtUPS1 and AtUPS2 reportedly showed normal growth phenotype (Schmidt *et al.*, 2004). Schmidt *et al*. (2004) proposed that the main function of AtUPSs is attributable to pyrimidine transport for its salvage in early developmental stages, because ureides are not generally regarded as quantitatively important remobilized N in non-leguminous species, and because the characterized AtUPSs showed rather broad substrate specificities with higher affinity to pyrimidine bases than ureides.

Stress physiological roles of plant purine catabolism

Plant purine catabolism provides N nutrition and supports healthy plant growth at least in legumes; however, it has also emerged as a crucial

component of stress responses and adaptation. The best-known example of its stress-physiological role is the contribution of XDH to abiotic and biotic stress resistance. Although plant XDH proteins generally prefer NAD^+ as an electron acceptor, some of them concomitantly show reactive oxygen species (ROS)-generating xanthine generating (XO) activity. For instance, AtXDH1 transfers 22% of electron derived from xanthine to O_2 to yield superoxide anion (O_2^-) (Hesberg *et al.*, 2004). In addition to XO activity, AtXDH1 also has a weak NADPH oxidase activity that also results in O_2^- generation (Yesbergenova et al., 2005). These ROS-generating activities of XDH are likely to confer pathogen defense. Studies of Italian researchers have shown that allopurinol, a potent XDH inhibitor, suppresses hypersensitive response (HR) induced by rust and virus infections (Montalbini, 1995; Montalbini and Torre Della, 1996; Silvestri *et al.*, 2008). Recently, Ma *et al*. (2016) genetically showed that ROS burst brought by AtXDH1 was required for the host resistance of Arabidopsis to powdery mildew. NADPH oxidases such as RBOHD are thought to be mostly responsible for ROS burst during plant immunity (Kadota *et al.*, 2014); however, this study revealed that AtXDH1 as a new component for ROS generation in pathogen defense, and highlighted the potential link between plant purine catabolism and immune responses. AtXDH1 is required not only for biotic, but also abiotic stress adaptation. Although AtXDH1 is an O_2^- -producing enzyme, its genetic lesion paradoxically resulted in H_2O_2 overaccumulation and enhanced susceptibility to drought, dark and oxidative stresses (Brychkova *et al.*, 2008; Watanabe *et al.*, 2010, 2014). These reports suggest that metabolic intermediates downstream of xanthine contribute to ROS homeostasis and abiotic stress resistance. A possible purine compound is uric acid, which is long known for its antioxidative effect (Glantzounis *et al.*, 2005). Recently, Ma *et al*. (2016)

have shown that, in mesophyll cells, AtXDH1 was localized to tonoplast that attaches to chloroplasts, suggesting that AtXDH1 provides uric acid to chloroplast to protect it from ROS. According to previous research (Watanabe *et al.*, 2010), however, uric acid levels are apparently rather low in Arabidopsis. Thus, it is also possible that stress protection is conferred by the metabolic intermediates downstream of uric acid.

The ureides allantoin and allantoate are most quantitatively abundant metabolic intermediates of purine catabolism. It is long known that these ureides are accumulated in plants exposed to environmental adversity (Montalbini 1991; Sagi *et al*., 1998; Nikiforova *et al*., 2005; Brychkova *et al*., 2008, Alamillo *et al*., 2010; Kanani *et al*., 2010; Rose *et al*., 2012; Yobi *et al*., 2013, Watanabe *et al*., 2014*b*). Ureide accumulation in stressed plants is apparently a consequence of inhibitory effects on metabolism; however, plants rather seem to actively accumulate ureides through transcriptional regulation of the metabolic enzymes (Fig. 2). In Arabidopsis, *XDH1* transcript levels were upregulated by stress factors and stress-related phytohormone such as drought, salinity, dark, H_2O_2, powdery mildew infection and ABA (Hesberg *et al*., 2004; Brychkova *et al*., 2008; Lescano *et al*., 2016; Ma *et al*., 2016). *UOX* was responsive to cadmium, drought, salinity and darkness (Brychkova *et al.*, 2008; Irani and Todd, 2016; Nourimand and Todd, 2016). *AS* transcription responded positively to salinity treatments (Lescano *et al.*, 2016). On the other hand, expression levels of *ALN* decreased in response to salinity and mannitol treatments (Irani and Todd, 2016; Lescano *et al.*, 2016). *AAH* transcript levels were also repressed in salinity conditions (Irani and Todd, 2016). Taken together, Arabidopsis exhibit contrasting expression pattern of upstream and downstream genes of purine catabolism in a way to enhance ureide accumulation.

Stress-physiological roles of ureide accumulation have so far been reported in both legume and non-legume plants. In ureide-type legume plants, although still under dispute, it is long thought that ureides act as signaling molecules that suppress symbiotic N fixation in response to drought (Serraj *et al.*, 1999). Ureides, however, also accumulate in response to stress in non-legume plants like Arabidopsis and rice (*Oryza sativa* L.). One of the putative physiological functions of ureides is scavenging reactive oxygen species (ROS). Exogenous allantoin and allanoate reportedly mitigate oxidative stress symptoms of Arabidopsis leaf discs (Brychkova *et al.*, 2008). Ureide levels in Arabidopsis, however, are generally much lower than other antioxidants such as ascorbic acid even under stress conditions (e.g. below 1 μmol g^{-1} FW) (Brychkova *et al.*, 2008). Moreover, *in vitro* tests pointed that allantoin barely had antioxidant capacity (Wang *et al.*, 2012). Therefore, it is still controversial whether ureide compounds function as ROS scavengers *in planta*.

Apart from the potential role in ROS scavenging, Watanabe *et al*. (2014*b*) showed a possible regulatory role of allantoin in stress adaptation that activated ABA production and therefore elicited ABA-mediated stress responses. Arabidopsis knockout mutants for *ALN* (*aln*), which constitutively accumulated allantoin, exhibited moderately increased ABA levels even under normal growth conditions and were highly tolerant to drought and osmotic stress. These results suggest that allantoin accumulation affected ABA metabolism. In Arabidopsis, stress-induced ABA production is regulated by two biochemical routes: *de novo* biosynthesis and regeneration from inactive ABA-glucosyl esters (ABA-GE) (Fig. 3). In the regeneration pathway, BGLU18 (also known as BG1), a key enzyme that hydrolyses ABA-GE to liberate free ABA, is thought to be activated through its polymerization (Lee

et al., 2006). Since ABA regeneration probably proceeds *de novo* synthesis that is at least partly under a positive feedback by elevated levels of free ABA in response to stress (Xiong *et al.*, 2001), ABA regeneration is regarded as the trigger of ABA production. Interestingly, both ALN and BGLU18 localize to the ER, suggesting the possible link between allantoin and ABA regeneration. Watanabe *et al*. (2014*b*) also found that both endogenous accumulation and exogenous supplementation of allantoin caused BGLU18 polymerization. Furthermore, in addition to the regeneration pathway, allantoin enhanced expression levels of *9-CIS-EPOXYCAROTENOID DIOXIGENASE3* (*NCED3*) that is a rate-limiting gene for ABA *de novo* synthesis. Based on these results, it is speculated that allantoin first activates BGLU18 in the ER, followed by up-regulation of ABA *de novo* synthesis by a positive feedback of regenerated ABA (Fig. 3). ABA and other phytohormones, however, constitute complex signaling networks, and interact each other. It still remains unknown whether, and if so how, allantoin accumulation affects overall plant stress signaling and responses mediated by phytohormone responses.

4. The aims of this study

The aim of this study was to investigate and establish a dual role of purine catabolism in maintaining plant growth under normal conditions and responding to stressful conditions for environmental adaptation. In CHAPTER I, I focused on the physiological impacts of purine catabolism on the growth and efficient N utilization in Arabidopsis plants. For this purpose, I examined the various aspects of the phenotypes of Arabidopsis knockout mutants for ureide-degrading enzymes (ALN and AAH) and ureide transporters (UPS1 and UPS2). This was because, if ureide degradation and transport played a

significant part in N metabolism and recycling, the effects of these knockout mutations would become apparent as mutant plants grow to maturity where N is required in large quantities for reproduction. The results obtained from this study suggest that purine-derived N contributes significantly to plant growth and reproduction through the ureide degradation and transport. In CHAPTER II, I investigated the possible regulatory role of purine catabolism in activating stress responses, specifically focusing on the effects of ureide allantoin on the responses mediated by the phytohormone jasmonic acid (JA). This was because microarray analysis of an *aln* mutant (*aln-1*) raised the possibility that allantoin accumulation up-regulates not only ABA-responsive genes, but also JA-responsive genes (Watanebe *et al*., 2014*b*). JA is well known for its pivotal roles in biotic stress resistance. In this study, therefore, I investigated the effect of allantoin accumulation on the expression profile of JA-responsive genes and defense response to bacterial pathogens. I also conducted genetic analysis to elucidate the mechanism through which JA responses are activated by allantoin. The results in this part highlight new insights into the regulatory roles of allantoin in stress phytohormone responses.

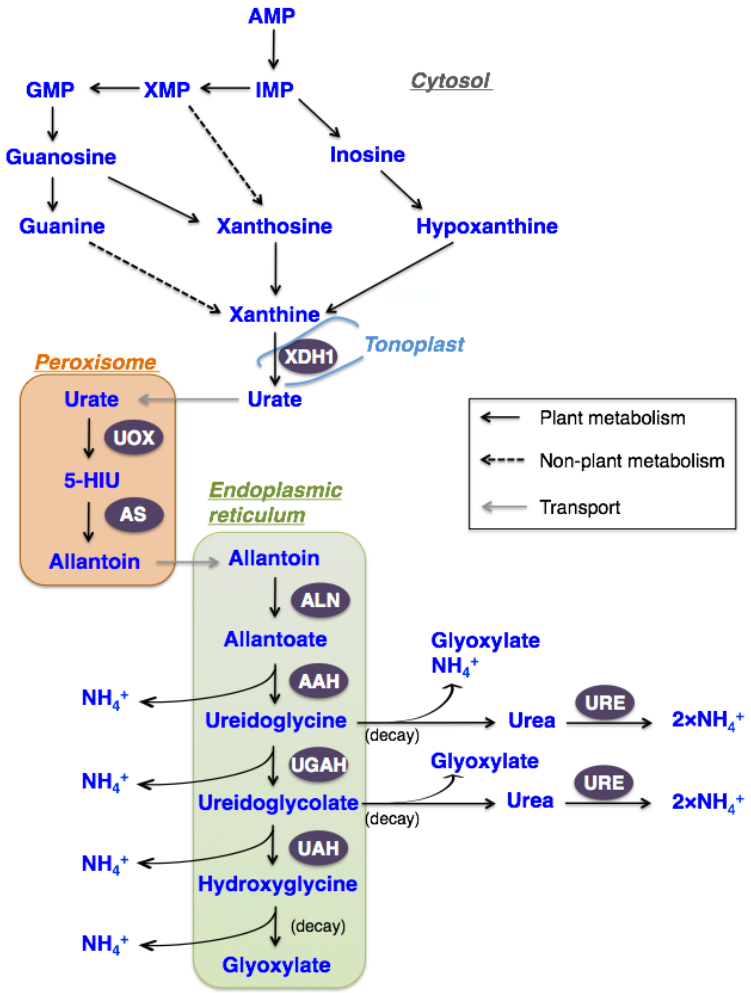

Figure 1. The purine catabolism pathway and metabolites derived therefrom.

The catabolic route is schematically illustrated beginning with AMP. Only catabolic enzymes after xanthine are shown: XDH, xanthine dehydrogenase; UOX, urate oxidase; AS, allantoin synthase; ALN, allantoinase (allantoin amidohydrolase); AAH, allantoate amidohydrolase; UGAH, ureidoglycine aminohydrolase; UAH, ureidoglycolate amidohydrolase.

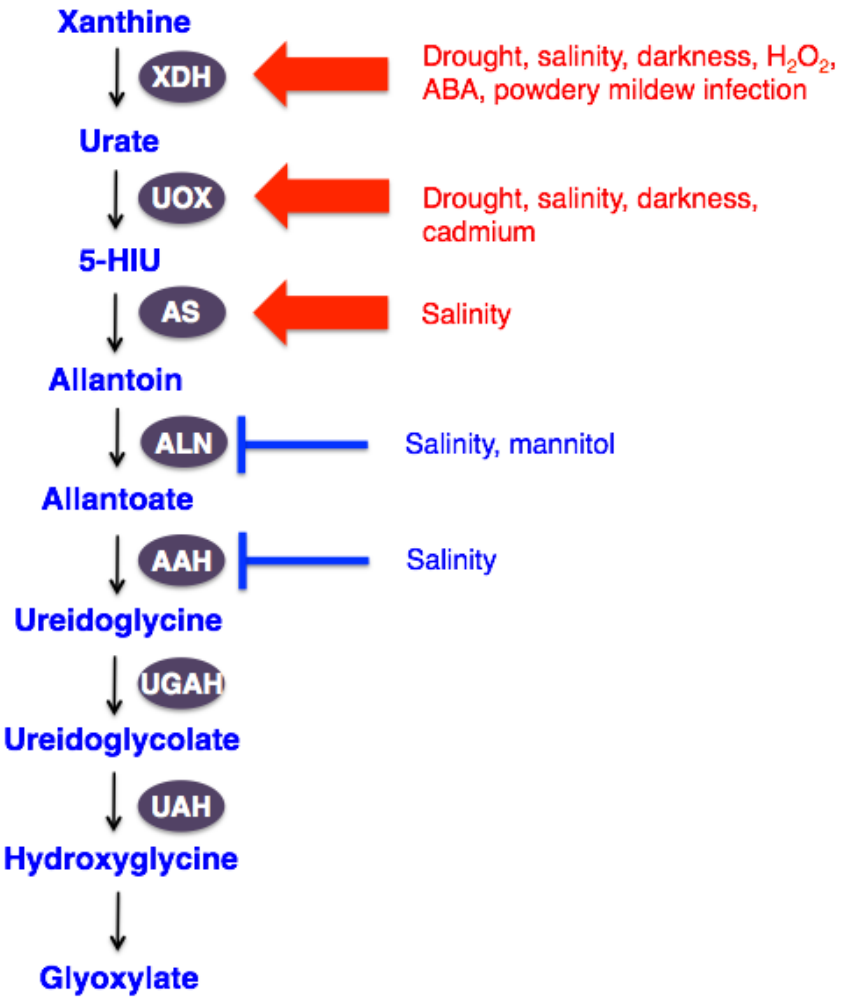

Figure 2. Transcriptional regulation of purine catabolic genes under stress conditions that result in ureide accumulation in Arabidopsis.
Genes involved in ureide biosynthesis (*XDH*, *UOX* and *AS*) are upregulated, whereas genes involved in ureide degradation (*ALN* and *AAH*) are downregulated in response to environmental stress.

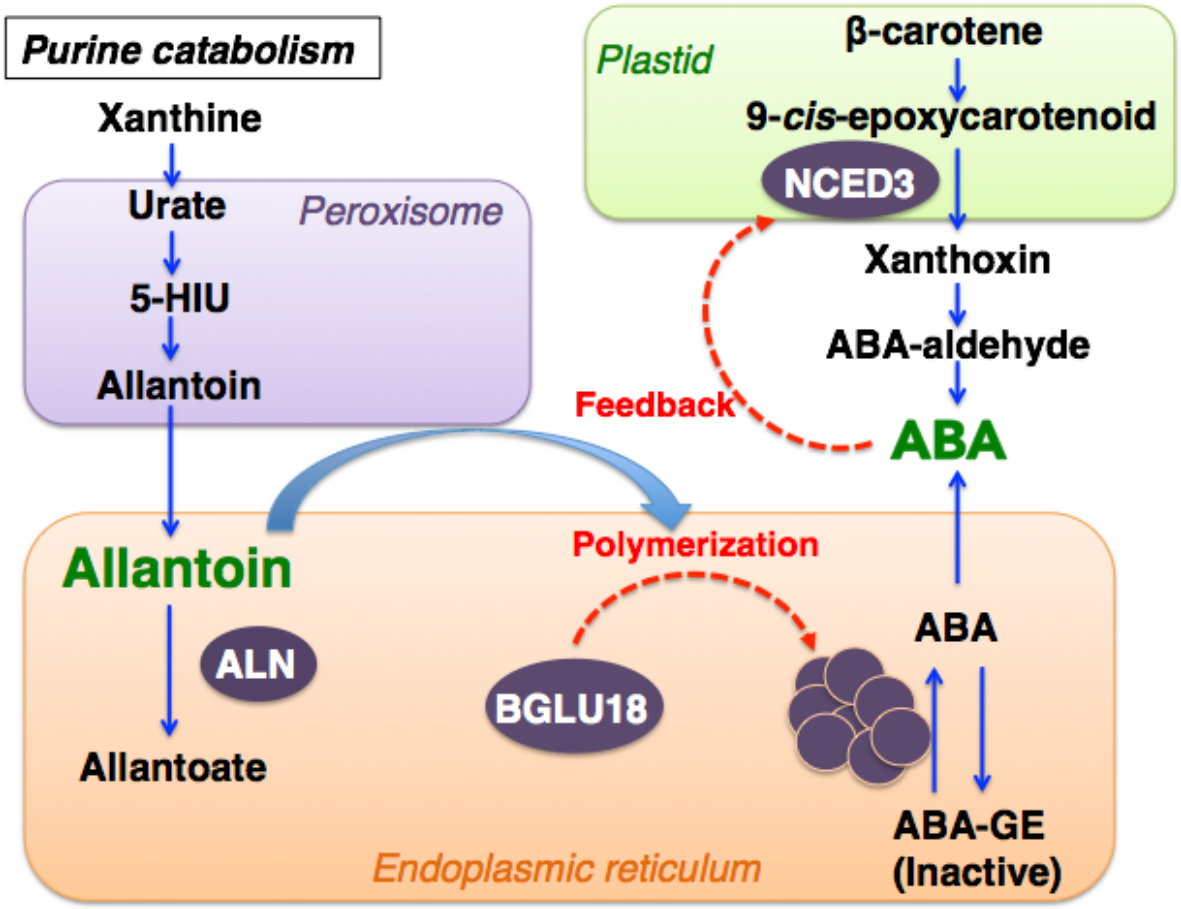

Figure 3. Possible model for mode of allantoin action on ABA metabolism. Allantoin activates an ABA-regenerating ß-glucosidase, BGLU18 (also known as BG1), through its polymerization to release free ABA from inactive ABA-glucose esters (ABA-GE). Regenerated ABA causes positive feedback regulation on ABA *de novo* synthesis (Watanabe *et al*., 2014*b*).

CHAPTER I

Ureide catabolism impacts on plant growth and efficient nitrogen utilization in Arabidopsis

Introduction

N is the mineral element used in large quantities by plants, and its availability is considered rate limiting for plant growth, productivity, and yields. Therefore, under natural and agricultural environments, critically important is how plants efficiently use N, which involves various physiological processes such as sensing, uptake and assimilation of inorganic N into organic forms, and recycling and redistribution of stored N in cellular macromolecules (*i.e.*, proteins and nucleic acids) (Masclaux-Daubresse *et al*., 2010). The senescence-induced remobilization of leaf N plays a major role in source–sink N redistribution, supporting the vegetative and reproductive phases of growth, such as new leaf formation and seed development. Major chloroplast proteins, particularly ribulose-1,5-bisphosphate carboxylase/oxygenase, are considered the main source of remobilized leaf N, since most plants allocate large amounts of leaf N to chloroplasts (Mae *et al*., 1983; Evans and Seemann, 1989). A great deal of research efforts have been made to understand the regulatory mechanisms of protein breakdown associated with chloroplast dismantling during leaf senescence (Kato *et al*., 2004; Ishida *et al*., 2008; Martínez *et al*., 2008; Carrión *et al*., 2013; Lee *et al*., 2013; Ono *et al*., 2013). Following proteolysis and deamination of constituent amino acids, protein-derived N is eventually liberated as ammonium that is re-assimilated into glutamine by cytosolic GS. Glutamine and asparagine are

amido-amino acids that generally serve as mobile reservoirs to transport N from source to sink organs during N remobilization (Masclaux-Daubresse *et al*., 2010).

Nucleic acids are also considered as an important source of remobilized N during senescence, yet their precise contribution remains largely unexplored (Buchanan-Wollaston, 1997). Purines and pyrimidines constitute the nitrogenous components of nucleic acids, and unless converted to nucleotides through salvage reactions, the free form of these nucleobases provide re-usable N upon the decomposition thereof (Stasolla *et al*., 2003; Zrenner *et al*., 2006). Purines are the more valuable N source than pyrimidines because in plants, all the four N atoms in the purine ring can be recycled as ammonium whereas only one of the two N atoms is mineralized from the pyrimidine ring. When catabolized, all purines are converged to xanthine, the first common intermediate of the purine catabolic pathway. In Arabidopsis, and most probably in other species, this pathway consists of a series of biochemical reactions that are mediated by seven enzymes distributed in the cytosol, peroxisomes and ER (Werner and Witte, 2011). The xanthine is oxidized to urate by XDH in the cytosol (Datta *et al*., 1991; Hesberg *et al*., 2004). Urate is then transported into the peroxisomes and converted to the ureide allantoin via a three-enzymatic step, first mediated by UOX, then followed by a bifunctional enzyme AS catalyzing the last two reactions (Lamberto *et al*., 2010; Pessoa *et al*., 2010). The subsequent ureide degradation is accomplished stepwise by four ER-localized hydrolases to release four ammonium ions. Allantoin is decomposed by ALN (Yang and Han, 2004) to allantoate, which is degraded by AAH (Todd and Polacco, 2006) to ureidoglycine and an ammonium ion. This ureido intermediate is further hydrolyzed to release another ammonium by UGAH (Serventi *et al*., 2010), and the resultant

ureidoglycolate is finally metabolized to glyoxylate and two molecules of ammonium, by UAH and the subsequent spontaneous decomposition (Werner *et al*., 2010). The purine-derived ammonium is almost probably recycled for glutamine synthesis in the cytosol, as is that derived from proteins, although little is known how this inorganic ion is exported from the ER.

Purine metabolism is adopted as an integral part of symbiotically fixed N_2 utilization in leguminous species of tropical and sub-tropical origin. The ureides allantoin and allantoate, the principal products of N_2 fixation in these legumes, occur at very significant levels in the xylem and translocate the bulk of N from root nodules to shoots for transient storage, catabolism, or further distribution to reproductive organs (Schubert, 1986). Certain members of the UPS family, such as PvUPS1 from common bean and GmUPS1-1 and GmUPS1-2 from soybean (*Glycine max* L.), have been shown to mediate symplasmic transport of allantoin and its xylem loading in nodulated roots (Pélissier *et al*., 2004; Collier and Tegeder, 2012). PvUPS1 is also possibly involved in the phloem loading (Pélissier and Tegeder, 2007). Although no evidence has so far been presented for long-distance translocation of the ureides in Arabidopsis, its genome contains five paralogous genes encoding UPS (AtUPS1–5), suggesting that the possible involvement of ureide transport in purine-derived N recycling and remobilization in this non-N_2-fixing plant. Among these members, AtUPS1, AtUPS2 and AtUPS5 have been shown to be able to transport allantoin using heterologous expression in yeast and in *Xenopus* oocytes (Desimone *et al*., 2002; Schmidt *et al*., 2004, 2006). However, these characterized AtUPS proteins exhibited several-fold higher affinity for uracil (AtUPS1 and AtUPS2) and xanthine (AtUPS5), pointing to their primary function *in planta* as transporting nucleobases rather than ureides (Schmidt *et al*., 2004, 2006).

Purine-catabolic mutants of Arabidopsis have been isolated, such as those that lack or down-regulate *XDH*, *UOX*, *ALN* or *AAH*, thus unable to use purine-derived N by blocking ureide synthesis or degradation. Recent studies using these mutants revealed that defects in purine catabolism significantly influenced abiotic stress tolerance of the plant. Loss-of-function *xdh1* mutation and post-transcriptional gene suppression (PTGS) of *AtXDH1* and *AtXDH2*, both rendering the whole catabolic pathway inoperative, resulted in enhanced sensitivity to extended dark and drought stress (Brychkova *et al*., 2008; Watanabe *et al*., 2010, 2014a). Conversely, interrupting the catabolism halfway by knocking out *ALN,* but not *AAH*, allowed the mutants to be more tolerant to drought, osmotic and salt stress, probably through the accumulation of allantoin that could act as antioxidant or activate stress responses (Watanabe *et al*., 2014b; Irani and Todd, 2016; Lescano *et al*., 2016). Under normal growth conditions, the *AtXDH1*/*2*-PTGS lines exhibited age-dependent growth retardation and precocious leaf senescence (Nakagawa *et al*., 2007). However, none of the knockout mutations (*xdh1*, *aln*, and *aah*) reportedly affected the growth phenotypes, with the exception of *uox* that hampers the early development due to peroxisomal disorder (Yang and Han, 2004; Todd and Polacco, 2006; Brychkova *et al*., 2008; Werner *et al*., 2013; Hauck *et al*., 2014). When grown normally, no phenotypic alteration was also reported for the ureide-transporter mutants, *AtUPS1*-PTGS lines and *ups2* knockout mutants (Schmidt *et al*., 2004). Overall, these reverse-genetic studies, while highlighting an emerging role in stress protection, provide little evidence to support the general role that has been attributed to purine catabolism (*i.e.* recycling and remobilizing N), despite the importance of efficient N use in plant growth and development.

The aim of this study is to re-examine the role of purine catabolism as

fundamental N metabolism to sustain normal growth and development of Arabidopsis plants. For this, we conducted a detailed evaluation of the growth phenotype of the Arabidopsis mutants (*aln*, *aah*, *ups1* and *ups2*), particularly focusing on ureide degradation and transport, the key processes for the utilization of purine-derived N. Here we show that dysfunction of these physiological processes severely impacted on the growth to maturity when the large amounts of N is recycled and remobilized, which led consistently to early flowering and senescence, and low biomass accumulation in these ureide-related mutants. Moreover, the growth defects were accompanied by significant alterations in N use efficiency and the sink–source distribution of allantoin and allantoate. Our results thus suggest that the role of purine degradation becomes evident and substantial towards the later stage of Arabidopsis growth, probably through contributing to efficient N utilization.

Materials and Methods

Plant materials, growth conditions and flowering time measurement

Arabidopsis plants were grown on soil at 23 °C, long light (16 h Light, 8h dark) with 70 μmol photons m^{-2} s^{-1}. Seeds were directly sown on garden soil "Hanasaki Monogatari" (Akimoto-tensanbutsu, Iga, Japan) which has following nutrient compositions: 290 mg L^{-1} N; 620 mg L^{-1} P; 285 mg L^{-1} K; small amount of Mg, B, Fe and Mn. Plants were irrigated with 1/2000 Hyponex (Hyponex-Japan, Osaka, Japan) once a week, and tap water to prevent from dryness. Seeds of the following mutants and T-DNA insertion lines were obtained from the Arabidopsis Biological Resource Center (Ohio State University, Columbus, Ohio, USA): *aah* (SALK_112631; Todd and Polacco, 2006), *aln-1* (SALK_000325; Yang and Han, 2004; Watanabe *et al*., 2014b; also known as *aln*), *aln-2* (SALK_146783; Watanabe *et al*., 2014b), *ups1* (SAIL_549_F06) and *ups2* (SALK_044551C; Schmidt *et al*., 2004; also known as *ups2-2*). Flowering time was expressed with the number of rosette leaves when primary inflorescence (about 1 cm) was observed.

Biomass, leaf size and ureide contents

Aerial parts of 5-week-old plants were cut into leaf blades (rosette leaves), petioles, cauline leaves, inflorescence stems and siliques, and used for fresh weight (FW) measurements. The largest leaf was selected by naked eyes, and used to measure length and width of leaf blade, and length of petiole. Shoots of 9-week-old plant were dried in air-forced oven at 65 °C for dry weight (DW) measurement. For ureide measurements, 5- and 9-week-old plants were

cut and freeze-dried. Ureide contents were determined as described previously (Watanabe *et al*., 2014b).

Nitrogen-deficient conditions

Seeds were sown on 1/2 MS medium and vernalized for 2 days at 4 °C. After plates were placed in growth chamber for 2 weeks, plants were transplanted into pots containing vermiculite:pertlite (1.5:1), and grown for 4 weeks. We irrigated culture solution 2 or 20 mM N once a week. The component of culture solution was shown in Table I-1. Aerial parts were freeze-dried, and used for DW and ureide measurements.

The number of siliques and size of siliques and seeds

To measure silique length and seed numbers per silique, 10 matured siliques were detached from every plant. The average silique length and seed numbers in the individual plant were defined as one sample. We used 10 individual 9-week-old plants for these experiments. The length of siliques was measured using ImageJ software version 1.45 (http://rsbweb. nih.gov/ij/, accessed 22 February 2016). The numbers of undetached siliques were counted once a week.

Inorganic analysis and nitrogen use efficiency

Aerial parts of 9-week-old plants were freeze-dried and grounded to a fine powder, and N and C contents were determined by combustion and thermal conductivity separation in a CHN analyzer (Perkin Elmer Series II CHNS/O

Analyzer, Perkin Elmer, Norwalk, Connecticut, USA). Nitrogen use efficiency (NUE) was calculated following the equation of Good *et al*., (2004).

Gene expression analyses

Total RNA was extracted using the NucleoSpin RNAII extraction kit (Macherey-Nagel GmbH & Co, Düren, Germany) following the manufacturer's protocol. Aliquots (500 ng) of RNA were used as templates for reverse transcription with the ReverTra Ace qPCR RT kit (Toyobo, Osaka, Japan), and RT-quantitative PCR (RT-qPCR) was performed by the SYBR green methods using a 7300 Real-Time PCR System (Applied Biosystems, Foster City, CA, USA). The PCR program consisted of an initial denaturation and Taq polymerase activation step of 10 min at 95°C, followed by 40 cycles of 15 s at 95°C and 1 min at 60°C. The specificity of primers was confirmed with dissociation curve analysis. Relative gene expression levels were calculated by the $2^{-\Delta\Delta Ct}$ method (Livak and Schmittgen, 2001) after normalization to *ACTIN 2* (*ACT2*), *UBIQITIN CONJUGATING ENZYME 9* (*UBC9*) and MONESIN SENSITIVITY 1 (*MON1*) expression levels. Primer sequences for target genes are listed in Table I-2.

Phytohormone measurements

Hormones were extracted and quantified following the method of Tsukahara *et al*., (2015) with small modifications. Aerial parts of 5-week-old plants were freeze-dried and grounded to a fine powder, extracted with mixed with 4 mL of 80% (v/v) acetonitrile containing 1% (v/v) acetic and known amount of stable isotope-labeled internal standards at 4°C for 1h. After removal of cell debris by centrifugation at 3000g for 10 min, the resultant residues were

extracted with 80% (v/v) acetonitrile containing 1% (v/v) acetic again. The two supernatants were combined, evaporate in a vacuum centrifugal evaporator (miVac quattro concentrator, Genevac Ltd., Ipswich, UK) and dissolved in 1% (v/v) acetic acid. The extracts were loaded onto pre-equilibrated Oasis HLB column cartridge (Waters Corporation, Milford, MA, USA). After washed with water acidified with 1% acetic acid, the column was eluted with 80% (v/v) acetonitrile containing 1% (v/v) acetic acid. The eluted samples were evaporated to obtain extracts in water acidified with 1% acetic acid, and loaded onto a pre-equilibrated Oasis MCX column cartridge (Waters). The cartridge was washed with 1% acetic acid (v/v), and the acidic fraction was eluted with 80% acetonitrile containing 1% acetic acid. A portion of the acidic elute was analyzed for salicylic acid (SA). The cartridge was further washed with 5% aqueous ammonia, and the basic fraction was eluted with 40% acetonitrile containing 5% ammonia and analyzed for trans-zeatin (tZ) and N^6-(Δ^2-isopentenyl)adenine (iP). The remaining acidic fraction was evaporated, dissolved in 1% acetic acid, and loaded onto pre-equilibrated Oasis WAX column cartridges (Waters). The cartridge was washed with 1% acetic acid (v/v) and 80% acetonitrile, and remaining hormones were eluted with 80% acetonitrile containing 1% acetic acid. The elute was analyzed for indole-3-acetic acid (IAA), GA_4, ABA, JA, and jasmonoyl-L-isoleucine (JA-Ile). All fractions were analyzed on an Agilent 6410 Triple Quadrupole system with a ZORBAX Eclipse XDB-C18 column and MassHunter software version B.01.02 (Agilent Technology, Palo Alto, CA, USA).

Statistical analyses

Means of two groups were compared by Student's *t*-test at a 5% level of significance with Microsoft Excel. Means of three or more groups were

compared by Tukey's multiple comparison test, which was performed with IBM SPSS statistic, version 21.0 (IBM, New York, NY, USA).

Results

Disruption of ureide degradation accelerates the transition to reproductive growth

To evaluate possible impacts of disrupting ureide degradation on the growth and development of Arabidopsis, we first compared the normal growth phenotype of three T-DNA knockout mutants with that of the WT plants. Two of such mutants, *aln-1* and *aln-2*, were loss-of-function alleles of *ALN* incapable of degrading allantoin and another mutant, *aah*, was deficient in allantoate hydrolysis due to the disrupted *AAH* (Watanabe *et al*., 2014b). When grown on soil under long day conditions, these mutants started bolting and flowering as early as at 4 (week after germination) WAG whereas WT plants remained non-bolting (Fig. I-1A). The early flowering of *aln* and *aah* mutants resulted in fewer than 10 rosette leaves per plant versus about 14 for WT plants that were not florally induced (Fig. I-1B). The three mutants also displayed slight but significant decreases in foliar chlorophylls (Fig. I-2). At 5 WAG, although there were little differences from the WT in terms of above-ground FW, these mutants had less FW for rosette leaves (leaf blades and petioles) but more FW for inflorescence stems and cauline leaves (Fig. I-1C and D). Associated with the lower FW, the rosette leaves of these mutants were significantly shorter in the length of leaf blades and petioles (Table I-3). These results suggest that disruption of ureide degradation accelerated the transition from vegetative to reproductive growth under long-day conditions.

Disruption of ureide degradation impairs the reproductive growth

To know whether *aln* and *aah* mutations affected the subsequent growth and reproduction, we examined the mutant phenotypes at the late growth stage. At 9 WAG, the three mutants were relatively smaller in appearance, with the whole-plant DW being approximately half of WT plants (Fig. I-3A). Correlated with the early flowering phenotype, these mutants tended to form more siliques than did WT plants during the early stages of inflorescence development (up to 7 WAG; Fig. I-3B). However, consistent with the lower DW, total silique numbers of the three mutants were reduced at 9 WAG, ranging between 50% and 67% of WT plants, dependent on the mutant lines (Fig. I-3B). Moreover, the siliques of these mutants were significantly shorter and contained much less seeds than those of WT plants (Fig. I-3C and D). These reproduction-associated phenotypes suggest that ureide degradation has physiological impact especially in the late stages of Arabidopsis growth.

Disruption of ureide degradation accelerates leaf senescence in mature plants

The vegetative-to-reproductive growth transition generally coincides with the onset of leaf senescence. We therefore examined whether ureide degradation mutants accelerated this physiological process. At 9 WAG, these mutants showed more yellowing of the rosette leaves when compared with those of the WT plants (Fig. I-4A). To confirm the early senescence phenotype in these mutants at the molecular level, we analyzed the expression of a canonical senescence marker *SENESCENCE-ASSOCIATED GENE 13* (*SAG13*) in 7-week-old rosette leaves by RT-qPCR using three different reference genes (Figs I-4B and I-5). In all cases, consistent with the early senescence symptom, *SAG13* showed significantly higher levels of expression in these mutants than in WT. The findings suggest that defective ureide

degradation leads to precocious leaf senescence in mature Arabidopsis plants.

Disruption of ureide degradation affects nitrogen status and reduces the growth under low nitrogen condition

Nutritional status in plants critically affects developmental and physiological phase transitions, and N starvation induces early flowering and leaf senescence, which often result in reduced growth. Since *aln* and *aah* plants displayed such N-deficiency-like phenotypes as they grew toward maturity (Figs I-1 to I-3), we examined relative N content, NUE and C/N ratio as indicators of N status in these mutants, and compared them with the same measures in WT plants. At 9 WAG, all the three mutants exhibited significant differences in these parameters from those of WT, with the increases in relative N content but the decreases in NUE and C/N ratio (Table I-4). The results suggested that *aln* and *aah* mutants were relatively inefficient at using N for their growth and C assimilation. To test this, we examined whether these mutants were more susceptible than WT to N-deficient conditions, because limited N supply would aggravate further the inefficiency on N usage in these mutants. Two-week-old aseptic seedlings were transplanted to soil, and then they were grown for 4 weeks under sufficient (20 mM) and low (2 mM) N regimes. At this growth stage (6 WAG), sufficient N supply resulted in no statistical differences in DW-based growth between WT and the mutants except for *aln-2*, whereas under low N conditions, all the three mutants reduced the DW significantly compared to WT plants (Fig. I-6A). Simultaneous measurements of the ureide contents showed that, irrespective of N regimes, *aln* and *aah* mutants accumulated high levels of allantoin and allantoate, respectively (Fig. I-6B). WT plants, however, responded to low N

regimes by significantly decreasing allantoate levels, implying activated allantoate degradation under N deficiency. Taken together, these results suggest a possible role of ureide degradation in efficient N use when Arabidopsis plants grow to maturity or experience N scarcity.

Hormone responses may be not responsible for growth attenuation of degradation mutants

The results described above suggest that purine catabolism is involved in efficient N utilization. Watanabe *et al*., (2014b), however, demonstrated that 2-week-old *aln* mutants grown on 1/2 MS medium overaccumulated ABA. Therefore, it is possible that the growth reduction of ureide accumulating mutants is attributed to the effect of hormonal responses rather than N use efficiency. To test it, 5-week-old plants grown on soil were used for phytohormone measurements (Table I-5). The *aln-2* mutant significantly increased ABA and JA-Ile; however, the *aln-1* and *aah* mutants showed no significant change in ABA and JA contents. In addition to ABA and JA-Ile, the *aln-2* mutants increased IAA, and decreased tZ contents, suggesting antagonistic auxin‐cytokinin interactions. Increased GA_4 contents in the *aln* mutants may be related to early flowering phenotypes. Based on these results, I cannot clearly exclude the possibility that growth reduction comes from enhanced stress hormone responses, especially in the *aln-2* mutant; however, I think that these stress hormones may be not mainly responsible for growth restriction, because levels of stress hormones such as ABA and JA in the *aln-1* and *aah* mutants were comparable with WT plants.

Reproductive tissues contain relatively high ureide levels that are augmented

by disruption of ureide degradation

Source–sink allocation and redistribution of N constitute an important physiological process for efficient N use when plants grow to maturity and reproduce seeds, or when available N is limited. We therefore examined tissue distribution of allantoin and allantoate in the above-ground parts of Arabidopsis plants. At 5 WAG when most WT plants were still not bolting yet (Fig. I-1C), the rosette leaves contained allantoin equally in the leaf blades and petioles whereas allantoate was found 3-fold higher in the petioles (Fig. I-7). By this stage, both *aln* and *aah* mutants already started bolting (Fig. I-1) and had significantly greater levels of allantoin and allantoate than the WT, respectively, with a tendency to accumulate more in inflorescence stems and/or cauline leaves (Fig. I-7). At 9 WAG, WT plants exhibited higher levels of allantoate than allantoin in every tissue examined (leaf blades, petioles, caulines, stems and siliques) and the highest level was detected in siliques (Fig. I-8). Such accumulation profiles were consistent and augmented in the *aah* mutant where allantoate degradation is blocked. Compared to allantoate, allantoin was distributed relatively evenly in the WT and *aah* mutant, although the *aln* mutants appeared to accumulate this ureide slightly more in siliques and caulines than in the other tissues. Mature dry seeds from the WT contained allantoin almost exclusively and its level further increased in the *aln-1* mutant (Fig. I-9). The *aah* mutant also accumulated more allantoin than allantoate, suggesting that allantoin serves as the major storage form of purine-derived N in Arabidopsis seeds (Fig. I-9). Overall, these results indicate that the two ureides occurred predominantly in the reproductive parts of Arabidopsis during the growth to maturity and seed production, with the highest levels found in siliques for allantoate and in dry seeds for allantoin.

The differential distribution of allantoin and allantoate is likely to result from the different metabolic and/or transport activities for these metabolites within the above-ground tissues.

Disruption of ureide transporters results in a similar growth defect to ureide degradation mutants but lowers ureide levels in reproductive tissues

The above results suggested that not only the degradation, but also the partitioning of ureides that involves membrane transport, is critical for supporting the growth at the later stage of Arabidopsis. We thus investigated the effect of disrupting ureide transport on the growth phenotype and tissue distribution of allantoin and allantoate using *ups1* and *ups2*, two knockout mutants for functionally characterized Arabidopsis UPS proteins, AtUPS1 and AtUPS2, respectively (Fig. I-10). Similar to *aln* and *aah* mutants, *ups1* and *ups2* mutants showed early flowering (Fig. I-11A), and at 9 WAG, significantly reduced the whole-plant DW by 50% and 25%, respectively, compared with the WT (Fig. I-11B). Tissue distribution of the two ureides was determined at 7 WAG when both the WT and two *ups* mutants were bolting and developing siliques (Fig. I-12). As shown in Figure I-11C, no significant difference was found in allantoin levels between the WT and the mutants in any of the tissues examined. However, when compared to the WT, allantoate levels decreased significantly in inflorescence stems of both *ups1* and *ups2* mutants and in siliques of the *ups1* mutant, while increased in rosette leaf blades of the *ups2* mutant. These results indicate that dysfunction of UPS transporter genes negatively impacted at the reproductive stage of Arabidopsis growth and reduced allantoate accumulation mainly in the inflorescence stems.

Genes involved in ureide synthesis and transport are activated upon vegetative-to-reproductive phase transition

To examine the relationship of tissue distribution of allantoin and allantoate with the associated gene expression, we determined changes in transcript levels of genes involved in ureide metabolism (*XDH*, *ALN* and *AAH*) and transport (*UPS1* and *UPS2*) in the WT plants upon transition from vegetative (5 WAG, see Fig. I-1C) to reproductive phase (7 WAG, see Fig. I-11). RT-qPCR using different reference genes resulted in overall consistent data (Figs I-13A, I-14A, I-15A), which showed that transcript levels for *XDH* and *ALN* increased, while those for *AAH* remained little changed, in rosette leaf blades during the growth phase transition. Coincident with *XDH* and *ALN* expression, *UPS1* and *UPS2* significantly enhanced their transcript levels in both leaf blades and petioles (Figs I-13B, I-14B, I-15B). In the reproductive organs, all genes were expressed higher in cauline leaves than in stems. These results suggest that ureide synthesis, particularly of allantoate, and UPS-mediated transport are activated in source organs (*i.e*. rosette leaves for inflorescence; caulines for siliques) as Arabidopsis plants shift from vegetative to reproductive growth.

Discussion

Purine catabolism is required for efficient nitrogen utilization

Purine catabolism is well known for its pivotal role in store and utilization of symbiotically fixed N (Smith and Atkins, 2002). However, its general roles in plants still remain elusive (Werner and Witte, 2011). This catabolic pathway has been thought as N recycling metabolism, since complete breakdown of a purine compound releases four molar equivalents of ammonia; however, experimental evidence is still limited. Although previous studies reported that disruption of ureide degradation and transport did not affect plant growth (Schmidt *et al*., 2004; Yang and Han, 2004; Todd and Polacco, 2006; Werner *et al*., 2008), results in this study showed that ureide degradation and transport are required for healthy plant growth and reproduction.

The *aln* and *aah* mutants showed early transition to reproductive stages and low chlorophyll contents (Figs I-1, I-2). Since early flowering and leaf yellowing are typical symptoms of N deficiency, we further investigated the growth phenotypes of ureide degradation mutants. These mutants showed the decrease of biomass (Fig. I-3) and early leaf senescence (Fig. I-4) in late growth stage. Early leaf senescence is inconsistent with previous study that showed ureides protect from oxidative stresses (Brychkova *et al*., 2008). This suggests that the antioxiadative effect of ureides *in planta* is limited at least in late growth stage. The results of this study also raised the possibility that impaired growth and accelerated senescence in *AtXDH1*/*2*-PTGS lines (Nakagawa *et al*., 2007) are mainly attributed to the decreased N use efficiency, rather than excessive cell oxidation.

The mutants defective in ureide degradation showed symptoms like N

deficiency; however, the question whether these mutant phenotypes come from N deficiency or other effects remained elusive. To test it, we measured N contents in 9-week-old plants. Ureide degradation mutants showed significantly increased N contents, and decreased NUE and C:N ratio (Table I-4). These results suggest that ureide catabolism is essential for efficient N utilization. These results prompted us to cultivate mutants for ureide degradation under N-deficient and sufficient conditions. In N-deficient conditions, all mutants defective in ureide degradation decreased DW compared with WT; in N sufficient (20 mM N) conditions, only the *aln-2* mutant reduced significantly (Fig. I-6). Interestingly, WT plants showed higher allantoate contents under N-sufficient conditions than N-deficient condition. This supports the idea that ureides are used as a potential N source. It was recently reported that, however, allantoin accumulation affected ABA responses in 2-week-old plants (Watanabe *et al*., 2014*b*), thus it is also possible that growth reduction of ureide degrading mutants comes from enhanced stress hormone responses. We measure phytohormone contents using 5-week-old plants. The levels of stress hormones, ABA and JA-Ile, were increased in the *aln-2* mutant, but not in the *aln-1*and *aah* mutants (Table I-5). In the light of discrepancy between 2-week-old and 5-week-old plants, I speculate that the effect of allantoin on hormone responses depends on developmental stages. Based on the results of hormone contents, I think the effect on hormone responses is not to be direct and main reasons of growth reduction.

UPS1 and UPS2 may transport allantoate to upper parts for N recycling

In this study, WT and the *aah* mutant accumulated allantoate in siliques;

however, this tendency was not clear in allantoin in the *aln* mutants (Figs I-7, I-8). I thus further investigated the effect of genetic impairment of ureide transporters using the *ups1* and *ups2* mutants (Fig. I-11). Although previous report described that AtUPS1 and AtUPS2 protein showed very low affinity for allantoate (Schmidt *et al.*, 2004), the results of this study showed that the *ups1* and *ups2* mutation significantly decreased allantoate levels in inflorescent stems and siliques. So far, only known example of proteins that showed affinities to allantoate are soybean GmUPS1-1 and GmUPS1-2 (Collier and Tegeder, 2012). These authors found that knockdown mutations of these transporters resulted in the significant inhibition of nodule–shoot allantoate transport, while the effect on allantoin transport was weaker compared with allantoate. In biochemical assays, however, allantoin showed higher affinity for GmUPS1 proteins than allantoate. In the light of the discrepancy between biochemical and physiological experiments, I think that it is possible that AtUPS1 and AtUPS2 proteins transport allantoate *in planta*, although it was denied in biochemical assays in the previous study (Schmidt *et al.*, 2004).

Schmidt *et al*., (2004) concluded that the main physiological function of UPS proteins is pyrimidine transport for its salvage in early growth stages, but not N remobilization. Therefore, the growth reduction of the *ups1* and *ups2* mutant were thought as the results of impaired pyrimidine transports, rather than attenuated N recycling and remobilization. However, gene expression analysis in this study showed mRNA level of *UPS1* and *UPS2* increased at late growth stage (Figs I-13B, I-14B, I-15B). In contrast to N recycling, the physiological importance of nucleotide salvage usually decreases in the late growth stage, because *de novo* synthesis covers almost all of pyrimidine bases. Therefore, impaired growth in the *ups1* and *ups2* might be not attributed to the

disruption of pyrimidine transport.

Previously, it was shown that five members of *AtUPS* family have different gene expression patterns (Schmidt *et al*., 2006), suggesting their distinctive roles. In this study, the *ups2* mutant decreased allantoate content in inflorescence stems, but increased it in rosette leaves (Fig. I-11). Consistent with this, the expression levels of *UPS2* strongly increased in 7-week-old leaves compared with 5-week-old leaves (Fig. I-13B, 14B, 15B). UPS2 may transport allantoate from leaf blades to upper parts. In the *ups1* mutant, source organs such as leaf blades did not increase allantoate concentration, although it was significantly decreased in upper parts (Fig. I-11C). Recent study showed that *ups5* mutant decreased root–shoot allantoin transport (Lescano *et al*., 2016). Perhaps, UPS1 is also involved in root–shoots ureide transports. Further analyses will be required to understand the mode of action of UPS proteins.

Allantoate biosynthesis and transport may be coordinately regulated

In this study, we also attempted to unveil how N recycling and remobilization by purine catabolism is regulated. To investigate this, we tested gene expression levels of purine catabolic genes (*XDH1*, *ALN* and *AAH*), and ureide transport genes (*UPS1* and *UPS2*). *XDH1*, *ALN*, *UPS1* and *UPS2* were upregulated with senescence, but *AAH* expression did not change significantly (Figs I-13A, I-14A, I-15A). This expression pattern is consistent with the increase of allantoate contents in late growth stages in sink organs. It is generally known that allantoin to allantoate ratio increase with senescence (Collier and Tegeder, 2012). Moreover, in common bean, senescence-associated allantoate biosynthesis and translocation was

independent from nodule activation (Díaz-Leal *et al.*, 2012). Activation of allantoate synthesis and transport in late growth stages might be conserved mechanism among legume and non-legume plants.

Previous reports have showed that genes encoding UPS proteins are expressed surrounding phloem in Arabidopsis, common bean and soybean (Pélissier *et al*., 2004; Schmidt *et al*., 2004; Pélissier and Tegeder, 2007; Collier and Tegeder, 2012). In most cases, remobilized N translocated to young tissues through phloem sap (Masclaux-Daubresse *et al*., 2010), thus it is highly likely that allantoate is also remobilized through pheloem sap (Fig. I-16). Although allantoate accumulated in siliques, allantoate was hardly observed in seeds (Fig. I-9). In ureide-transporting legumes, large quantity of ureides is transported to pod wall where ureide catabolism occurs and the ammonia is re-assimilated into amino acids (reviewed by Tegeder, 2014). Therefore, like legume plants, Arabidopsis might use allantoate as N source for pod formation, rather than as N storage substance.

In this study, we investigated whether purine catabolism works as functional N recycling metabolism using Arabidopsis mutants defective in ureide degradation and transport. The results of this study suggest that purine catabolism is required for efficient N utilization, and coordinated allantoate biosynthesis and transport is possible mechanism for N recycle and remobilization by purine catabolism.

Table I-1. Nutrient contents in culture solution.

	2 mM N	20 mM N
NH_4NO_3 (mM)	1.00	10.00
KCl	9.39	9.39
$CaCl_2 \cdot 2H_2O$	1.50	1.50
$MgSO_4 \cdot 7H_2O$	0.75	0.75
KH_2PO_4	0.62	0.62
H_3BO_3	0.05	0.05
MnSO4·5H2O	0.05	0.05
$ZnSO4 \cdot 7H_2O$	0.015	0.015
KI	0.0025	0.0025
$Na_2MoO_4 \cdot 2H_2O$	0.00059	0.00059
$CuSO_4 \cdot 5H_2O$	0.00005	0.00005
$CoCl \cdot 6H_2O$	0.00005	0.00005
Na_2-EDTA	0.05	0.05
$FeSO4 \cdot 7H_2O$	0.05	0.05
Thiamin Hydrichloride	0.0007	0.0007
Nicotinic acid	0.0020	0.0020
Pridoxine hydrochloride	0.0012	0.0012
Glycine	0.013	0.013
myo-inositol	0.278	0.278

Table I-2. Nucleotide sequneces of primers used in this study.

AGI code	Gene symbol	Direction	Sequence (Designation)	Use
At4g20070	AAH	Forward	5'-CTTTTGTGCTCCATTGAACGAAAGC-3'	RT-qPCR
		Reverse	5'-AACAACATTCCCACCTTGGTTAAGTGT-3'	RT-qPCR
At3g18780	ACT2	Forward	5'-ACCGTATGAGCAAAGAAATCAC-3'	RT-qPCR
		Reverse	5'-GAGGGAAGCAAGAATGGAAC-3'	RT-qPCR
At4g04955	ALN	Forward	5'-CCTGGTCTCATTGATGTGCATGTTC-3'	RT-qPCR
		Reverse	5'-TGTTTTTCGCAGCTTCAATCTTGAGT-3'	RT-qPCR
AT2g28390	MON1	Forward	5'-AACTCTATGCAGCATTTGATCCACT-3'	RT-qPCR
		Reverse	5'-TGATTGCATATCTTTATCGCCATC-3'	RT-qPCR
AT4g27960	UBC9	Forward	5'-TCACAATTTCCAAGGTGCTGC-3'	RT-qPCR
		Reverse	5'-TCATCTGGGTTTGGATCCGT-3'	RT-qPCR
At2g03590	UPS1	Forward	5'-TCATTGCTTCTCTAGAAACCCA-3' (F1)	PCR genotyping
		Reverse	5'-TCTGCTCGGACCTATTTCTCC-3' (R1)	PCR genotyping
		Forward	5'-GGATCCATTGAAGGAAGAGTTAC-3'	RT-qPCR
		Reverse	5'-CCAATTGTTGTTAGCAAAGCC-3'	RT-qPCR
At2g03530	UPS2	Forward	5'-GGTATCGTGCTTAGCCTCGGGAATC-3' (F2)	PCR genotyping
		Reverse	5'-GCTGGAGAGAAGAGGGAGAAAC-3' (R2)	PCR genotyping
		Forward	5'-GACTGGAATGGTCGTTACTGG-3'	RT-qPCR
		Reverse	5'-AGCCTGAACGGAGTCAGCA-3'	RT-qPCR
At4g34890	XDH1	Forward	5'-TGATGTTGGACAAATAGAAGGAGCGTTT-3'	RT-qPCR
		Reverse	5'-TATTCGGATTCCCCTTGAGAAGCGAAACA-3'	RT-qPCR
−	T-DNA (LBa1)	−	5'-TGGTTCACGTAGTGGGCCATCG-3'	PCR genotyping
	T-DNA (SAIL LB1)	−	5'-GCCTTTTCAGAAATGGATAAATAGCCTTGCTTCC-4'	PCR genotyping

Table I-3. The effect of disruption of ureide degradation on leaf size.

	WT	*aln-1*	*aln-2*	*aah*
Leaf length (mm)	31.2 ± 0.9	26.6 ± 1.2 **	27.8 ± 1.0 *	27.0 ± 1.2 **
Leaf width	15.8 ± 0.4	14.8 ± 0.5	14.9 ± 0.4	14.7 ± 0.7
Petiole length	18.0 ± 0.6	12.4 ± 0.6 ***	14.8 ± 0.5 ***	9.9 ± 0.8 ***

The biggest leaf in individual 5-week-old plant were selected by naked eyes. Length of leaf blades and petioles, and width of leaf blades was measured by the scale. *$P < 0.05$, **$P < 0.01$, ***$P < 0.001$ ($n \geq 9$, Student's *t*-test).

Table I-4. Nitrogen (N) contents, Nitrogen use efficiency (NUE) and Carbon: Nitrogen ratio (C/N) in 9-week-old plants. □

	WT	aln-1	aln-2	aah
N (%)	3.39 ± 0.13	4.45 ± 0.13 **	4.10 ± 0.04 **	4.09 ± 0.15 *
NUE	29.65 ± 1.14	22.53 ± 0.65 **	24.38 ± 0.26 *	24.55 ± 0.89 *
C/N	11.60 ± 0.57	8.60 ± 0.27 **	9.23 ± 0.22 **	8.89 ± 0.38 **

*P < 0.05, **P < 0.01 (n = 4, Student's t-test). □

Table I-5. Phytophormone contents in 5-week-old plants.

	WT	aln-1	aln-2	aah
Phytohormone (ng g^{-1} DW)				
ABA	78.6 ± 3.2	90.8 ± 6.4	113.2 ± 3.3 **	86.2 ± 8.1
JA	99.5 ± 60.8	86.0 ± 26.9	188.0 ± 71.1	132.5 ± 57.9
JA-Ile	5.4 ±2.3	6.6 ±1.6	13.9 ±1.0*	6.9 ±1.6
IAA	180.7 ±2.4	402.8 ±72.3	718.3 ±64.5*	264.5 ±40.2
GA_4	2.3 ±0.5	4.6 ±0.5*	5.4 ±0.2**	3.4 ± 0.2
SA	3198.3 ± 134.9	3926.3 ±1134.5	2862.8 ±245.5	3985.3 ±343.3
tZ	10.8 ±0.5	7.6 ±1.1	6.4 ±1.1*	7.8 ±1.3
iP	1.6 ±0.1	2.6 ± 0.4	2.2 ±0.3	1.7 ±0.4

*P < 0.05, **P < 0.0 (n ≥ 9, Student's t-test).

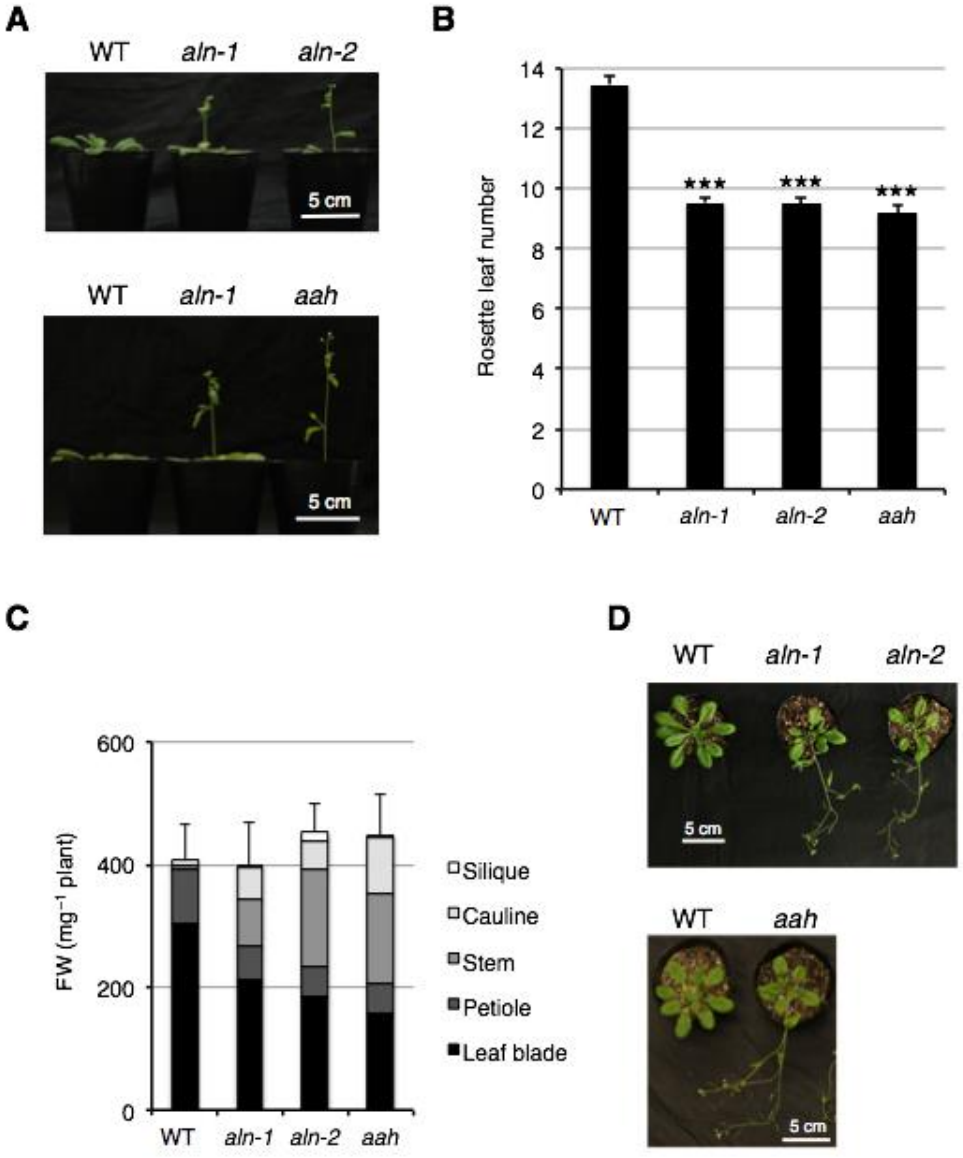

Figure I-1. Early flowering phenotype of mutants defective in ureide degradation. Seeds of WT, *aln-1*, *aln-2* and *aah* were directly sown on soil, and plants were grown under long day conditions (16h light and 8h dark). (A) Representatives of 4-week-old plants. Bar = 5 cm. (B) The number of rosette leaves when the primary inflorescence (about 1 cm) were detected ($n \geq 32$). (C) Biomass of rosette leaves, petioles, stems, cauline leaves and siliques obtained from 5-week-old plants ($n \geq 9$). FW, fresh weight. (D) Representatives of 5-week-old plants. Asterisks denote significant differences between WT and mutant plants (***$P < 0.001$ by Student's *t*-test).

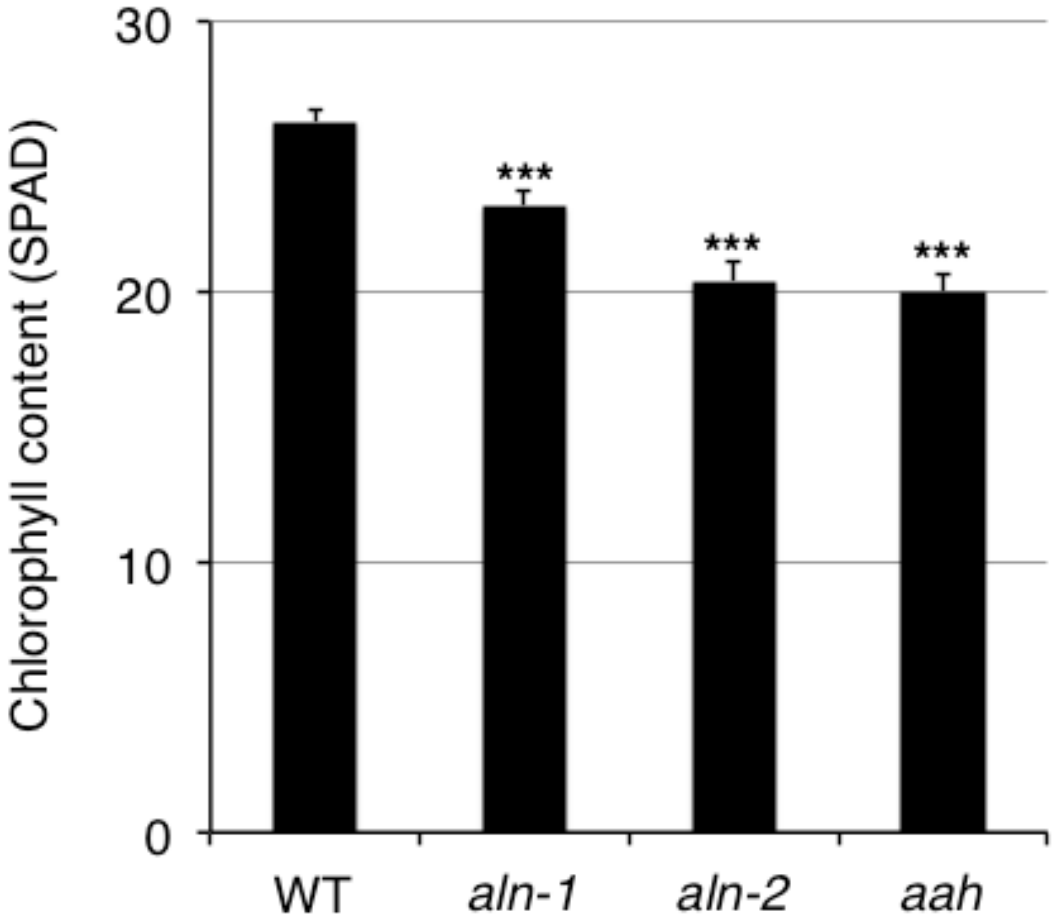

Figure I-2. Chlorophyll contents (SPAD units) in 4-week-old rosette leaves.
***$P < 0.001$ ($n \geq 15$, Student's *t*-test).

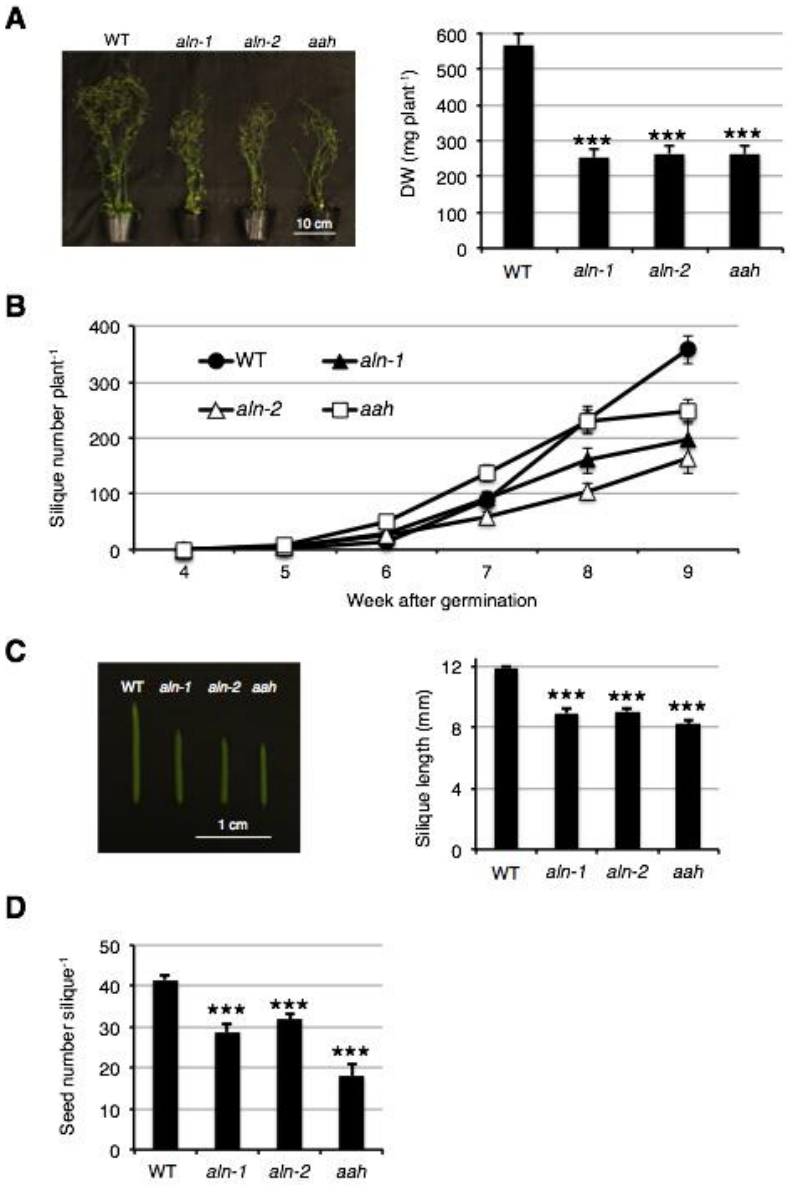

Figure I-3. Reduced growth and fertility of mutants defective in ureide degradation. (A) Reduced growth of 9-week-old plants. Bar = 10 cm. DW was measured at 9 WAG. DW, dry weight ($n \geq 15$). (B) The number of siliques in 4- to 9-week-old plants. (C) The length of siliques detached from 9-week-old plants ($n = 10$). (D) The number of seeds in siliques detached from 9-week-old plants ($n = 10$). Asterisks denote significant differences between WT and mutant plants (***$P < 0.001$ by Student's *t*-test).

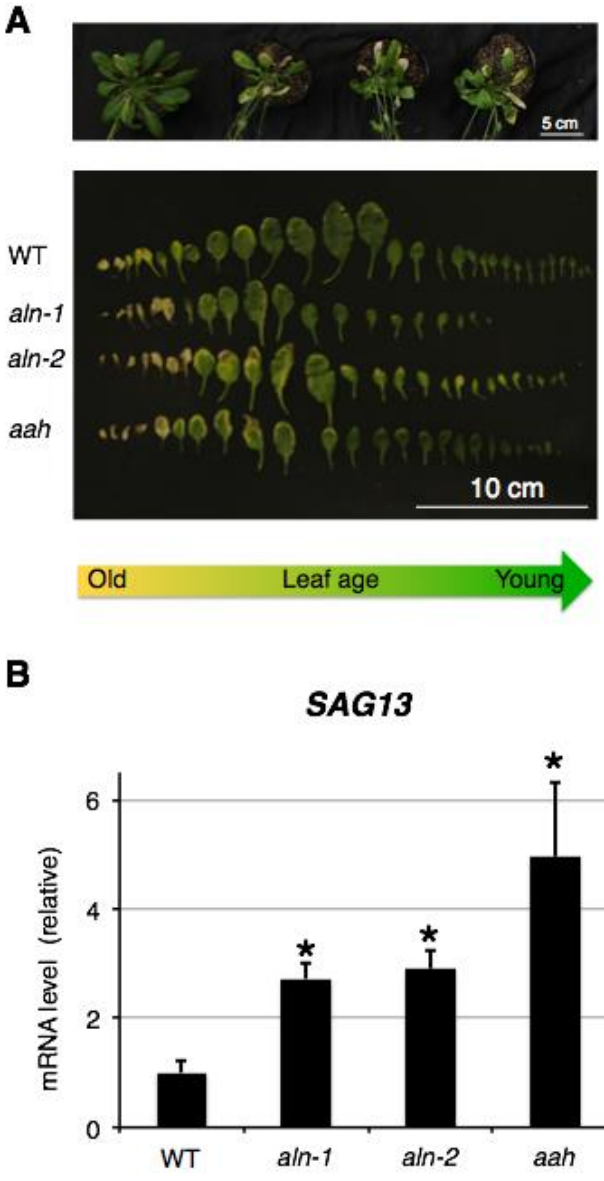

Figure I-4. Accelerated leaf senescence of mutants defective in ureide degradation.
(A) Representatives of 9-week-old WT, *aln-1*, *aln-2* and *aah* leaves. (B) *SAG13* expression levels. RNA was extracted from all leaves detached from 7-week-old plnats grown on soil. Relative mRNA levels were determined using *ACT2* expression as reference and presented as values relative to those of WT (n = 3). Asterisks denote significant differences between WT and mutant plants (*$P < 0.05$ by Student's t-test).

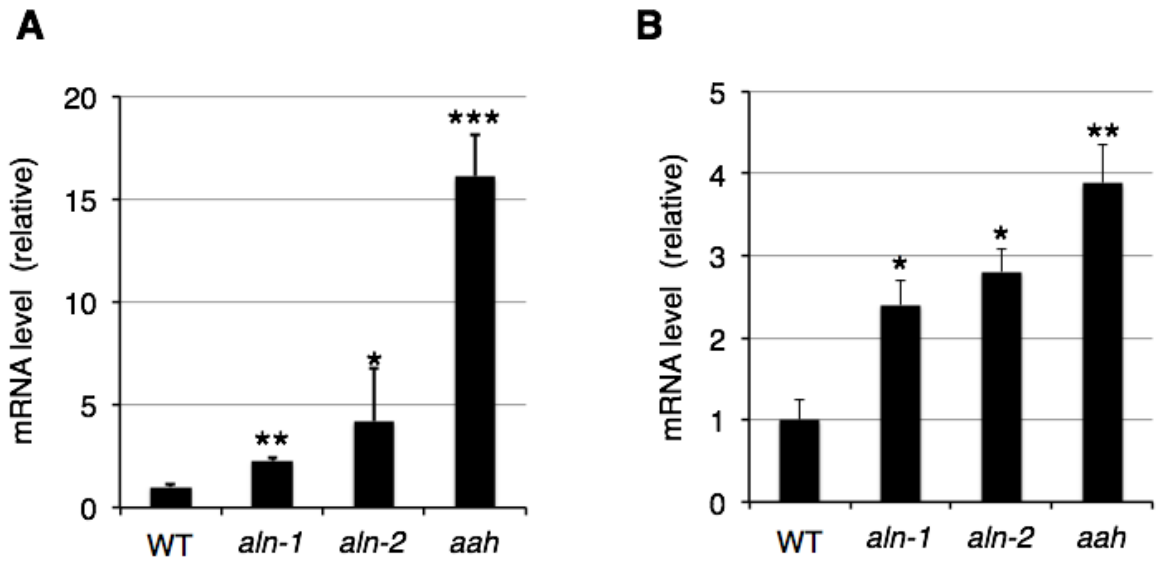

Figure I-5. Relative *SAG13* expression levels determined using *UBC9* (A) or *MON1* (B) expression as reference.
Data are presented as values relative to those of WT ($n = 3$). Asterisks denote significant differences between WT and mutant plants (*$P < 0.05$; **$P < 0.01$; ***$P < 0.001$ by Student's *t*-test).

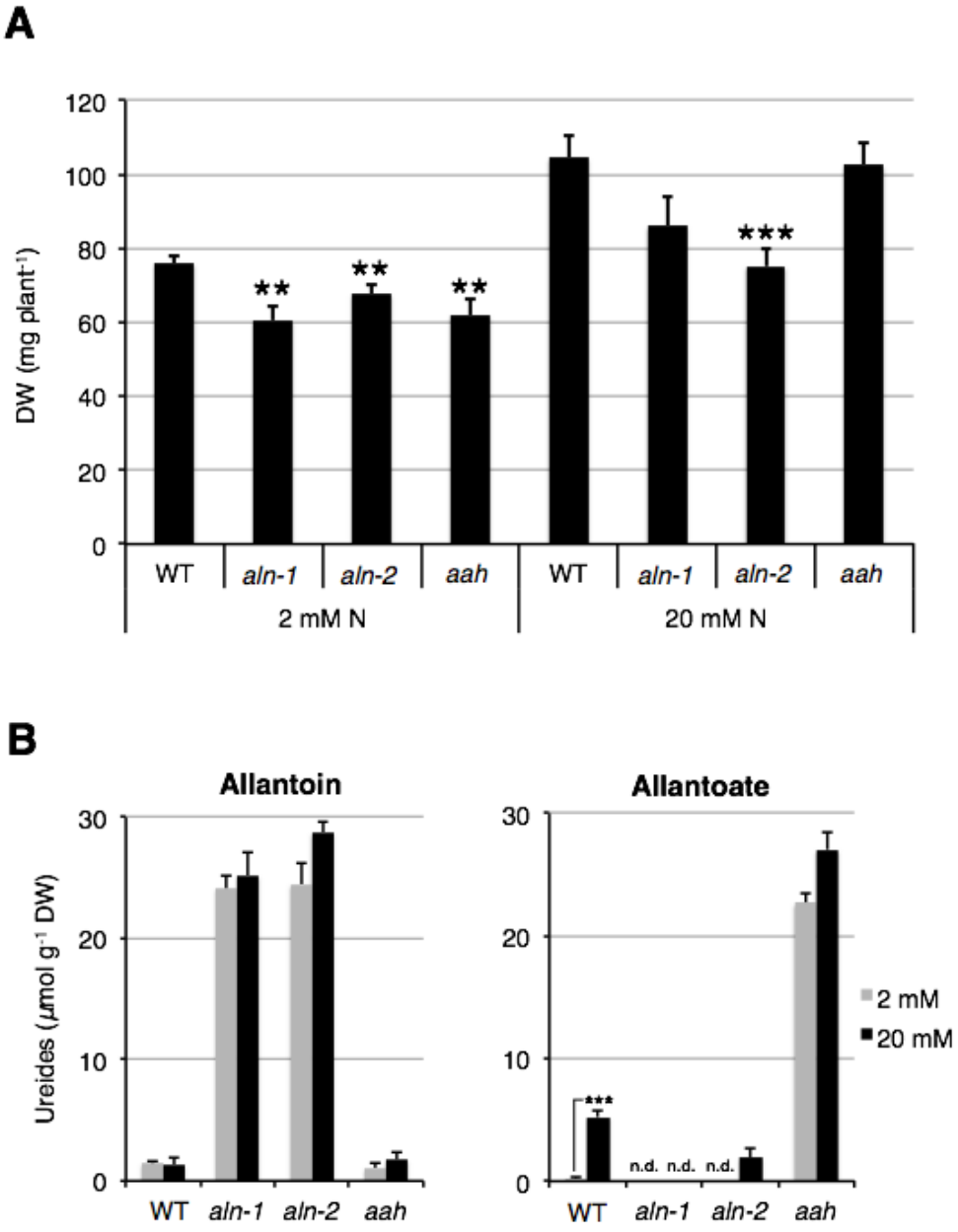

Figure I-6. Effect of N deficiency on plant growth and ureide contents.
Seeds of WT, *aln-1, aln-2* and *aah* were directly sown half-strength MS medium, and 2-week-old plants were transplanted on vermiculite:perlite (1.5:1). (A) Aerial parts were collected 4 weeks after transplanting, and biomass was measured ($n = 16$). (B) Crude extractions for ureide measurements were obtained from freeze-dried whole shoots. DW and n.d indicate dry weight and not detected, respectively ($n = 3$). Asterisks denote significant differences between WT and mutant plants (**$P < 0.01$; ***$P < 0.001$ by Student's *t*-test).

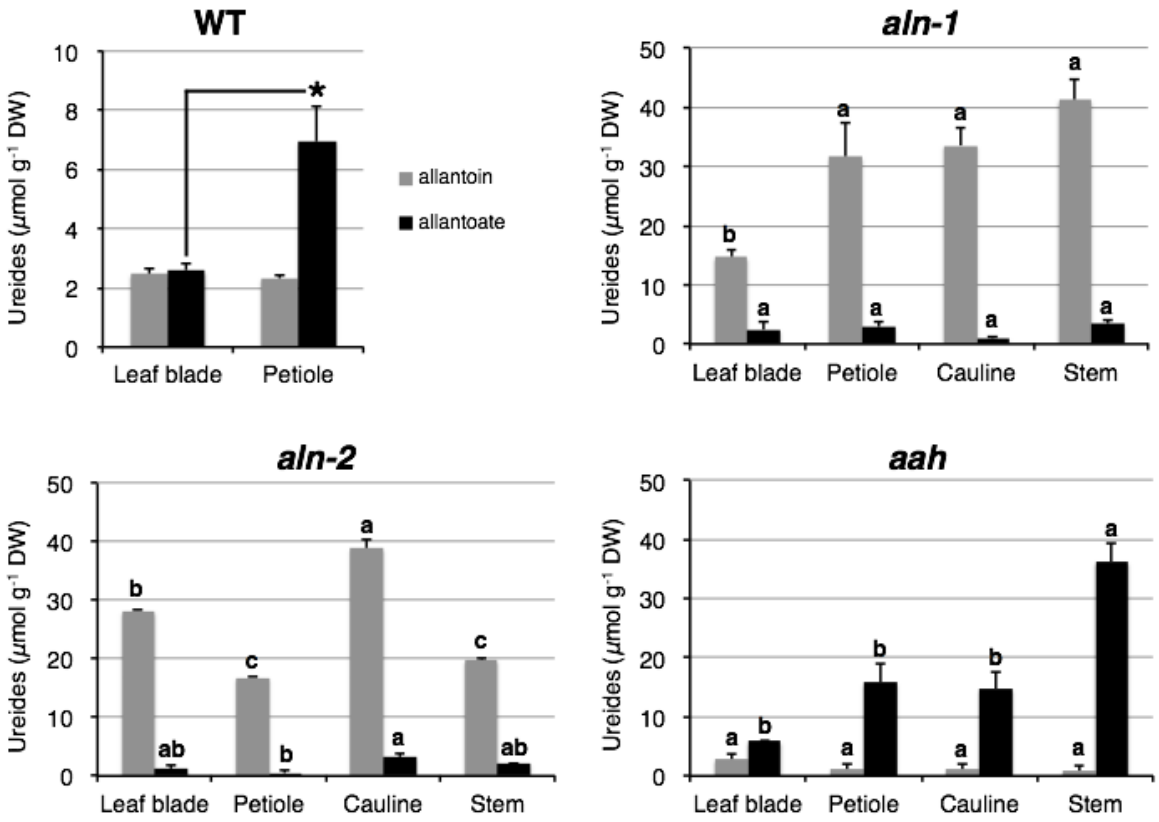

Figure I-7. Ureide concentration in different parts obtained from 5-week-old plants. Five-week-old WT, *aln-1*, *aln-2* and *aah* plants were cut into leaf blades, petioles, cauline leaves and stems. Crude extractions were obtained from freeze-dried samples. DW, dry weight. Different letters indicate significant difference ($n = 3$, Tukey's test). Asterisks denote significant differences between WT and mutant plants (*$P < 0.05$ by Student's *t*-test).

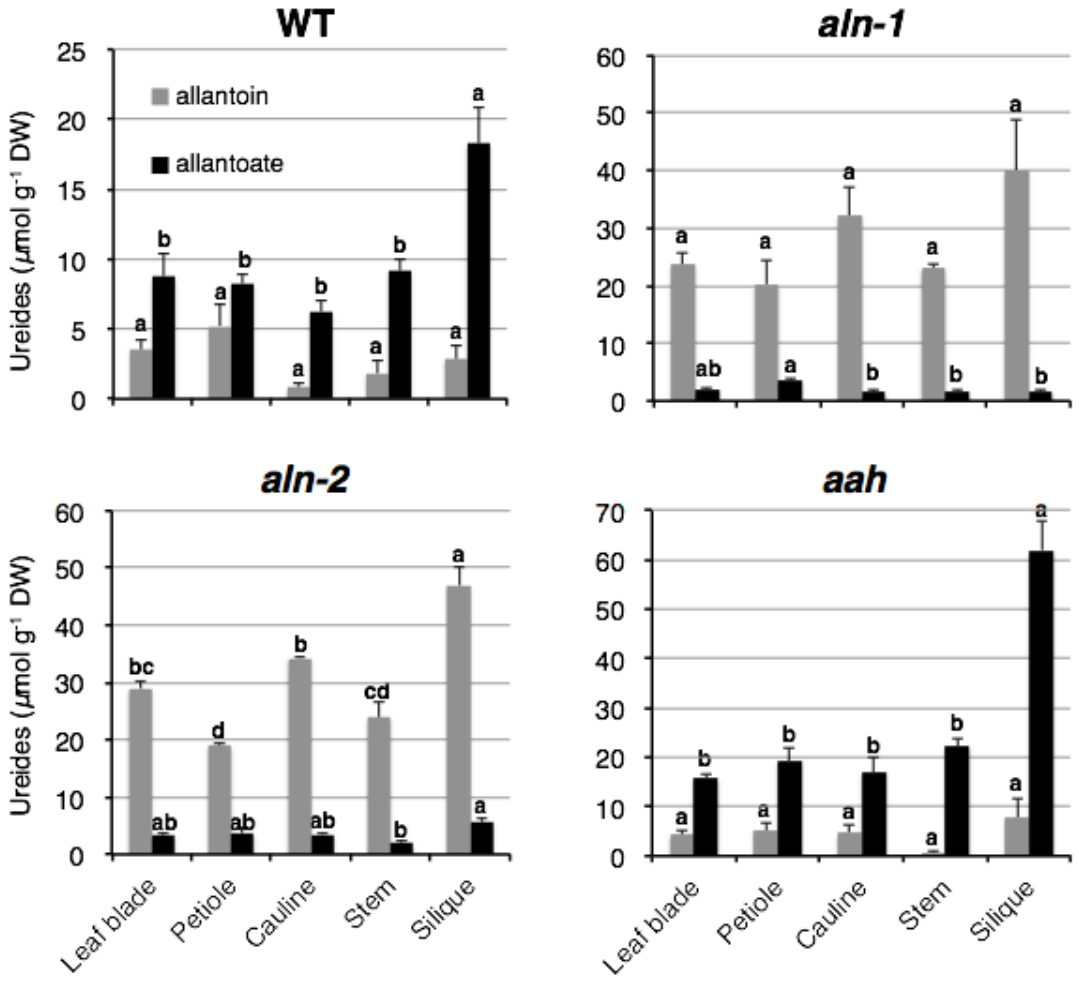

Figure I-8. Ureide concentration in different parts obtained from 9-week-old plants. WT, *aln-1*, *aln-2* and *aah* plants were cut into leaf blades, petioles, cauline leaves, stems and siliques. Crude extractions were obtained from freeze-dried tissues. DW, dry weight. Different letters indicate significant difference (n = 3, Tukey's test).

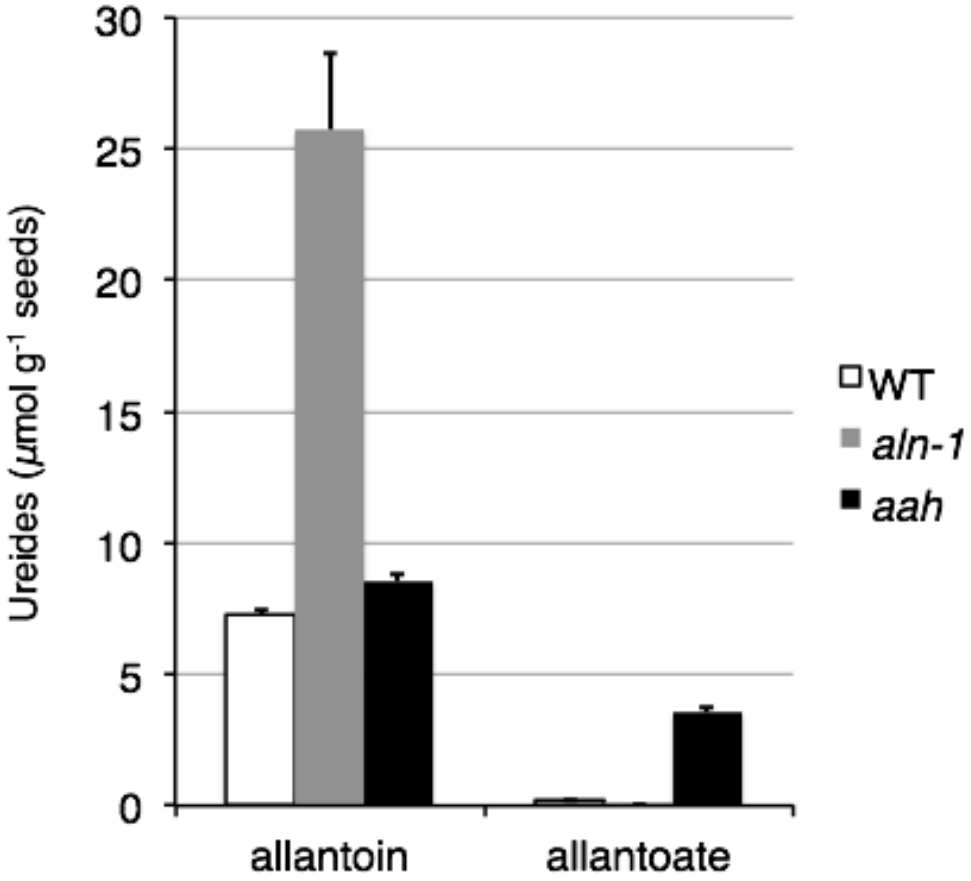

Figure I-9. Ureide concentration in matured seed.

Crude extractions were obtained from bulked seeds (*n* =3).

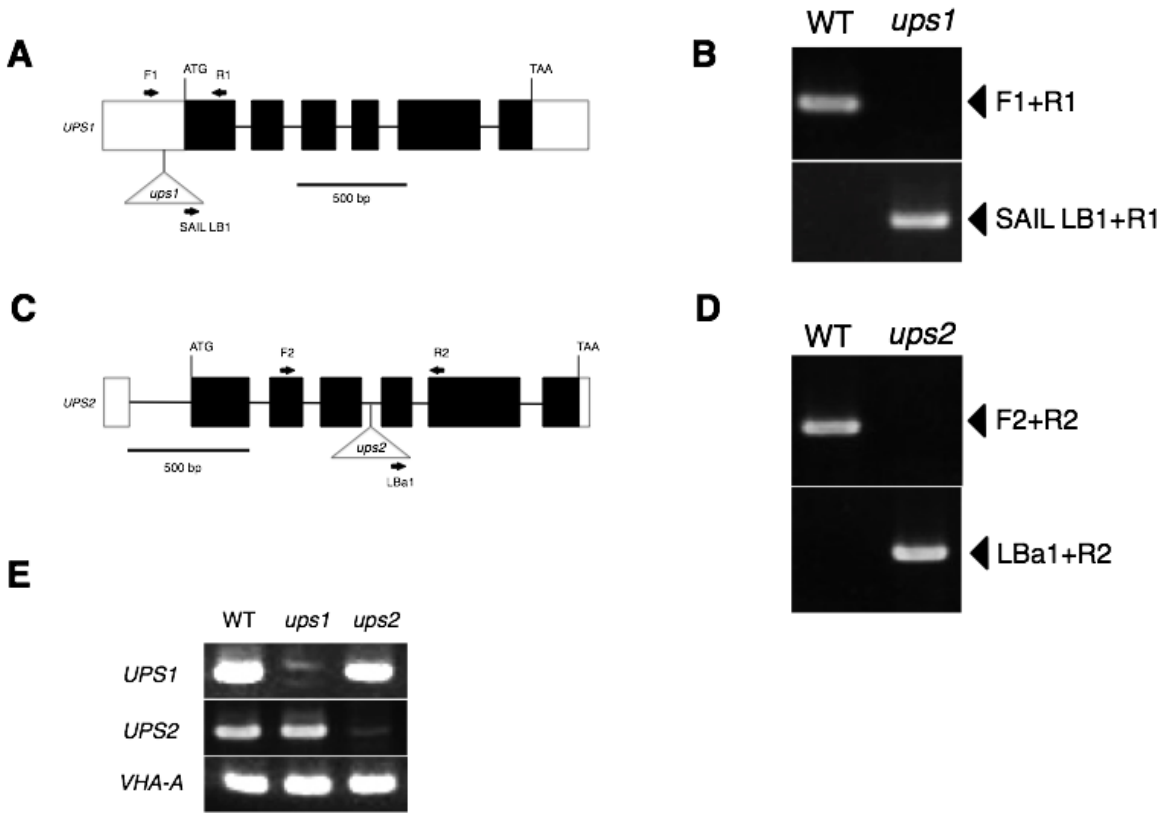

Figure I-10. Characterization of the *ups1* and *ups2* mutant.
(A) Diagram of T-DNA insertion in the *UPS1* gene structure for the *ups1* mutant. Arrows denote PCR primers. (B) PCR-based genotyping of the *ups1* mutant using primers specific to UPS1 (F1 and R1) and the left border sequence of T-DNA (SAIL LB1). (C) Diagram of T-DNA insertion in the *UPS2* gene structure for the *ups2* mutant. Arrows denote PCR primers. (D) PCR-based genotyping of the *ups1* mutant using primers specific to UPS1 (F2 and R2) and the left border sequence of T-DNA (LBa1). (E) Semi-quantitative RT-PCR for estimating *UPS1* and *UPS2* mRNA levels in the mutant lines. *VHA-A* expression was simultaneously analyzed as internal control (Nakagawa *et al*. 2007).

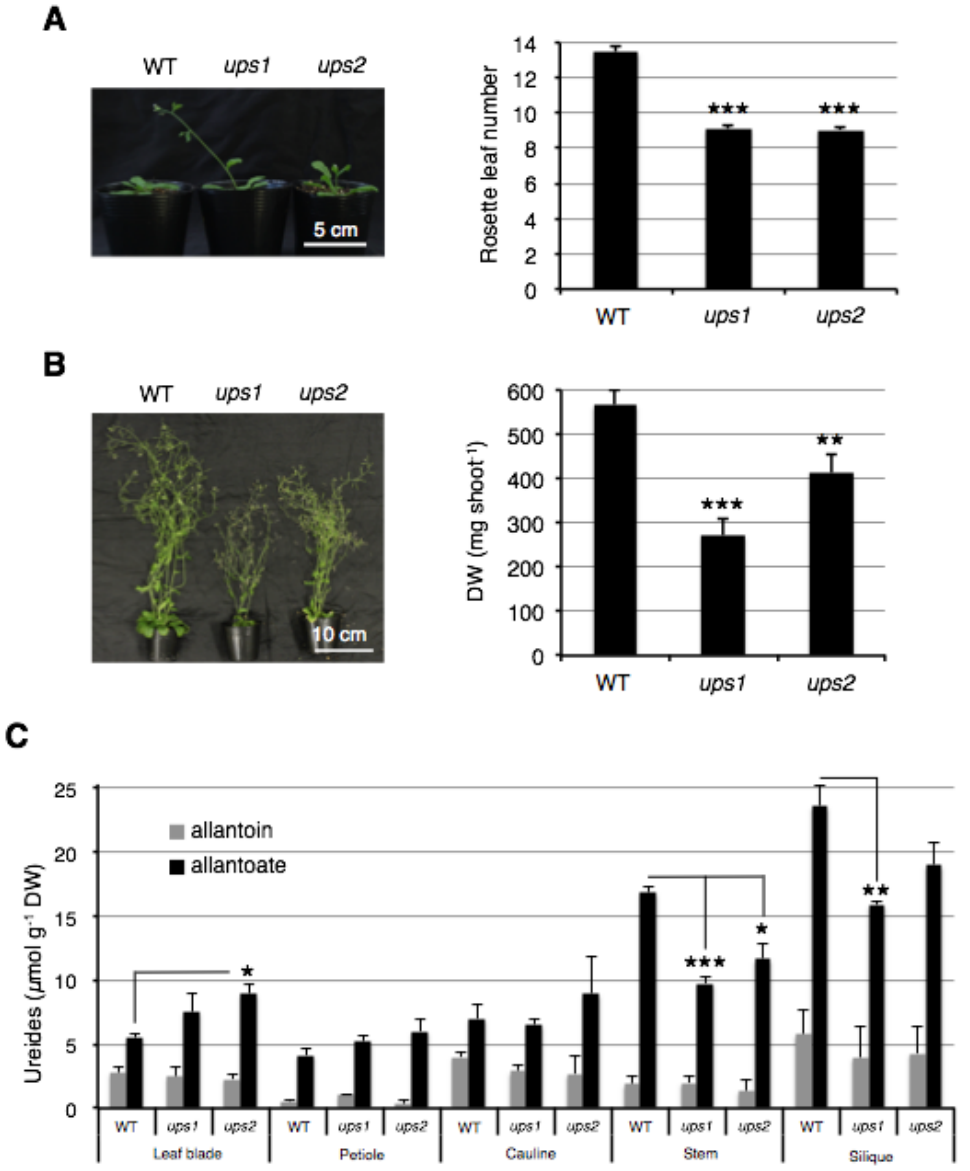

Figure I-11. The effects of disruption of ureide permease (UPS) on plant growth and ureide concentration.
(A) Early flowering of the *ups1* and *ups2* mutants. The number of rosette leaves when the primary inflorescence (about 1 cm) was detected ($n \geq 28$). (B) Biomass of 9-week-old plants ($n \geq 12$). (C) The ureide concentration in different plant parts. Seven-week-old WT, *ups1*, and *ups2* plants were cut into rosette leaves, petioles, cauline leaves, stems and siliques. Crude extractions were obtained from freeze-dried tissues. DW, dry weight ($n = 3$). Asterisks denote significant differences between WT and mutant plants (*$P < 0.05$; **$P < 0.01$; ***$P < 0.001$ by Student's *t*-test).

Figure I-12. Representatives of 7-week-old mutants defective in ureide transport.

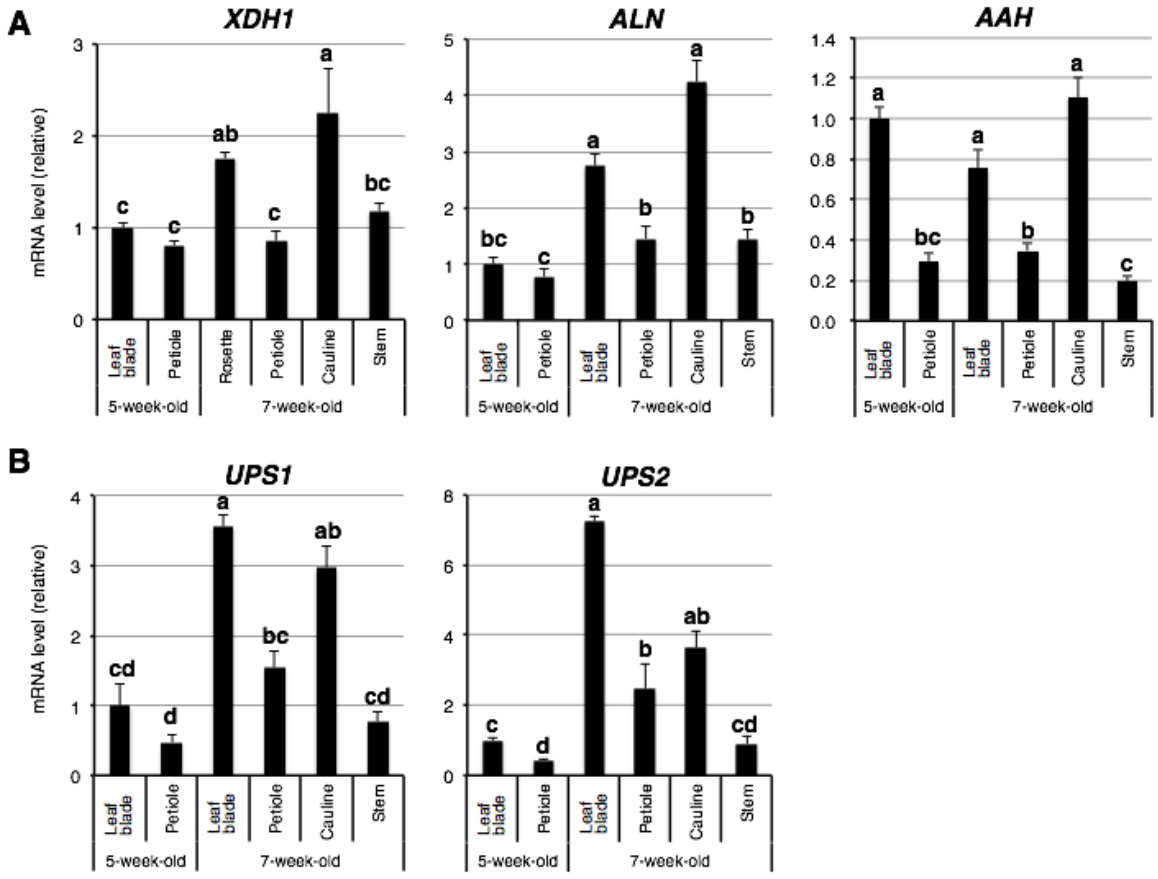

Figure I-13. Effect of senescence progression on the expression of genes for purine catabolism and ureide transport.
(A) Purine catabolic genes: *XDH1*, *ALN* and *AAH*, and (B) ureide transporting gene: *UPS1* and *UPS2*. RNA was extracted from different parts obtained from 5- and 7-week-old plnats grown on soil. Relative mRNA level were determined using *ACT2* expression as reference, and presented as values relative to those of 5-week-old lead blade. Different letters indicate significant difference (n = 3, Tukey's test).

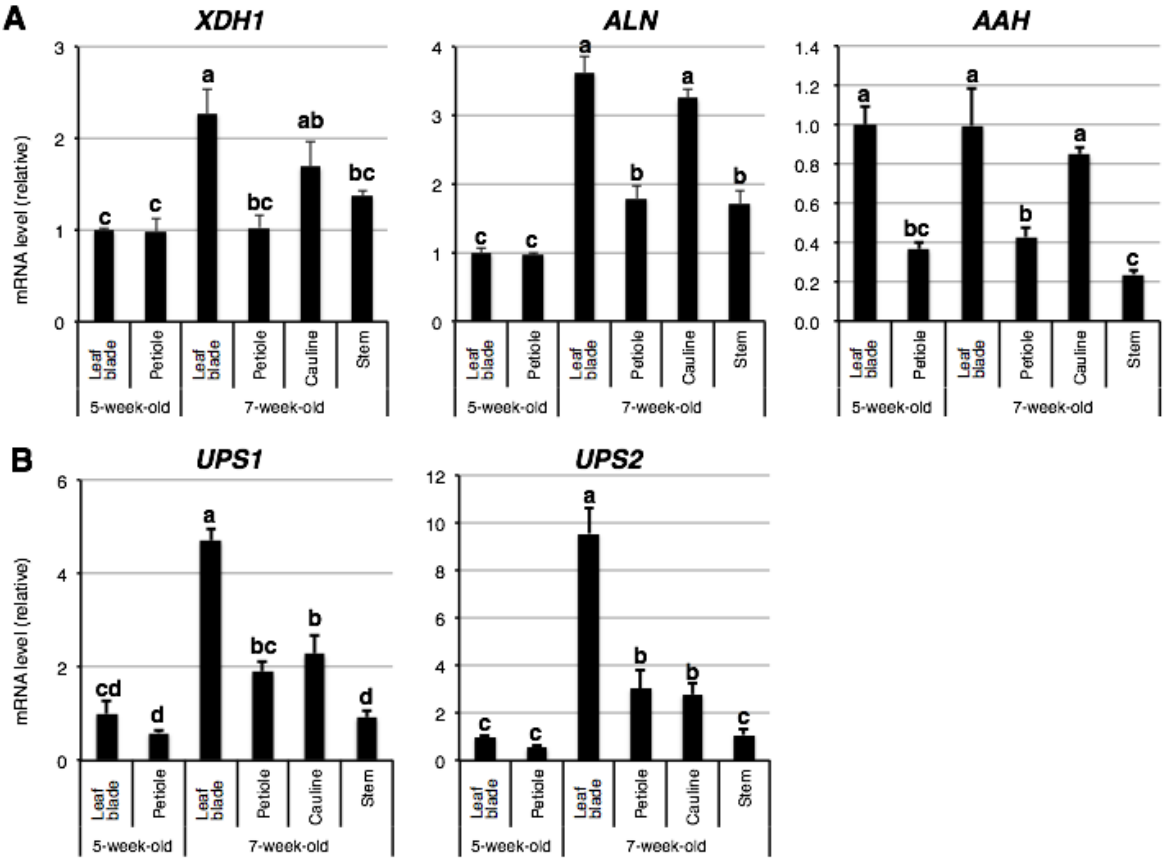

Figure I-14. Relative mRNA levels determined using *UBC9* expression as reference. (A) Purine catabolic genes: *XDH1*, *ALN* and *AAH*, and (B) ureide transporting gene: *UPS1* and *UPS2*. RNA was extracted from different plant parts obtained from 5- and 7-week-old plnats grown on soil. Data are presented as values relative to those of 5-week-old leaf blade. Different letters indicate significant difference (n = 3, Tukey's test).

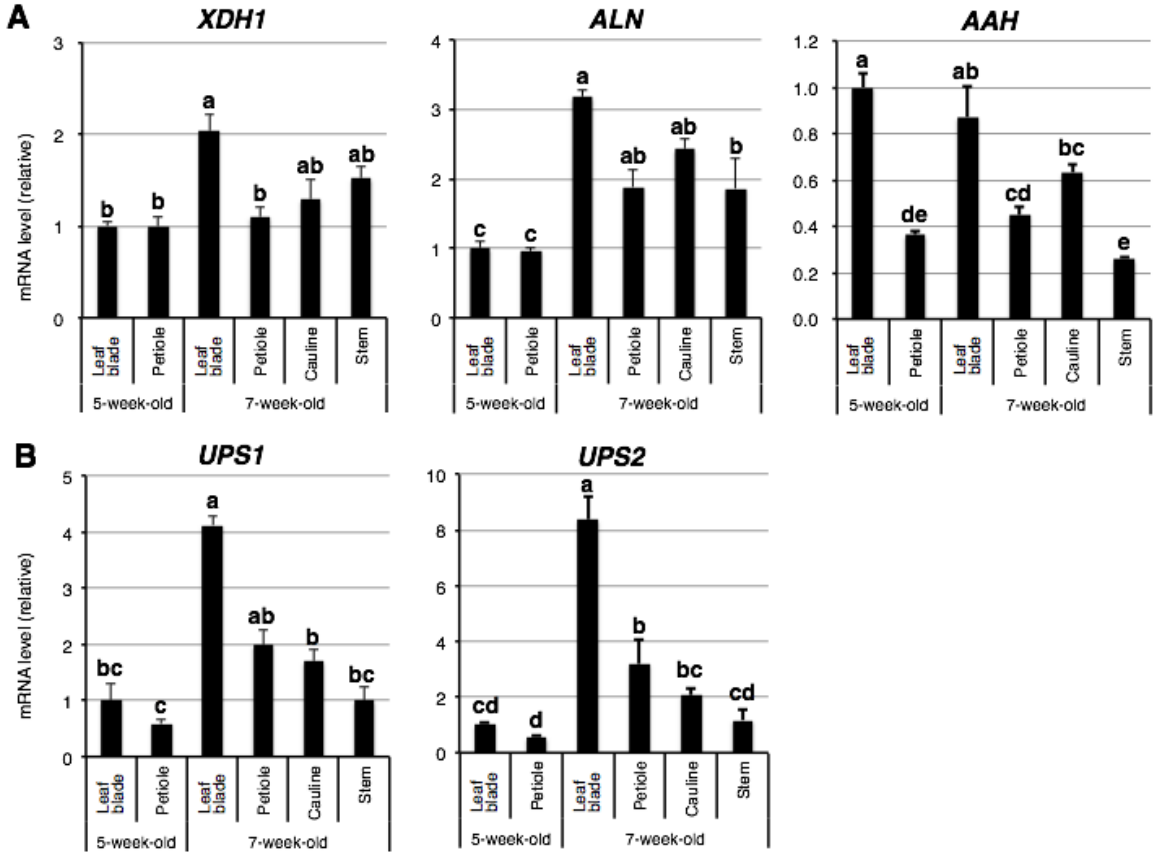

Figure I-15. Relative mRNA levels determined using *MON1* expression as reference. (A) Purine catabolic genes: *XDH1*, *ALN* and *AAH*, and (B) ureide transporting gene: *UPS1* and *UPS2*. RNA was extracted from different plant parts obtained from 5- and 7-week-old plnats grown on soil. Data are presented as values relative to those of 5-week-old leaf blade. Different letters indicate significant difference (n = 3, Tukey's test). Different letters indicate significant difference (n = 3, Tukey's test).

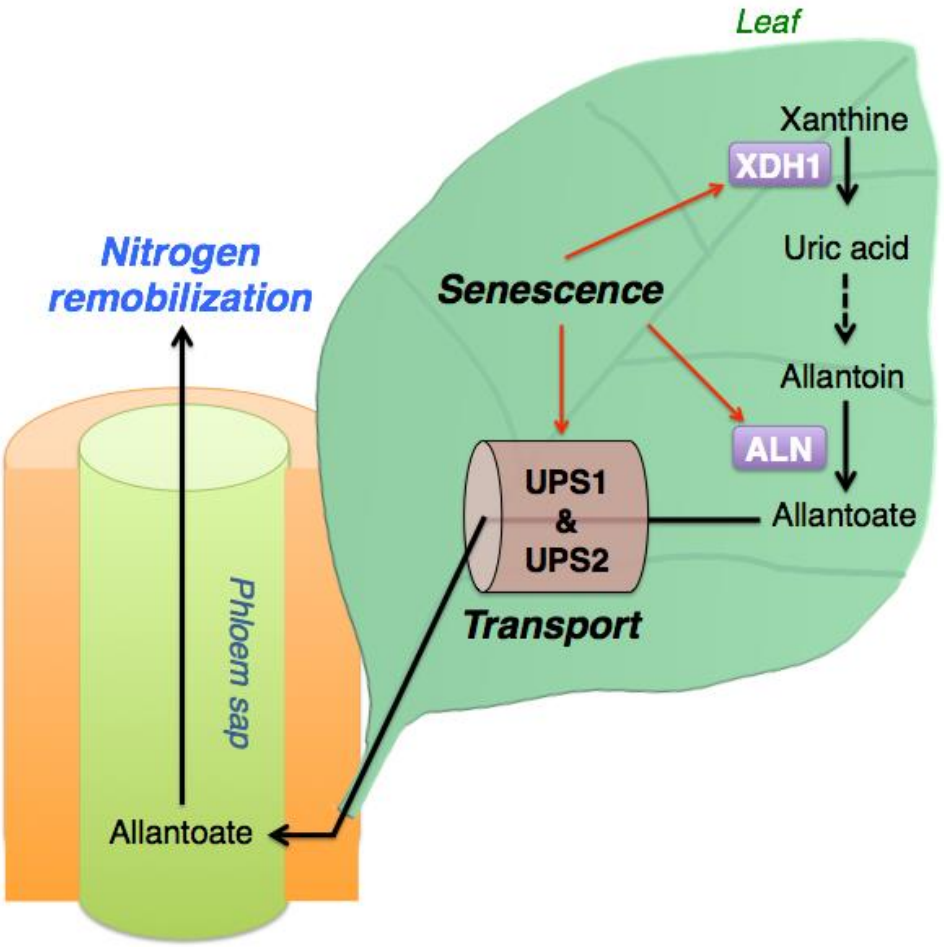

Figure I-16. Model for N remobilization by purine catabolism.
Senescence induces *XDH1*, *ALN*, *UPS1* and *UPS2* expression in leaves, resulting in activation of allantoate biosynthesis and transport. Allantoate may be transported to upper plant parts via pheloem sap, and used as N source.

CHAPTER II

Allantoin, a stress-related purine metabolite, can activate jasmonate signaling in a MYC2-regulated and abscisic acid-dependent manner

Introduction

Plants have evolved a complex diversity of metabolic pathways to maintain and improve their growth and survival in natural environments, including stressful conditions. Plants confronted with stressful conditions typically accumulate an amazing array of small organic compounds, including metabolic products and intermediates. Numerous *in vitro* and *in vivo* studies have shown that various small metabolites serve specialized functions in cellular protection, such as scavenging ROS, osmoregulation, stabilization of protein structure, and maintenance of membrane integrity (Chen and Murata, 2002). Certain small metabolites also play signaling and regulatory roles in mediating plant responses and adaptation to stress (see, for example, Szabados and Savouré, 2010; Wind *et al*., 2010; Hussain *et al*., 2011; Lunn *et al*., 2014). However, the physiological function and significance of the accumulation of many stress-associated small compounds remain elusive.

Allantoin, a N-rich heterocyclic compound, occurs ubiquitously in plants as an intermediary metabolite of purine catabolism. Allantoin and its acyclic metabolite allantoate are collectively called ureides and, in tropical legumes, they serve as the vehicle for storage and xylem transport of symbiotically fixed N (Smith and Atkins, 2002). In non-legume plants, purine catabolism is believed to function as a fundamental route for N recycling and remobilization,

since the sequential degradation of the purine ring, which initiates from oxidation of xanthine, proceeds through ureide hydrolysis and releases four molar equivalents of ammonia (Zrenner *et al*., 2006; Werner and Witte, 2011). However, conventional metabolite analyses and recent metabolomics studies revealed allantoin as a major purine metabolite in Arabidopsis, rice (*Oryza sativa* L.), and other species under various stress conditions such as drought (Oliver *et al*., 2011; Silvente *et al*., 2011; Yobi *et al*., 2013), high salinity (Kanani *et al*., 2010; Wu *et al*., 2012; Wang *et al*., 2016), cold (Kaplan *et al*., 2004), nutrient constraint (Nikiforova *et al*., 2005; Rose *et al*., 2012; Coneva *et al*., 2014), extended darkness (Brychkova *et al*., 2008), and pathogen invasion (Montalbini, 1991).

The possible involvement of allantoin in stress protection was initially suggested from studies on *XDH* knockout/knockdown mutants (*xdh1* and RNAi lines) of Arabidopsis. In these mutants, defects in xanthine oxidation resulted in significantly impaired stress tolerance, as well as stress-induced symptoms such as early senescence (Nakagawa *et al*., 2007; Brychkova *et al*., 2008; Watanabe *et al*., 2010, 2014a). The stress-susceptible *xdh* phenotype might be at least in part attributable to purine metabolite deficiency, because supplementation with allantoin or its precursor uric acid, a product of XDH, reversed the mutant phenotype. Recent studies on knockout mutants (*aln*) of the Arabidopsis *ALN* provided more direct evidence; the *aln* mutants showed constitutive accumulation of allantoin and enhanced seedling survival and growth under drought and osmotic stress (Watanabe *et al*., 2014b). Allantoin may function in stress protection by scavenging ROS; indeed, leaf disc assays showed that exogenous allantoin alleviated ROS accumulation and cell death (Brychkova *et al*., 2008). Allantoin may also activate stress responses, as its accumulation in *aln* mutants or supplementation of WT seedlings increased

basal levels of the stress phytohormone ABA, with concomitant activation of stress-related gene expression (Watanabe *et al*., 2014b).

ABA has pivotal roles in plant growth and adaptive responses to various environmental stresses, mostly through antagonistic, synergistic, and additive interactions with other phytohormones such as JA, SA, and ethylene. ABA, in particular, has long been known to regulate JA responses positively. JA and its metabolites, such as the bioactive metabolite JA-Ile, are collectively known as jasmonates; the jasmonates regulate diverse aspects of plant development and defense responses to insect herbivores and microbial pathogens (Wasternack and Hause, 2013). The complex interplay of the ABA and JA pathways controls defense gene expression in response to biotic stress. Early studies in potato and tomato plants reported that ABA elicits wounding responses and wound-inducible JA production (Pēna-Cortés *et al*., 1989, 1995). Recent studies in Arabidopsis demonstrated that ABA can increase JA levels in disease conditions, and activate JA signaling for systemic induced resistance against herbivores (Adie *et al*., 2007; Fan *et al*., 2009; Vos *et al*., 2013).

In Arabidopsis, the JA signaling pathway consists of two antagonistically acting branches, the ABA-co-regulated MYC branch and the ethylene-co-regulated ETHYLENE RESPONSE FACTOR (ERF) branch. The MYC branch responds to herbivore feeding and mechanical wounding, and is controlled by the basic helix–loop–helix leucine zipper transcription factors MYC2/3/4 (Anderson *et al*., 2004; Fernández-Calvo *et al*., 2011; Niu *et al*., 2011). The ERF branch responds to infection with necrotrophic pathogens and is controlled by the APETALA2 (AP2)/ERF domain transcription factors ERF1 and *OCTADECANOID-RESPONSIVE ARABIDOPSIS AP2/ERF 59* (ORA59) (Penninckx *et al*., 1998; Lorenzo *et al*., 2004; Pré *et al*., 2008). ABA

acts synergistically on the MYC branch and antagonistically on the ERF branch pathways (Anderson *et al*., 2004).

The effects of ABA on these branches are mediated, at least in part, through transcriptional regulation by the ABA/JA-responsive MYC2 transcription factor [also known as JAI1/JIN1] (Anderson *et al*., 2004; Kazan and Manners, 2013). Originally identified as a positive regulator of ABA-dependent drought responses (Abe *et al*., 1997), MYC2 orchestrates the expression of early JA-responsive genes that play key roles in JA signaling and responses. While activating herbivore and wounding responses, MYC2 acts as a negative regulator of resistance to necrotrophic pathogens by repressing ERF1 and ORA59 (Lorenzo *et al*., 2004; Dombrecht *et al*., 2007). MYC2 also suppresses SA-dependent defenses against biotrophic pathogens and innate immune responses (Laurie-Berry *et al*., 2006; Millet *et al*., 2010). In addition to its antagonistic co-ordination of biotic stress responses to herbivores and pathogens, MYC2 also participates in regulation of a broad spectrum of JA-related responses, including the biosynthesis of JA and anthocyanin, JA-induced root growth inhibition, and oxidative stress tolerance (Lorenzo *et al*., 2004; Dombrecht *et al*., 2007; Kazan and Manners, 2013; Wasternack and Hause, 2013). Thus, MYC2 is considered a master regulator of most aspects of the JA signaling pathway as well as a hub that integrates ABA and JA signaling.

Given the critical role of JA and its intimate regulatory interaction with ABA in plant stress responses, this study investigated whether allantoin affects JA signaling and responsiveness in Arabidopsis. Detailed phenotypic and transcriptomic analyses of allantoin-accumulating *aln* mutants revealed activation of JA responses at the levels of gene expression, metabolism, physiology, and pathophysiology, in a MYC2-regulated manner. These

JA-related mutant phenotypes involve allantoin because exogenous application of allantoin in WT Arabidopsis plants induced the expression of MYC2 and MYC2-regulated JA-responsive genes. However, disrupting JA signaling or blocking ABA production abrogated the effect of both the *aln* mutation and exogenous allantoin. The results presented here thus provide evidence that allantoin can activate JA responses via ABA, and suggest that purine catabolism may have the potential to affect the homeostasis of these phytohormones and their interplay in stress signaling.

Materials and Methods

Plant materials and growth conditions

Arabidopsis thaliana (L.) Heynh., accession Columbia-0, was used for all experiments. Seeds of the following mutants and T-DNA insertion lines were obtained from the Arabidopsis Biological Resource Center (Ohio State University, Columbus, OH, USA): *aah* (SALK_112631; Todd and Polacco, 2006), *aba2-1* (CS156; Léon-Kloosterziel *et al*., 1996), *aln-1* (SALK_000325; Yang and Han, 2004; Watanabe *et al*., 2014b; also known as *aln*), *aln-2* (SALK_146783; Watanabe *et al*., 2014b), *bglu18* (SALK_075731C; Ogasawara *et al*., 2009), *jar1-1* (CS8072; Staswick *et al*., 1992), *myc2-3* (SALK_061267; identical to *jin1-8* reported in Lorenzo *et al*., 2004), and *xdh1* (SALK_148366; Watanabe *et al*., 2014b). The double mutants *aln-1 bglu18* and *aln-1 jar1-1* were constructed by manual cross-pollination. A homozygous complemented line of *aln-1* (*aln-1 35S:ALN*) was described in our previous study (Watanabe *et al*., 2014b). Under standard conditions, surface-sterilized seeds were sown on solid medium containing half-strength Murashige and Skoog (1/2MS) salts, 1.0% (w/v) sucrose, and 0.3% (w/v) gellan gum. After 2 d at 4 °C to break seed dormancy, plates were placed in a growth chamber maintained at 23 °C under long-day conditions (16h light/8h dark) with 70 μmol photons m^{-2} s^{-1}.

Gene expression analyses

For transcriptome analysis, the previously deposited raw data from the microarray data sets (NCBI Gene Expression Omnibus GSE44922) were

parametrically normalized by the three-parameter lognormal distribution method (Konishi, 2004), using the SuperNORM data service (Skylight Biotech Inc., Akita, Japan). The renormalized data have been deposited under accession number GSE73841. The significance of differentially expressed genes showing ≥ 3-fold changes was statistically tested by a two-way ANOVA with a significance threshold set at 0.001 (Konishi, 2011). Functional enrichment analyses of the Biological Process Gene Ontology (GO) terms were carried out using the BioMaps tool of VirtualPlant version 1.3 (Katari *et al*., 2010; http://virtualplant.bio.nyu.edu/cgi-bin/vpweb/, accessed 22 February 2016) in the default-setting mode (Fisher's exact test with false discovery rate correction, $P < 0.01$), with the Arabidopsis genome annotation (TAIR release 10; https://www.arabidopsis.org/, accessed 22 February 2016) as the background.

For quantitative transcript analysis, samples of aerial parts were collected from 2-week-old seedlings that were grown aseptically on solid 1/2MS medium with or without added allantoin (Wako Pure Chemical Industries, Ltd, Osaka, Japan) or allantoic acid (Carbosynth Limited, Berkshire, UK). RNA extraction and RT-qPCR were performed as described previously (Watanabe *et al*., 2014b). Relative gene expression levels were calculated by the $2^{-\Delta\Delta Ct}$ method (Livak and Schmittgen, 2001) after normalization to *ACT2* expression levels. Primer sequences for target genes are listed in Table II-1.

Quantification of jasmonic acid (JA) and JA-Ile

Extraction and quantification of JA and JA-Ile were performed following the method of Preston *et al*. (2009) with minor modifications. The stable isotope-labeled compounds used as internal standards were: [$^2H_2$]JA (Tokyo

Chemical industry Co., Ltd., Tokyo, Japan) and [$^{13}C_6$]JA-Ile, which was synthesized with [$^{13}C_6$]Ile (Cambridge Isotope Laboratories, Andover, MA, USA) as described in Jikumaru *et al*. (2004). Aerial parts (500 mg) from 2-week-old seedlings grown aseptically on solid half-strength MS medium were frozen in liquid N_2, ground, and extracted with 80% (v/v) methanol containing 1% (v/v) acetic acid at 4°C for 1 h. After removal of cell debris by centrifugation, the supernatants were condensed and dried *in vacuo*, and the resultant residues were extracted twice with methanol. The extracts were evaporated to dryness and resuspended with 80% methanol containing 1% acetic acid and internal standards, which were again evaporated and then extracted with water acidified with 1% (v/v) acetic acid. The extracts were loaded onto pre-equilibrated Oasis HLB column cartridge (Waters Corporation, Milford, MA, USA). After washed with water acidified with 1% acetic acid, the column was eluted with 80% (v/v) acetonitrile containing 1% (v/v) acetic acid. The eluted samples were evaporated to obtain extracts in water acidified with 1% acetic acid, and loaded onto a pre-equilibrated Oasis MCX column cartridge (Waters). The cartridge was washed with water acidified with 1% acetic acid and eluted with 80% acetonitrile containing 1% acetic acid. The eluate was loaded onto pre-equilibrated Oasis WAX column cartridges (Waters) followed by washing, first with water acidified 1% acetic acid and then with 80% acetonitrile, and the fraction containing JA and JA-Ile was eluted with 80% acetonitrile containing 1% acetic acid. The obtained fraction was dried and reconstituted in ultra-pure water acidified with 1% (v/v) acetic acid for quantification of JA and JA-Ile by liquid chromatography-electrospray ionization-tandem mass spectrometry (LC-ESI-MS/MS) on an Agilent 6410 Triple Quadrupole system with a ZORBAX Eclipse XDB-C18 column and MassHunter software version

B.01.02 (Agilent Technology, Palo Alto, CA, USA). The LC column was eluted with a binary solvent system of 0.01% (v/v) acetic acid in water (solvent A) and 0.05% (v/v) acetic acid in acetonitrile (solvent B) using a linear gradient of solvent B in solvent A, from 3% to 50%, in 20 min at the flow rate of 0.4 ml min^{-1}. The MS/MS operation parameters are summarized in Table II-2.

Metabolite analyses

Anthocyanin was extracted from the aerial parts of 8-day-old seedlings with methanol acidified with 1% (v/v) hydrochloric acid, and the anthocyanin level was calculated based on the absorbance at 530 nm and 657 nm according to Teng *et al*. (2005). Allantoin was determined in 2-week-old seedlings as described previously (Watanabe *et al*., 2014b).

Root growth inhibition assay

Seeds were surface sterilized and sown onto square plates of solid 1/2MS medium containing methyl jasmonate (MeJA) (Sigma-Aldrich, St Louis, MO, USA). Square plates were set vertically in a growth chamber and, 8 d after germination, the length of each primary root was measured using ImageJ version 1.45 (http://rsbweb.nih.gov/ij/, accessed 22 February 2016).

Wounding treatment

All rosette leaves of 2-week-old aseptically grown seedlings were wounded mechanically once by crushing with tweezers. Aerial parts of the

plants were collected at the indicated time after wounding and then quick-frozen in liquid N for RNA extraction.

Pathogen inoculation

Surface-sterilized seeds were germinated and grown on 0.3% (w/v) Phytagel-solidified 1/2MS medium at 24 °C under a photoperiod of 12h light/12h dark with a light intensity of 150–200 μmol photons m^{-2} s^{-1}. Two weeks after germination, seedlings were used for evaluation of resistance to *Pseudomonas syringae* pv. *tomato* (*Pst*) strain DC3000 according to Ishiga *et al*. (2011) and to *Pectobacterium carotovorum* subsp. *carotovorum* (*Pcc*) EC1 as described in Higashi *et al*. (2008). For *Pst* DC3000, seedlings were inoculated by flooding with a bacterial suspension [5×10^6 colony-forming units (CFU) ml^{-1}]. At 48h and 96h post-inoculation (hpi), aerial parts were collected. After being surface sterilized with 5% (v/v) H_2O_2, samples were homogenized in sterile water to recover internal bacteria and, upon appropriate dilution, bacterial populations were determined by colony formation on MG agar medium containing rifampicin. For infection with *Pcc* EC1, intact leaves were drop-inoculated with 5 μl of a bacterial suspension in 0.9% (w/v) NaCl; this suspension was pre-adjusted to a 600 nm optical density of 0.01. The levels of disease symptoms were categorized as: level 0, no symptoms; level 1, symptoms restricted within the inoculated region; level 2, symptoms extended outside of the inoculated region.

Statistical analyses

All data are shown as means ± SE. Means of two groups were compared by Student's *t*-test at a 5% level of significance with Microsoft Excel. Means of three or more groups were compared by Tukey's multiple comparison test, which was performed with IBM SPSS statistic, version 21.0 (IBM, New York, NY, USA). Statistical difference of *Pcc* EC1 resistance was tested with Fisher's exact test using RStudio (version 0.98; https://www.rstudio.com/, accessed 22 February 2016).

Accession numbers

Arabidopsis Genome Initiative numbers for the genes mentioned in this article are as follows: *AAH*, At4g20070; *ABA2*, At1g52340; *ACT2*, At3g18780; *ALN*, At4g04955; *ANAC019*, At1g52890; *ANAC055*, At3g15500; *ANAC072*, At4g27410; *AOC1*, At3g25760; *AOS*, At5g42650; *BGLU18*, At1g52400; *BSMT1*, At3g11480; *CYP94B3*, At3g48520; *ERF1*, At3g23240; *ICS1*, At1g74710; *JAM1*, At2g46510; *JAR1*, At2g46370; *JAZ1*, At1g19180; *JAZ3*, At3g17860; *JAZ5*, At1g17380; *JAZ6*, At1g72450; *JAZ7*, At2g34600; *JAZ10*, At5g13220; *JAZ12*, At5g20900; *LOX2*, At3g45140; *LOX3*, At1g17420; *LOX4*, At1g72520; *MYC2*, At1g32640; *OPR3*, At2g06050; *ORA59*, At1g06160; *PDF1.2a*, At5g44420; *PDF1.2b*, At2g26020; *PR-1*, At2g14610; *SAGT1*, At2g43820; *VSP1*, At5g24780; and *XDH1*, At4g34890.

Results

The aln *mutants show increased expression of ABA- and JA-responsive genes and decreased expression of SA-related genes*

Previous work reported that normally grown 2-week-old *aln* mutant (*aln-1*) seedlings exhibited genome-wide alterations in the levels of transcripts associated with stress responses, with increased expression of ABA-responsive genes. Although not conspicuous in the GO analysis (Table 1 of Watanabe *et al*., 2014b), the *aln* mutants also showed increased expression of JA response signatures including genes involved in JA metabolism and signaling, such as *13-LIPOXYGENESE* (*LOX*) and *JASMONATE ZIM-DOMAIN* (*JAZ*) *PROTEINS* (Supplementary Table S2 of Watanabe *et al*., 2014b). For this reason, and to improve the interpretation of the transcriptome profiles, the first step in this study was to renormalize these microarray data according to a three-parameter lognormal distribution model (Konishi, 2004). This refinement of the data resulted in identification of 324 genes (211 increased, Table II-3; 113 reduced, Table II-4) with a significant change of at least 3.0-fold in their transcript levels ($P < 0.001$). The physiological and functional aspects of these differentially expressed genes were assessed by GO enrichment analysis for biological process terms using VirtualPlant software ($P < 0.01$). As shown in Fig. II-1 as a hierarchical tree graph, 21 out of 47 of the significantly enriched GO terms for genes with increased transcript levels were relevant to the 'response to stimulus' category, which included genes associated with ABA and abiotic stress responses ('response to abscisic acid stimulus' and 'response to abiotic stimulus' along with its eight descendant GO terms), and also genes associated with JA-related stress responses

('response to jasmonic acid stimulus', 'response to wounding', 'defense response to fungus', and 'response to biotic stimulus'). Moreover, 'jasmonic acid metabolic process' was identified as significantly enriched in the 'cellular process' category. For genes with reduced transcript levels, more than half (20 out of 33) of the significantly enriched GO terms belonged to three related categories ('response to stimulus', 'multi-organism process', and 'immune system process'), which emphasized biotic defense responses mainly involving SA, such as innate and acquired immunity (Fig. II-2). This downward shift in basal expression levels of SA-responsive genes was confirmed by RT-qPCR of the canonical SA-marker *PATHOGENESIS-RELATED PROTEIN 1* (*PR-1*) (Fig. II-3). Taken together, the results of re-examining the transcriptome profiling suggested that the *aln* mutation caused increased transcript levels of ABA- and JA-responsive genes but decreased transcript levels of SA-related genes at the seedling stage under normal growth conditions.

The aln *mutants show altered basal expression of* MYC2 *and MYC2-regulated genes in JA metabolism, signaling, and responses*

Next, mapping of the relevant microarray-derived expression data onto the current model of the MYC2-modulated JA signaling pathways was conducted to obtain a more detailed picture of JA-associated gene expression in the *aln-1* mutant (Kazan and Manners, 2013), with emphasis on the crosstalk with ABA and SA (Fig. II-4A). In the ABA-co-regulated MYC branch, this mapping revealed a significant increase in basal expression levels of two of the three genes encoding ANAC (Arabidopsis NAM/ATAF/CUC) transcription factors, ANAC019, ANAC055, and ANAC072, immediate target genes positively

regulated by MYC2 (Bu *et al*., 2008). Transcript levels of downstream MYC branch marker genes that these ANAC transcription factors regulate, positively or negatively, also showed major changes. Genes with increased transcript levels included the marker *VEGETATIVE STORAGE PROTEIN 1* (*VSP1*) along with *SABATH METHYLTRANSFERASE* (also known as *BSMT1*) and *SALICYLIC ACID GLUCOSYLTRANSFERESE* (*SAGT1*), both of which encode SA-inactivating enzymes. Genes with decreased transcript levels included *ISOCHORISMATE SYNTHASE 1* (*ICS1*), which encodes an SA biosynthetic enzyme. For ERF branch genes, markedly reduced basal expression was observed for the key transcription factor gene *ORA59* whose expression is negatively regulated by MYC2 (Dombrecht *et al*., 2007), and the ORA59 downstream target and representative ERF branch marker *PLANT DEFENSIN 1.2* (*PDF1.2a* and *PDF1.2b*). Overall, the altered expression of these JA and SA markers was in accordance with the known modes of MYC2 action on its direct and downstream target genes.

MYC2 also acts as a transcriptional activator of JA-responsive genes encoding JA metabolic enzymes such as LOX, allene oxide synthase (AOS), allene oxide cyclase (AOC), 12-oxophytodienoate reductase (OPR), jasmonate-amido synthetase (also known as JASMONATE RESISTANCE 1; JAR1), and cytochrome P450 monooxygenase 94B3 (CYP94B3) (Lorenzo *et al*., 2004; Sasaki-Sekimoto *et al*., 2013). MYC2 also activates genes encoding JA signaling components including JAZ and JASMONATE-ASSOCIATED MYC2-LIKE1 (JAM1) repressor proteins (Chini *et al*., 2007; Nakata *et al*., 2013; Sasaki-Sekimoto *et al*., 2013). As shown by microarray analysis (Fig. II-4B), the basal expression levels of most of these genes significantly increased in the *aln-1* mutant. This was confirmed by RT-qPCR for selected genes (*LOX3*, *LOX4*, *AOS*, *OPR3*, *JAZ3*, *JAZ10*, and *MYC2*) using a separate

set of RNA samples from those used for microarray analysis (Fig. II-4C). The RT-qPCR clearly demonstrated the significant activation of MYC2 expression, although the microarray analysis only showed a modest increase in the MYC2 transcript level (Fig. II-4A, B). Genetic complementation of the *aln-1* mutant with the WT *ALN* cDNA (*aln-1 35S:ALN*) resulted in the reversion of the transcript levels of all these genes to the normal WT levels, corroborating the effect of the mutation.

The increased expression of these JA-responsive genes could be caused by general inhibition of the purine catabolic pathway, rather than by the specific blockage of allantoin degradation. To exclude this possibility, two other knockout mutations, *xdh1* and *aah* were examined which impair the metabolic steps upstream and downstream of allantoin degradation, respectively. The basal expression levels of JA-responsive genes in *xdh1* and *aah* mutants were comparable with or lower than those of the WT (Fig. II-4C), supporting the idea that the *aln* mutation preventing allantoin degradation was indeed responsible for the observed gene expression phenotype.

The aln *mutants have increased levels of endogenous JA and JA-Ile*

Based on the observation that expression of genes involved in JA metabolism was significantly increased in the *aln-1* mutant (Fig. II-4B, C), endogenous JA and JA-Ile levels were measured in the WT and the mutant by LC-ESI-MS/MS (Fig. II-4D). The concentrations of JA and JA-Ile in WT seedlings (4.0 ± 0.6ng g^{-1} FW and 0.22 ± 0.12ng g^{-1} FW, respectively) were similar to those reported previously (Pan *et al*., 2010). Compared with WT seedlings, the *aln-1* mutant showed a 2-fold increase in JA levels and a 6-fold increase in JA-Ile levels. This increase in jasmonates correlated with the

observed expression profiles (Fig. II-4B, C), suggesting that the *aln* mutation promotes jasmonate accumulation in normally grown Arabidopsis seedlings, probably through the transcriptional activation of JA biosynthetic genes.

The aln *mutants show enhanced sensitivity to exogenous jasmonate*

In addition to JA biosynthesis, MYC2 also positively regulates jasmonate-induced root growth inhibition and anthocyanin production (Dombrecht *et al*., 2007). To determine whether the *aln* mutants show increased activation of these MYC2-modulated JA responses, the sensitivity of the WT, *aln-1* mutants, and the complemented line to exogenous MeJA was tested. When these genotypes were grown for 8 d on medium containing MeJA, they seemed to develop lateral roots well (Fig. II-5A), probably reflecting the stimulatory effect of MeJA (Raya-González *et al*. 2012). Simultaneously, the *aln-1* seedlings showed a slight but statistically significant reduction in primary root length, compared with the WT and the complemented mutant (Fig. II-5B). However, when the *aln* mutation was introduced into the JA-insensitive *jar1-1* mutant, which is defective in JA-Ile production (Staswick *et al*., 1992), the resultant *aln-1 jar1-1* double mutant displayed no change in root growth in the presence of MeJA (Fig. II-6). Similar to the results of root growth inhibition, the *aln-1* mutant responded more strongly than the WT to exogenous MeJA in anthocyanin production, further increasing its anthocyanin accumulation in response to MeJA treatment (Fig. II-5C). Conversely, the complemented line was the least responsive to MeJA treatment as it had lower levels of anthocyanin than the WT and the *aln-1* mutant. The *aah* mutant also compromised the metabolic response to MeJA (Fig. II-7). These results support the idea that the *aln*

mutation enhances the MYC2-mediated physiological and metabolic responses to JA.

The aln *mutants show enhanced wounding-inducible expression of JA-responsive genes*

Next, this study investigated whether the *aln* mutation has a stimulatory effect on MYC2-mediated JA responses under stress conditions known to activate the JA signaling pathway. Wounding stress strongly enhances the transcript levels of genes involved in JA biosynthesis and signaling in a MYC2-dependent manner (Reymond *et al*., 2000; Lorenzo *et al*., 2004; Chung *et al*., 2008). Thus, the expression of these JA-responsive genes (*LOX3*, *LOX4*, and *OPR3* for JA biosynthesis and *JAZ3* and *JAZ10* for JA signaling) was monitored in wounded leaves of 2-week-old seedlings (Fig. II-8). Although the transcripts for these genes accumulated in response to wounding, in all cases the maximum levels were significantly higher in the mutant than in the WT, possibly reflecting the increased basal expression levels. The complemented mutant showed essentially the same transcript expression profiles as those observed in the WT. These results suggest that the *aln* mutation activates the MYC2-mediated JA response in normal growth conditions and under JA-associated stress conditions.

The aln *mutation affects basal resistance to* Pseudomonas syringae *DC3000*

MYC2 negatively regulates the SA signaling pathway and suppresses SA-mediated host defenses against the bacterial pathogen *Pst* DC3000 (Nickstadt *et al*., 2004; Laurie-Berry *et al*., 2006). Because the gene

expression data described above suggested that the *aln* mutation led to attenuation of SA signaling through activation of MYC2 (Figs II-2, II-3, II-4A), the resistance of two *aln* mutant alleles, *aln-1* and *aln-2*, to *Pst* DC3000 was examined by monitoring bacterial growth in inoculated seedlings (Fig. II-9A). At 48 hpi, bacterial growth was evident in both the WT and the mutants, but the *aln-2* mutants had significantly more bacteria (11-fold, $P<0.05$) than the WT. Although not statistically significant, the same tendency was observed in the *aln-1* mutant (a 9-fold higher population; $P=0.068$). At 96 hpi, bacterial populations showed further increases, but no longer differed between the WT and the *aln* mutants. Simultaneous monitoring of expression of the SA marker *PR-1* during the course of infection with *Pst* DC3000 gave overall results consistent with those of the infection experiments, as induction of *PR-1* expression was compromised in the *aln-1* and *aln-2* mutants (Fig. II-9B). These results suggest that the *aln* mutation reduced the resistance to *Pst* DC3000 at early stages of pathogen infection, probably due to constitutive activation of the MYC branch of JA signaling.

The aln *mutation suppresses basal resistance against* Pectobacterium carotovorum

MYC2 down-regulates the ERF branch of JA signaling, which is critical for Arabidopsis resistance to phytopathogens such as *Pcc* EC1 (Norman-Setterblad *et al*., 2000; Hiruma *et al*., 2011). To test if the *aln* mutation altered resistance to this bacterium, *Pcc* EC1 was drop-inoculated onto intact leaves of 2-week-old seedlings and disease symptoms were evaluated at 24 hpi. As shown in Fig. II-9C, the *aln-1* and *aln-2* mutants had compromised resistance to *Pcc* EC1, showing a significantly higher proportion

of level 2 (most serious) symptoms and a lower proportion of level 0 (no detectable) symptoms, compared with the WT. The complemented *aln-1* mutant plants showed substantially recovered disease resistance, with a proportion of level 2 symptoms non-significantly different from the WT. The expression levels of the disease resistance gene *PDF1.2a*, a marker of the ERF branch, were also examined at early stages of infection (0, 3, and 6 hpi). As expected from the enhanced susceptibility to *Pcc* EC1, the *aln* mutants showed consistently lower levels of *PDF1.2a* expression compared with the WT (Fig. II-9D). For unknown reasons, complementation of the *aln-1* mutant failed to restore *PDF1.2a* expression to the WT levels, which might explain why the resistance of the complemented mutant to *Pcc* EC1 was not fully recovered. Nevertheless, these results showed the compromised resistance of the *aln* mutants to *Pcc* EC1, providing more evidence for *aln*-mediated activation of MYC2.

Allantoin activates expression of MYC2 *and MYC2-modulated JA-responsive genes*

To address whether the observed JA-related *aln* phenotype was attributable to the accumulation of allantoin as a result of the *aln* mutation, the effects of exogenous allantoin on expression of MYC2 and the MYC2-modulated JA-responsive genes *LOX3*, *LOX4*, and *OPR3* were examined. When seedlings of the WT were grown aseptically for 2 weeks on standard medium containing 100 μM allantoin, the four genes showed significantly increased transcript levels, compared with the non-treated control (Fig. II-10A). Allantoate, which is similar in structure to allantoin as the immediate downstream metabolite, was also tested. When exogenously

supplied at 100 μM, allantoate did not affect transcript levels, or caused a decrease in transcript levels (Fig. II-10A), further supporting the specific efficacy of allantoin in inducing these JA-responsive genes. These results supported the idea that the JA-related *aln* mutant phenotypes result from accumulation of allantoin.

Allantoin requires ABA to activate JA-responsive genes

To gain insight into how allantoin activates JA-dependent responses, the next step was to investigate the effects of exogenous allantoin on JA-responsive gene expression in the two mutants, JA-insensitive *jar1-1* and MYC2-deficient *myc2-3*. In marked contrast to the WT, both *jar1-1* and *myc2-3* mutants showed no responses to allantoin (Fig. II-10B), demonstrating that the action of allantoin relies on an intact JA signaling pathway and requires the formation of bioactive JA-Ile. Because MYC2 is responsive to ABA (Abe *et al*., 1997), and because ABA levels increase in the *aln* mutants and in response to exogenous allantoin in WT plants (Watanabe *et al*., 2014b), expression of JA-responsive genes was also examined in the ABA-deficient mutants *aba2-1* (*abscisic acid deficient 2-1*) and *bglu18* (*ß-glucosidase 18*), which impair *de novo* ABA synthesis and regeneration of ABA from inactive ABA glucosides, respectively (Léon-Kloosterziel *et al*., 1996; Lee *et al*., 2006; Ogasawara *et al*., 2009). Similar to the JA-insensitive mutants, neither *aba2-1* nor *bglu18* mutants showed increases in the transcript levels of JA-responsive genes in response to exogenous allantoin (Fig. II-10C).

To obtain further evidence supporting this, the next experiments tested if these JA- and ABA-related mutations also suppress the effect of allantoin accumulation in the *aln-1* background. For this, the *aln-1* mutant was crossed

with the *bglu18* mutant to establish the *aln-1 bglu18* double mutant (Fig. II-11), and the transcript levels of seven JA-responsive genes (the same set as reported in Fig. II-4C) were measured in the *aln-1 jar1-1* and *aln-1 bglu18* double mutants. Although these double mutants exhibited allantoin levels comparable with the *aln-1* mutant (Fig. II-12A), the expression levels of seven JA-responsive genes no longer increased significantly (Fig. II-12B). Thus, ABA may be required for activation of JA responses by allantoin.

Discussion

Evidence for the involvement of purine catabolism in stress protection in plants has only recently emerged (Brychkova *et al*., 2008; Watanabe *et al*., 2010), and the mechanism behind this remains unclear. Previous studies using Arabidopsis mutants defective in purine catabolism showed that the intermediary metabolite allantoin stimulated ABA production and enhanced abiotic stress tolerance (Watanabe *et al*., 2010, 2014a, b). To gain more insight into the relationship between this purine metabolite and stress hormones, the present study investigated the effects of allantoin on JA signaling and responses, because the interplay between ABA and JA constitutes a fundamental regulatory mechanism in plant defense reactions (Kazan and Manners, 2013; Wasternack and Hause, 2013). The current results show that allantoin can activate JA metabolism, signaling, and responses via mechanisms involving ABA, which is supported by several lines of evidence. First, with the improved microarray data using a superior renormalization technique and a stringent cut-off threshold (Konishi, 2004, 2011), GO-based over-representation analysis of the *aln-1* mutant, which accumulates allantoin, revealed a strong effect on JA responses (Fig. II-1). This was supported by the significantly increased levels of JA and JA-Ile in the *aln-1* mutants (Fig. II-4D). This analysis also reproduced the enhanced responses to ABA and abiotic stress conditions that were previously observed with the *aln-1* mutant (Watanabe *et al*., 2014b), indicating that the *aln* mutation could cause the activation of both JA and ABA responses. Such transcriptome profiles provided a plausible explanation for the simultaneous suppression of SA responses (Figs II-2, II-3, II-4A), since antagonistic action of JA and ABA on SA signaling has been reported (Laurie-Berry *et al*., 2006; Yasuda *et al*.,

2008; Millet *et al*., 2010). Secondly, the detailed transcriptome profiling and RT-qPCR analyses emphasized the massive influence of MYC2, a master regulator of JA signaling, on global gene expression in this mutant (Fig. II-4A–C). As discussed below, this finding was supported by significant alterations in metabolic, physiological, and pathophysiological responses that are mainly controlled by MYC2 (Figs II-5, II-8, II-9). Most of these alterations were reversed upon genetic complementation of the *aln* mutation (Figs II-4C, II-5, II-8, II-9C, D), while the other mutations that disrupt different steps in purine degradation had little effect on activating JA-responsive genes (Fig. II-4C). These results confirmed the *aln* mutation as the primary cause behind the observed phenotype, and ruled out non-specific effects of inhibiting purine catabolism. Thirdly, exogenously supplied allantoin, but not its immediate metabolite allantoate, activated expression of JA-responsive genes in the WT plants (Fig. II-10A). The observation is consistent with the expression data for *aln-1* and *aah* mutants, which endogenously accumulate allantoin and allantoate, respectively (Fig. II-4C). It thus appears that the accumulation of allantoin as a result of the *aln* mutation indeed triggers JA responses. Finally, not only JA-insensitive mutants, but also ABA-deficient mutants, showed no effect of allantoin that was either exogenously supplied or endogenously accumulated due to the *aln-1* mutation (Figs II-10B, C, II-12). These findings revealed the requirement for ABA in the action of allantoin to elicit JA responses, suggesting that allantoin may exert its effects through the interplay between the two phytohormones.

In Arabidopsis, the MYC and ERF branches of the JA signaling pathway play critical roles in JA-mediated defense responses, and their antagonistic interaction is co-ordinated mainly by the MYC2 transcription factor (Kazan and Manners, 2013). Surprisingly, the *aln* mutation resulted in highly

contrasting effects on these two major branches, activating the MYC branch while repressing the ERF branch (Fig. II-4A). This finding suggested that MYC2 activity was augmented in the *aln-1* mutant. Indeed, the *aln-1* mutant showed significantly increased MYC2 transcript levels, which most probably accounted for transcriptional activation of MYC2 target genes (Fig. II-4A–C). Consistent with these observations, *aln-1* mutants also showed enhanced sensitivity to exogenous MeJA and mechanical wounding (Figs II-5, II-8), which are established MYC2-mediated responses. Modestly compromised resistance of *aln* mutants to bacterial pathogens (Fig. II-9) also seems to result from high levels of MYC2 expression, perhaps due to suppression of SA signaling and the ERF branch of JA signaling (Fig. II-4A). Some features of the *aln* mutant phenotype, such as enhanced sensitivity to exogenous JA, coincided with the phenotypes of transgenic Arabidopsis plants expressing MYC2 under a strong constitutive promoter (Lorenzo *et al*., 2004; Dombrecht *et al*., 2007). All together, these phenotypes of *aln* mutants can be interpreted as the consequences of MYC2 activation, suggesting that allantoin may activate JA responses by enhancing expression of this master regulator.

Arabidopsis MYC2 is rapidly induced by ABA (Abe *et al*., 1997), and it has been shown that ABA acts upstream of JA to regulate MYC2 expression (Lorenzo *et al*., 2004). Previous work showed that allantoin could increase ABA levels in Arabidopsis seedlings via two possible mechanisms: by stimulating the expression of a rate-limiting enzyme NCED3 in *de novo* synthesis; and by post-translational activation of an enzyme (BGLU18 also known as BG1) responsible for hydrolytic conversion of inactive ABA glucosides (Watanabe *et al*., 2014b). Therefore, allantoin might activate JA responses through ABA-dependent MYC2 activation, although in Arabidopsis the *aln* mutation or exogenous allantoin increases ABA only at modest levels

(Watanabe *et al*., 2014b) and increased ABA levels do not always result in significantly enhanced JA responses (García-Andrade *et al*., 2011). Here, this possibility was examined by quantifying expression of MYC2 and MYC2-regulated genes in ABA-deficient single mutants treated with exogenous allantoin, and in ABA-deficient *aln-1* double mutants. The results revealed ABA to be an essential factor in allantoin-mediated MYC2 activation (Figs II-10C, II-12B). The similar expression analysis using the *jar1-1* single and *aln-1 jar1-1* double mutants gave the same results as those for the ABA mutants (Figs II-10B, II-12B), indicating that the effect of ABA depends on the formation of bioactive JA (JA-Ile). These results, together with those of a previous study (Watanabe *et al*., 2014b), support the idea that ABA might precede JA in the activation of MYC2 by allantoin, although how ABA enhances JA remains to be elucidated (Fig. II-13).

Whether the activated JA response contributes to allantoin-mediated stress tolerance, as observed in the *aln* mutants (Watanabe *et al*., 2014b), remains an important question regarding the mechanism of action of allantoin. Although ABA plays a central role in drought tolerance, JA participates in the regulation of ABA-mediated physiological responses to drought such as stomatal closure (Suhita *et al*., 2004). JA also affects expression of a significant fraction of drought-related genes that are responsive to ABA (Huang *et al*., 2008) and positively regulates freezing tolerance (Hu *et al*., 2013), which may share common protective mechanisms with drought tolerance. In fact, allantoin-accumulating *aln* mutants enhance ABA levels, activate stress-related genes, and increase drought and osmotic stress tolerance (Watanabe *et al*., 2014b); the results described here show that the mutants also activate JA responses and JA-related gene expression. These observations may

suggest a possible contribution of JA signaling to the abiotic stress tolerance mediated by allantoin, through interactions with ABA.

These results point to a previously unrecognized connection between allantoin and JA signaling, and imply its potential influence on the interplay between JA and SA (Figs II-2, II-3, II-4A, II-9). This suggests that purine catabolism may play a role in biotic stress responses. Indeed, purine catabolism has been implicated in plant–microbe interactions: in beans and wheat, changes in the enzyme activities and metabolites, including allantoin, occur as an early response to pathogens (Montalbini, 1991, 1992b). Also, inhibition of the purine catabolic pathway by the XDH inhibitor allopurinol resulted in altered rust infection and compromised hypersensitive responses during incompatible interactions (Montalbini, 1992a), and the application of allopurinol enhanced virus susceptibility in tobacco (Silvestri *et al*., 2008). In addition, a recent transcriptome analysis of wheat revealed significantly increased expression of genes involved in ureide transport during fusarium infection (Lysøe *et al*., 2011). Although the above pathophysiological phenomena may be relevant to JA and SA signaling, further research is needed to obtain evidence that substantially supports the role of purine catabolism in biotic defense. In this context, it would be interesting to examine the effect of allantoin on herbivore resistance because the *aln* mutants activated the MYC branch pathway and enhanced wounding responses (Figs II-4, II-8).

An intriguing observation is that *aah* mutation and exogenous allantoate treatment, both causing allantoate accumulation, tend to suppress JA responses at the transcript and metabolite levels (Figs II-4C, II-7, II-10A). The *aah* mutation also tends to perturb the expression of certain ABA-related genes, although the ABA level in this mutant does not seem to be significantly

different from that of the WT (Watanabe *et al*., 2014b). These observations may imply that allantoate also affects stress-related gene expression, potentially with the opposite effect to that of allantoin reported here and previously (Watanabe *et al*., 2014b). If such a possibility were likely, then allantoate could ensure the elimination of the effect of allantoin after its degradation. However, this remains to be investigated. A more extensive analysis, including further examination of the physiological effects of ureide accumulation and in-depth characterization of *aln* and *aah* mutants, would shed light on the possible relationship between allantoin and allantoate in the mechanism of stress response and adaptation.

Recent metabolomic studies showed that allantoin levels significantly increased in Arabidopsis, rice, and other species subjected to various stress conditions (see the Introduction). Some possibilities have been proposed to explain the physiological significance of stress-induced allantoin accumulation. The conventional view argues that this phenomenon results from a metabolic counter-balance to optimize carbon to N ratios, because, under stress conditions, reduced photosynthesis causes a shortage of carbon skeletons, which restricts assimilation of purine-derived ammonia and leads to accumulation of this toxic N compound. However, recent studies using Arabidopsis mutants indicated that allantoin might participate in stress protection and tolerance mechanisms. Brychkova *et al*. (2008) reported that this ureide compound could act as an antioxidant. Our previous and current studies showed that allantoin elicited phytohormone-mediated stress responses (Watanabe *et al*., 2014b; this study). In cultivated rice, allantoin also induced stress responses by significantly increasing the levels of osmoprotectants such as soluble sugars and free proline (Wang *et al*., 2012). Although none of these lines of evidence is as yet conclusive, it is worth mentioning that these

possible actions of allantoin are not mutually exclusive, which suggests that this purine metabolite may have a role beyond its function as a metabolic intermediate or N reservoir under stress conditions. Multifunctionality of small metabolites, in particular their signaling and regulatory roles, has recently gained attention as part of the set of adaptive mechanisms that allow plants to survive and grow under changing environments. The importance of various effects on plant development and physiology has been documented for certain molecular species of sugars, amino acids, polyamines, and other kinds of small compounds that are not considered to be phytohormones (see the Introduction). Currently, the number of such small metabolites is limited, but is estimated to be much higher than that reported in the literature (Tholl and Aharoni, 2014). Thus, it seems possible that allantoin could serve in either N metabolism or stress protection, depending on the circumstances where plants live. For further substantiation of such a dual functionality of allantoin, its modes of action in stress responses and adaptation need to be firmly defined.

Table II-1. Primers used in this study.

AGI[a]	Gene symbol[b]	Direction	Sequence (Designation)	Use
At4g04955	ALN	Forward	5’-CCTTTATGTGCCCTTCAGGA-3’ (F1)	PCR genotyping
		Reverse	5’-GGCCTATCACTCCACCAAGA-3’ (R1)	PCR genotyping
		Reverse	5’-GGTTCCCACACAACAAGATCTGC-3’ (R4)	PCR genotyping
At1g52400	BGLU18	Forward	5’-GGCGACCCAGAAGTTATCAT-3’ (F3)	PCR genotyping
		Reverse	5’-GAATACCATTTGCCCGAAAC-3’ (R3)	PCR genotyping
At2g46370	JAR1	Forward	5'-CGCTACTGACCCTGAAGAAGCTTT-3' (F2)	DNA sequencing
		Reverse	5'-CAACATGTTAAGGCATAGTCG-3' (R2)	DNA sequencing
At1g17420	LOX3	Forward	5’-TGAACATTGAGAGAGTCAAGACTTTT-3’	RT-qPCR
		Reverse	5’-AGATAGTTCGAGTAGCATAGGCTTT-3’	RT-qPCR
At1g72520	LOX4	Forward	5’-TCGCTAACTTTGGTGAGATCGATAG-3’	RT-qPCR
		Reverse	5’-TCGTCATCTCGAAGCCATGCATATT-3’	RT-qPCR
At5g42650	AOS	Forward	5’-GGTGGCGAGGTTGTTTGTGA-3’	RT-qPCR
		Reverse	5’-GCGACGTACCAACCTCAATATCA-3’	RT-qPCR
At2g06050	OPR3	Forward	5’-ACGGACCACTCCCGGCGGTTTT-3’	RT-qPCR
		Reverse	5’-CGTGAACTGCTTCCACAACT-3'	RT-qPCR
At1g32640	MYC2	Forward	5’-CGCGAGTATGTCGGTGGTTA-3’	RT-qPCR
		Reverse	5’-TGCTCTGAGCTGTTCTTGCGTATA-3’	RT-qPCR
At3g17860	JAZ3	Forward	5’-GTTCTACCAATGTAATGGCTCCAACA-3’	RT-qPCR
		Reverse	5’-CAATATGGGGATACGCTCGT-3’	RT-qPCR
At5g13220	JAZ10	Forward	5’-AGCTCTTTGGCCAGAATCTAGA-3’	RT-qPCR
		Reverse	5’-AGATGTTGATACTAATCTCTCCTTG-3’	RT-qPCR
At2g14610	PR-1	Forward	5'-CGTCTTTGTAGCTCTTGTAGGTGC-3'	RT-qPCR
		Reverse	5'-TGCCTGGTTGTGAACCCTTAG-3'	RT-qPCR
At5g44420	PDF1.2a	Forward	5'-CTTGTTCTCTTTGCTGCTTTCGAC-3'	RT-qPCR
		Reverse	5'-TTGGCTCCTTCAAGGTTAATGCAC-3'	RT-qPCR
At3g23240	ERF1	Forward	5'-CGATCCCTAACCGAAAACAG-3'	RT-qPCR
		Reverse	5'-TCCGATAGAATATTCCGGTGA-3'	RT-qPCR
At3g18780	ACTIN2	Forward	5’-ACCGTATGAGCAAAGAAATCAC-3’	RT-qPCR
		Reverse	5’-GAGGGAAGCAAGAATGGAAC-3’	RT-qPCR
–	T-DNA	–	5’-TGGTTCACGTAGTGGGCCATCG-3’ (LBa1)	PCR genotyping

[a] Arabidopsis thaliana gene identifier code assigned by the Arabidopsis Genome Initiatives (AGI; https://www.arabidopsis.org/portals/nomenclature/).

[b] Gene symbol as provided by The Arabidopsis Information Resource (TAIR; release 10; https://www.arabidopsis.org/) except for T-DNA of Agrobacterium tumefaciens.

Table II-2. LC-ESI-MS/MS parameters for jasmonate determination.

Analyte	Retention time on LC (min)	ESI mode	$[M–H]^{-1}$ (m/z)	Transition ion (m/z)	Collision energy (eV)	Fragmentor voltage (V)
JA	14.4	negative	209	59	15	135
$[^{2}H_{2}]$JA	14.4	negative	211	59	15	135
JA-Ile	18.0	negative	322.0	130	14	140
$[^{13}C_{6}]$JA-Ile	18.0	negative	328.4	136.2	14	140

Table II-3. Genes with significantly increased expression in the aln-1 mutant.

Listed are those whose changes in transcript levels increased by equal to or greater than 3-fold, with the statistical significance level of 0.001 by a two-way analysis of variance (ANOVA). These genes were selected from the revised microarray data (Gene Expression Omnibus accession number GSE73841) that had been parametrically renormalized using the SuperNORM data service (Skylight Biotech Inc, Akita, Japan), according to the three-parameter lognormal distribution method (Konishi 2004).

Affymetrix probe ID	AGI[a]	Fold change[b]	Gene symbol and description[c]	P-value[d]
248727_at	At5g47990	37.17	CYP705A5, THAD, THAD1, cytochrome P450, family 705, subfamily A, polypeptide 5	1.331E-06
252368_at	At3g48520	30.04	CYP94B3, cytochrome P450, family 94, subfamily B, polypeptide 3	1.282E-08
256601_s_at	At3g28290	18.06	AT14A, Protein of unknown function (DUF677)	1.411E-22
264415_at	At1g43160	16.76	RAP2.6, related to AP2 6	1.831E-14
267147_at	At2g38240	16.69	2-oxoglutarate (2OG) and Fe(II)-dependent oxygenase superfamily protein	3.205E-09
246340_s_at	At3g44860	14.61	FAMT, farnesoic acid carboxyl-O-methyltransferase	1.956E-21
249812_at	At5g23830	13.24	MD-2-related lipid recognition domain-containing protein	3.712E-16
263023_at	At1g23960	12.60	Protein of unknown function (DUF626)	6.221E-08
255065_s_at	At4g08870	12.06	Arginase/deacetylase superfamily protein	2.889E-26
265119_at	At1g62570	11.83	FMO GS-OX4, flavin-monooxygenase glucosinolate S-oxygenase 4	6.567E-13
248944_at	At5g45500	11.47	RNI-like superfamily protein	2.861E-06
247360_at	At5g63450	11.44	CYP94B1, cytochrome P450, family 94, subfamily B, polypeptide 1	5.902E-14
255257_at	At4g05050	10.42	UBQ11, ubiquitin 11	2.298E-25
261804_at	At1g30530	10.36	UGT78D1, UDP-glucosyl transferase 78D1	1.783E-21
266271_at	At2g29440	9.53	ATGSTU6, GST24, GSTU6, glutathione S-transferase tau 6	1.447E-09
267261_at	At2g23120	9.26	Late embryogenesis abundant protein, group 6	2.610E-14
256497_at	At1g31580	9.03	CXC750, ECS1, ECS1	1.596E-08
249600_s_at	At5g38000	8.90	Zinc-binding dehydrogenase family protein	5.939E-04
252487_at	At3g46660	8.73	UGT76E12, UDP-glucosyl transferase 76E12	4.360E-12
254481_at	At4g20480	8.62	Putative endonuclease or glycosyl hydrolase	6.565E-10
247175_at	At5g65280	8.21	GCL1, GCR2-like 1	1.076E-13
266901_at	At2g34600	7.87	JAZ7, TIFY5B, jasmonate-zim-domain protein 7	4.125E-16
263673_at	At2g04800	7.75	unknown protein; FUNCTIONS IN: molecular_function unknown; INVOLVED IN: N-terminal protein myristoylation; LOCATED IN: cellular_component unknown; EXPRESSED IN: hypocotyl, root; Has 4 Blast hits to 4 proteins in 1 species: Archae - 0; Bacteria - 0; Metazoa - 0; Fungi - 0; Plants - 4; Viruses - 0; Other Eukaryotes - 0 (source: NCBI BLink).	3.573E-05

[a] Arabidopsis thaliana gene identifier code assigned by the Arabidopsis Genome Initiatives (AGI; https://www.arabidopsis.org/portals/nomenclature/).

[b] Mean of two independent biological experiments (aln-1 versus wild-type).

[c] Gene symbol and description as provided by The Arabidopsis Information Resource (TAIR; release 10; https://www.arabidopsis.org/).

[d] P-value determined by a two-way ANOVA.

Table II-3. Genes with significantly increased expression in the aln-1 mutant (continued).

Affymetrix probe ID	AGI[a]	Fold change[b]	Gene symbol and description[c]	P-value[d]
256114_at	At1g16850	7.50	unknown protein; FUNCTIONS IN: molecular_function unknown; INVOLVED IN: response to salt stress; LOCATED IN: endomembrane system; EXPRESSED IN: leaf apex, leaf whorl, male gametophyte, flower, leaf; EXPRESSED DURING: LP.06 six leaves visible, LP.04 four leaves visible, LP.10 ten leaves visible, petal differentiation and expansion stage, LP.08 eight leaves visible; BEST Arabidopsis thaliana protein match is: unknown protein (TAIR:AT5G64820.1); Has 24 Blast hits to 24 proteins in 6 species: Archae - 0; Bacteria - 0; Metazoa - 0; Fungi - 0; Plants - 24; Viruses - 0; Other Eukaryotes - 0 (source: NCBI BLink).	6.812E-24
249599_at	At5g37990	7.10	S-adenosyl-L-methionine-dependent methyltransferases superfamily protein	2.658E-11
253104_at	At4g36010	7.06	Pathogenesis-related thaumatin superfamily protein	1.523E-16
263320_at	At2g47180	7.02	AtGolS1, GolS1, galactinol synthase 1	4.882E-18
249567_at	At5g38020	6.81	S-adenosyl-L-methionine-dependent methyltransferases superfamily protein	7.348E-16
263594_at	At2g01880	6.70	ATPAP7, PAP7, purple acid phosphatase 7	5.248E-11
260744_at	At1g15010	6.68	unknown protein; BEST Arabidopsis thaliana protein match is: unknown protein (TAIR:AT2G01300.1); Has 71 Blast hits to 71 proteins in 13 species: Archae - 0; Bacteria - 2; Metazoa - 0; Fungi - 0; Plants - 69; Viruses - 0; Other Eukaryotes - 0 (source: NCBI BLink).	7.417E-08
245689_at	At5g04120	6.23	Phosphoglycerate mutase family protein	4.586E-14
248205_at	At5g54300	6.15	Protein of unknown function (DUF761)	9.230E-12
265615_at	At2g25450	6.03	2-oxoglutarate (2OG) and Fe(II)-dependent oxygenase superfamily protein	1.288E-09
251513_at	At3g59220	5.98	ATPIRIN1, PRN, PRN1, pirin	2.923E-25
245444_at	At4g16740	5.97	ATTPS03, TPS03, terpene synthase 03	1.499E-11
246825_at	At5g26260	5.91	TRAF-like family protein	9.195E-12
247136_at	At5g66170	5.87	STR18, sulfurtransferase 18	4.901E-16
259286_at	At3g11480	5.84	ATBSMT1, BSMT1, S-adenosyl-L-methionine-dependent methyltransferases superfamily protein	2.060E-24
260549_at	At2g43535	5.84	Scorpion toxin-like knottin superfamily protein	4.788E-13
263482_at	At2g03980	5.82	GDSL-like Lipase/Acylhydrolase superfamily protein	1.014E-25
248392_at	At5g52050	5.71	MATE efflux family protein	1.438E-09
245555_at	At4g15390	5.70	HXXXD-type acyl-transferase family protein	4.897E-16
266743_at	At2g02990	5.64	ATRNS1, RNS1, ribonuclease 1	5.145E-10
265530_at	At2g06050	5.59	DDE1, OPR3, oxophytodienoate-reductase 3	2.070E-17
250793_at	At5g05600	5.56	2-oxoglutarate (2OG) and Fe(II)-dependent oxygenase superfamily protein	5.826E-15
251356_at	At3g61060	5.53	AtPP2-A13, PP2-A13, phloem protein 2-A13	2.022E-16
246488_at	At5g16010	5.52	3-oxo-5-alpha-steroid 4-dehydrogenase family protein	2.942E-12
245928_s_at	At5g24780	5.47	ATVSP1, VSP1, vegetative storage protein 1	3.363E-22
247600_at	At5g60890	5.40	ATMYB34, ATR1, MYB34, myb domain protein 34	9.715E-13
266246_at	At2g27690	5.38	CYP94C1, cytochrome P450, family 94, subfamily C, polypeptide 1	1.253E-12
252102_at	At3g50970	5.37	LTI30, XERO2, dehydrin family protein	4.219E-11
251241_s_at	At3g62460	5.37	Putative endonuclease or glycosyl hydrolase	9.894E-20
245713_at	At5g04370	5.34	NAMT1, S-adenosyl-L-methionine-dependent methyltransferases superfamily protein	1.362E-06

Table II-3. Genes with significantly increased expression in the aln-1 mutant (continued).

Affymetrix probe ID	AGI[a]	Fold change[b]	Gene symbol and description[c]	P-value[d]
267411_at	At2g34930	5.34	disease resistance family protein / LRR family protein	4.288E-11
263083_at	At2g27190	5.31	ATPAP1, ATPAP12, PAP1, PAP12, purple acid phosphatase 12	6.013E-21
245749_at	At1g51090	5.29	Heavy metal transport/detoxification superfamily protein	6.242E-13
250662_at	At5g07010	5.22	ATST2A, ST2A, sulfotransferase 2A	1.799E-06
264886_at	At1g61120	5.22	GES, TPS04, TPS4, terpene synthase 04	1.201E-08
259846_at	At1g72140	5.22	Major facilitator superfamily protein	2.148E-11
261919_at	At1g65980	5.21	TPX1, thioredoxin-dependent peroxidase 1	4.164E-11
261037_at	At1g17420	5.19	LOX3, lipoxygenase 3	1.737E-22
248337_at	At5g52310	5.11	COR78, LTI140, LTI78, RD29A, low-temperature-responsive protein 78 (LTI78) / desiccation-responsive protein 29A (RD29A)	1.912E-13
257638_at	At3g25820	5.06	ATTPS-CIN, TPS-CIN, terpene synthase-like sequence-1,8-cineole	3.374E-19
266799_at	At2g22860	5.06	ATPSK2, PSK2, phytosulfokine 2 precursor	3.091E-09
262226_at	At1g53885	4.94	Protein of unknown function (DUF581)	4.589E-07
249971_at	At5g19110	4.92	Eukaryotic aspartyl protease family protein	3.110E-16
256324_at	At1g66760	4.87	MATE efflux family protein	1.026E-06
249101_at	At5g43580	4.74	Serine protease inhibitor, potato inhibitor I-type family protein	1.325E-06
250292_at	At5g13220	4.73	JAS1, JAZ10, TIFY9, jasmonate-zim-domain protein 10	5.410E-15
255527_at	At4g02360	4.67	Protein of unknown function, DUF538	5.697E-16
260969_at	At1g12240	4.64	ATBETAFRUCT4, VAC-INV, Glycosyl hydrolases family 32 protein	1.631E-20
255132_at	At4g08170	4.61	Inositol 1,3,4-trisphosphate 5/6-kinase family protein	9.523E-16
264146_at	At1g02205	4.58	CER1, Fatty acid hydroxylase superfamily	1.358E-10
252377_at	At3g47960	4.58	Major facilitator superfamily protein	9.941E-12
251023_at	At5g02170	4.56	Transmembrane amino acid transporter family protein	2.740E-06
260012_at	At1g67865	4.56	unknown protein; BEST Arabidopsis thaliana protein match is: unknown protein (TAIR:AT1G67860.1); Has 13 Blast hits to 13 proteins in 2 species: Archae - 0; Bacteria - 0; Metazoa - 0; Fungi - 0; Plants - 13; Viruses - 0; Other Eukaryotes - 0 (source: NCBI BLink).	1.160E-12
266800_at	At2g22880	4.53	VQ motif-containing protein	2.547E-09
254085_at	At4g24960	4.51	ATHVA22D, HVA22D, HVA22 homologue D	1.755E-15
264953_at	At1g77120	4.49	ADH, ADH1, ATADH, ATADH1, alcohol dehydrogenase 1	2.059E-15
250648_at	At5g06760	4.45	LEA4-5, Late Embryogenesis Abundant 4-5	1.309E-13
254326_at	At4g22610	4.45	Bifunctional inhibitor/lipid-transfer protein/seed storage 2S albumin superfamily protein	5.600E-10
265698_at	At2g32160	4.30	S-adenosyl-L-methionine-dependent methyltransferases superfamily protein	1.780E-07
247933_at	At5g56980	4.29	unknown protein; FUNCTIONS IN: molecular_function unknown; INVOLVED IN: biological_process unknown; LOCATED IN: endomembrane system; EXPRESSED IN: 18 plant structures; EXPRESSED DURING: 12 growth stages; BEST Arabidopsis thaliana protein match is: unknown protein (TAIR:AT4G26130.1); Has 30201 Blast hits to 17322 proteins in 780 species: Archae - 12; Bacteria - 1396; Metazoa - 17338; Fungi - 3422; Plants - 5037; Viruses - 0; Other Eukaryotes - 2996 (source: NCBI BLink).	9.334E-12

Table II-3. Genes with significantly increased expression in the aln-1 **mutant (continued).**

Affymetrix probe ID	AGI[a]	Fold change[b]	Gene symbol and description[c]	P-value[d]
256417_s_at	At3g11170	4.27	FAD7, FADD, fatty acid desaturase 7	9.180E-14
245449_at	At4g16870	4.25	transposable element gene	1.839E-09
260399_at	At1g72520	4.20	PLAT/LH2 domain-containing lipoxygenase family protein	6.363E-16
258893_at	At3g05660	4.18	AtRLP33, RLP33, receptor like protein 33	4.862E-12
262496_at	At1g21790	4.17	TRAM, LAG1 and CLN8 (TLC) lipid-sensing domain containing protein	2.605E-19
264527_at	At1g30760	4.17	FAD-binding Berberine family protein	2.771E-08
251984_at	At3g53260	4.16	ATPAL2, PAL2, phenylalanine ammonia-lyase 2	2.247E-12
255942_at	At1g22360	4.12	AtUGT85A2, UGT85A2, UDP-glucosyl transferase 85A2	7.535E-13
248978_at	At5g45070	4.09	AtPP2-A8, PP2-A8, phloem protein 2-A8	7.511E-05
266486_at	At2g47950	4.07	unknown protein; FUNCTIONS IN: molecular_function unknown; INVOLVED IN: biological_process unknown; LOCATED IN: endomembrane system; EXPRESSED IN: root, flower; EXPRESSED DURING: petal differentiation and expansion stage; BEST Arabidopsis thaliana protein match is: unknown protein (TAIR:AT3G62990.1); Has 22 Blast hits to 22 proteins in 5 species: Archae - 0; Bacteria - 0; Metazoa - 0; Fungi - 0; Plants - 22; Viruses - 0; Other Eukaryotes - 0 (source: NCBI BLink).	2.353E-07
262010_at	At1g35612	4.07	transposable element gene	5.905E-06
263161_at	At1g54020	4.06	GDSL-like Lipase/Acylhydrolase superfamily protein	1.533E-12
245628_at	At1g56650	4.05	ATMYB75, MYB75, PAP1, SIAA1, production of anthocyanin pigment 1	2.806E-08
260557_at	At2g43610	4.04	Chitinase family protein	6.695E-19
258941_at	At3g09940	4.03	ATMDAR3, MDAR2, MDAR3, MDHAR, monodehydroascorbate reductase	1.933E-08
246125_at	At5g19875	4.03	unknown protein; FUNCTIONS IN: molecular_function unknown; INVOLVED IN: response to oxidative stress; LOCATED IN: endomembrane system; EXPRESSED IN: 21 plant structures; EXPRESSED DURING: 13 growth stages; BEST Arabidopsis thaliana protein match is: unknown protein (TAIR:AT2G31940.1); Has 30201 Blast hits to 17322 proteins in 780 species: Archae - 12; Bacteria - 1396; Metazoa - 17338; Fungi - 3422; Plants - 5037; Viruses - 0; Other Eukaryotes - 2996 (source: NCBI BLink).	3.758E-16
245736_at	At1g73330	4.03	ATDR4, DR4, drought-repressed 4	8.670E-15
248293_at	At5g53050	3.98	alpha/beta-Hydrolases superfamily protein	5.520E-14
258181_at	At3g21670	3.95	Major facilitator superfamily protein	9.060E-16
254561_at	At4g19160	3.95	unknown protein; Has 30201 Blast hits to 17322 proteins in 780 species: Archae - 12; Bacteria - 1396; Metazoa - 17338; Fungi - 3422; Plants - 5037; Viruses - 0; Other Eukaryotes - 2996 (source: NCBI BLink).	4.712E-21
245651_s_at	At1g24793	3.92	UDP-3-O-acyl N-acetylglycosamine deacetylase family protein	3.960E-25
267206_at	At2g30830	3.92	2-oxoglutarate (2OG) and Fe(II)-dependent oxygenase superfamily protein	5.079E-05
262637_at	At1g06640	3.91	2-oxoglutarate (2OG) and Fe(II)-dependent oxygenase superfamily protein	2.945E-14
258421_at	At3g16690	3.90	Nodulin MtN3 family protein	1.718E-06
258321_at	At3g22840	3.89	ELIP, ELIP1, Chlorophyll A-B binding family protein	9.380E-09
262887_at	At1g14780	3.88	MAC/Perforin domain-containing protein	5.670E-07
249216_at	At5g42240	3.88	scpl42, serine carboxypeptidase-like 42	5.393E-09
246286_at	At1g31910	3.88	GHMP kinase family protein	1.332E-22
254667_at	At4g18280	3.88	glycine-rich cell wall protein-related	2.040E-15
252170_at	At3g50480	3.86	HR4, homolog of RPW8 4	1.208E-10

Table II-3. Genes with significantly increased expression in the aln-1 mutant (continued).

Affymetrix probe ID	AGI[a]	Fold change[b]	Gene symbol and description[c]	P-value[d]
255403_at	At4g03400	3.84	DFL2, GH3-10, Auxin-responsive GH3 family protein	9.628E-16
245244_at	At1g44350	3.83	ILL6, IAA-leucine resistant (ILR)-like gene 6	4.611E-14
264424_at	At1g61740	3.83	Sulfite exporter TauE/SafE family protein	3.458E-17
253259_at	At4g34410	3.81	RRTF1, redox responsive transcription factor 1	1.297E-05
248079_at	At5g55790	3.80	unknown protein; BEST Arabidopsis thaliana protein match is: unknown protein (TAIR:AT1G45163.1); Has 1807 Blast hits to 1807 proteins in 277 species: Archae - 0; Bacteria - 0; Metazoa - 736; Fungi - 347; Plants - 385; Viruses - 0; Other Eukaryotes - 339 (source: NCBI BLink).	9.744E-06
246987_at	At5g67300	3.79	ATMYB44, ATMYBR1, MYB44, MYBR1, myb domain protein r1	2.831E-14
267058_at	At2g32510	3.78	MAPKKK17, mitogen-activated protein kinase kinase kinase 17	4.132E-15
256994_s_at	At3g25830	3.77	ATTPS-CIN, TPS-CIN, TPS-CIN, terpene synthase-like sequence-1,8-cineole	1.801E-16
264787_at	At2g17840	3.76	ERD7, Senescence/dehydration-associated protein-related	7.595E-15
249010_at	At5g44580	3.73	unknown protein; FUNCTIONS IN: molecular_function unknown; INVOLVED IN: biological_process unknown; LOCATED IN: endomembrane system; EXPRESSED IN: 18 plant structures; EXPRESSED DURING: 12 growth stages; BEST Arabidopsis thaliana protein match is: unknown protein (TAIR:AT5G44582.1); Has 30201 Blast hits to 17322 proteins in 780 species: Archae - 12; Bacteria - 1396; Metazoa - 17338; Fungi - 3422; Plants - 5037; Viruses - 0; Other Eukaryotes - 2996 (source: NCBI BLink).	1.500E-18
245450_at	At4g16880	3.72	Leucine-rich repeat (LRR) family protein	2.548E-06
253814_at	At4g28290	3.69	unknown protein; FUNCTIONS IN: molecular_function unknown; INVOLVED IN: biological_process unknown; LOCATED IN: chloroplast; EXPRESSED IN: 23 plant structures; EXPRESSED DURING: 15 growth stages; Has 45 Blast hits to 45 proteins in 11 species: Archae - 0; Bacteria - 0; Metazoa - 0; Fungi - 0; Plants - 45; Viruses - 0; Other Eukaryotes - 0 (source: NCBI BLink).	7.458E-08
247982_at	At5g56760	3.69	ATSERAT1;1, SAT-52, SAT5, SERAT1;1, serine acetyltransferase 1;1	2.241E-15
248522_at	At5g50565	3.69	unknown protein; BEST Arabidopsis thaliana protein match is: unknown protein (TAIR:AT5G50665.2); Has 6 Blast hits to 6 proteins in 1 species: Archae - 0; Bacteria - 0; Metazoa - 0; Fungi - 0; Plants - 6; Viruses - 0; Other Eukaryotes - 0 (source: NCBI BLink).	7.287E-08
246432_at	At5g17490	3.68	RGL3, RGA-like protein 3	2.466E-09
251642_at	At3g57520	3.67	AtSIP2, SIP2, seed imbibition 2	1.617E-12
256725_at	At2g34070	3.67	TBL37, TRICHOME BIREFRINGENCE-LIKE 37	2.501E-15
263098_at	At2g16005	3.67	MD-2-related lipid recognition domain-containing protein	9.852E-09
262517_at	At1g17180	3.66	ATGSTU25, GSTU25, glutathione S-transferase TAU 25	3.372E-05
259802_at	At1g72260	3.65	THI2.1, THI2.1.1, thionin 2.1	1.612E-13
254306_at	At4g22330	3.64	ATCES1, Alkaline phytoceramidase (aPHC)	7.765E-14
248790_at	At5g47450	3.63	ATTIP2;3, DELTA-TIP3, TIP2;3, tonoplast intrinsic protein 2;3	7.061E-13
263497_at	At2g42540	3.61	COR15, COR15A, cold-regulated 15a	6.977E-23
252563_at	At3g45970	3.60	ATEXLA1, ATEXPL1, ATHEXP BETA 2.1, EXLA1, EXPL1, expansin-like A1	3.517E-14
247478_at	At5g62360	3.58	Plant invertase/pectin methylesterase inhibitor superfamily protein	5.862E-08
257952_at	At3g21770	3.56	Peroxidase superfamily protein	4.333E-12
264835_at	At1g03550	3.56	Secretory carrier membrane protein (SCAMP) family protein	7.277E-17
251012_at	At5g02580	3.55	Plant protein 1589 of unknown function	4.499E-06
259442_at	At1g02310	3.53	MAN1, Glycosyl hydrolase superfamily protein	4.281E-12
259758_s_at	At1g77530	3.52	O-methyltransferase family protein	2.696E-10

Table II-3. Genes with significantly increased expression in the aln-1 **mutant (continued).**

Affymetrix probe ID	AGI[a]	Fold change[b]	Gene symbol and description[c]	P-value[d]
251229_at	At3g62740	3.51	BGLU7, beta glucosidase 7	1.563E-04
256577_at	At3g28220	3.51	TRAF-like family protein	2.151E-09
261199_at	At1g12950	3.46	RSH2, root hair specific 2	4.890E-06
245734_at	At1g73480	3.46	alpha/beta-Hydrolases superfamily protein	1.015E-15
264824_at	At1g03420	3.46	Sadhu4-2, transposable element gene	4.057E-11
259516_at	At1g20450	3.45	ERD10, LTI29, LTI45, Dehydrin family protein	1.119E-09
250161_at	At5g15240	3.45	Transmembrane amino acid transporter family protein	4.298E-07
261033_at	At1g17380	3.41	JAZ5, TIFY11A, jasmonate-zim-domain protein 5	1.707E-15
262516_at	At1g17190	3.41	ATGSTU26, GSTU26, glutathione S-transferase tau 26	1.011E-08
251028_at	At5g02230	3.41	Haloacid dehalogenase-like hydrolase (HAD) superfamily protein	2.489E-11
247431_at	At5g62520	3.40	SRO5, similar to RCD one 5	1.320E-04
257497_at	At1g51430	3.38	unknown protein; BEST Arabidopsis thaliana protein match is: unknown protein (TAIR:AT3G28370.1); Has 13 Blast hits to 13 proteins in 4 species: Archae - 0; Bacteria - 0; Metazoa - 0; Fungi - 0; Plants - 13; Viruses - 0; Other Eukaryotes - 0 (source: NCBI BLink).	7.165E-05
254809_at	At4g12410	3.37	SAUR-like auxin-responsive protein family	2.623E-17
254447_at	At4g20860	3.36	FAD-binding Berberine family protein	1.349E-04
256589_at	At3g28740	3.34	CYP81D1, Cytochrome P450 superfamily protein	3.269E-17
253832_at	At4g27654	3.34	unknown protein; FUNCTIONS IN: molecular_function unknown; INVOLVED IN: biological_process unknown; LOCATED IN: endomembrane system; EXPRESSED IN: 17 plant structures; EXPRESSED DURING: 9 growth stages; Has 30201 Blast hits to 17322 proteins in 780 species: Archae - 12; Bacteria - 1396; Metazoa - 17338; Fungi - 3422; Plants - 5037; Viruses - 0; Other Eukaryotes - 2996 (source: NCBI BLink).	1.072E-05
260357_at	At1g69260	3.32	AFP1, ABI five binding protein	6.224E-21
255723_at	At3g29575	3.32	AFP3, ABI five binding protein 3	5.297E-23
258498_at	At3g02480	3.30	Late embryogenesis abundant protein (LEA) family protein	1.938E-07
266832_at	At2g30040	3.29	MAPKKK14, mitogen-activated protein kinase kinase kinase 14	2.429E-11
258901_at	At3g05640	3.28	Protein phosphatase 2C family protein	6.072E-21
254909_at	At4g11210	3.27	Disease resistance-responsive (dirigent-like protein) family protein	2.215E-08
252677_at	At3g44320	3.26	AtNIT3, NIT3, nitrilase 3	5.307E-13
253827_at	At4g28085	3.26	unknown protein; Has 30201 Blast hits to 17322 proteins in 780 species: Archae - 12; Bacteria - 1396; Metazoa - 17338; Fungi - 3422; Plants - 5037; Viruses - 0; Other Eukaryotes - 2996 (source: NCBI BLink).	8.830E-13
264949_at	At1g77080	3.25	AGL27, FLM, MAF1, K-box region and MADS-box transcription factor family protein	1.637E-04
248524_s_at	At5g50570	3.24	Squamosa promoter-binding protein-like (SBP domain) transcription factor family protein	7.795E-20
262912_at	At1g59740	3.23	Major facilitator superfamily protein	2.947E-12
265305_at	At2g20340	3.23	Pyridoxal phosphate (PLP)-dependent transferases superfamily protein	1.336E-13
249265_at	At5g41700	3.22	ATUBC8, UBC8, ubiquitin conjugating enzyme 8	1.413E-15
245944_at	At5g19520	3.21	ATMSL9, MSL9, mechanosensitive channel of small conductance-like 9	7.007E-10

Table II-3. Genes with significantly increased expression in the *aln-1* mutant (continued).

Affymetrix probe ID	AGI[a]	Fold change[b]	Gene symbol and description[c]	P-value[d]
265188_at	At1g23800	3.20	ALDH2B, ALDH2B7, aldehyde dehydrogenase 2B7	5.979E-13
262133_at	At1g78000	3.20	SEL1, SULTR1;2, sulfate transporter 1;2	3.125E-11
265216_at	At1g05100	3.20	MAPKKK18, mitogen-activated protein kinase kinase kinase 18	6.727E-08
264289_at	At1g61890	3.19	MATE efflux family protein	1.851E-13
252419_at	At3g47510	3.18	unknown protein; FUNCTIONS IN: molecular_function unknown; INVOLVED IN: biological_process unknown; LOCATED IN: endomembrane system; EXPRESSED IN: 19 plant structures; EXPRESSED DURING: 11 growth stages; Has 15 Blast hits to 15 proteins in 7 species: Archae - 0; Bacteria - 0; Metazoa - 0; Fungi - 0; Plants - 15; Viruses - 0; Other Eukaryotes - 0 (source: NCBI BLink).	1.221E-17
253684_at	At4g29690	3.18	Alkaline-phosphatase-like family protein	9.631E-08
252076_at	At3g51660	3.18	Tautomerase/MIF superfamily protein	1.585E-17
255795_at	At2g33380	3.17	CLO-3, RD20, Caleosin-related family protein	4.371E-16
250781_at	At5g05410	3.17	DREB2, DREB2A, DRE-binding protein 2A	6.535E-14
260676_at	At1g19450	3.15	Major facilitator superfamily protein	1.216E-08
254996_at	At4g10390	3.15	Protein kinase superfamily protein	8.436E-17
263786_at	At2g46370	3.14	FIN219, JAR1, Auxin-responsive GH3 family protein	1.050E-12
259705_at	At1g77450	3.14	anac032, NAC032, NAC domain containing protein 32	7.980E-17
256848_at	At3g27960	3.13	Tetratricopeptide repeat (TPR)-like superfamily protein	1.037E-10
264145_at	At1g79310	3.13	AtMC7, MC7, metacaspase 7	4.761E-05
247717_at	At5g59320	3.11	LTP3, lipid transfer protein 3	8.271E-07
262164_at	At1g78070	3.11	Transducin/WD40 repeat-like superfamily protein	5.182E-11
246235_at	At4g36830	3.11	HOS3-1, GNS1/SUR4 membrane protein family	1.024E-08
249205_at	At5g42600	3.10	MRN1, marneral synthase	1.882E-13
264436_at	At1g10370	3.09	ATGSTU17, ERD9, GST30, GST30B, Glutathione S-transferase family protein	9.101E-09
247109_at	At5g65870	3.09	ATPSK5, PSK5, PSK5, phytosulfokine 5 precursor	1.305E-08
245267_at	At4g14060	3.08	Polyketide cyclase/dehydrase and lipid transport superfamily protein	1.080E-17
253872_at	At4g27410	3.07	ANAC072, RD26, NAC (No Apical Meristem) domain transcriptional regulator superfamily protein	2.721E-20
265058_s_at	At1g52040	3.07	ATMBP, MBP1, myrosinase-binding protein 1	3.468E-21
247026_at	At5g67080	3.07	MAPKKK19, mitogen-activated protein kinase kinase kinase 19	5.392E-16
260205_at	At1g70700	3.06	JAZ9, TIFY7, TIFY domain/Divergent CCT motif family protein	3.876E-15
251480_at	At3g59710	3.06	NAD(P)-binding Rossmann-fold superfamily protein	4.978E-07
248625_at	At5g48880	3.06	KAT5, PKT1, PKT2, peroxisomal 3-keto-acyl-CoA thiolase 2	7.153E-16
246376_at	At1g51950	3.05	IAA18, indole-3-acetic acid inducible 18	2.484E-15
262873_at	At1g64700	3.04	unknown protein; FUNCTIONS IN: molecular_function unknown; INVOLVED IN: N-terminal protein myristoylation; LOCATED IN: cellular_component unknown; EXPRESSED IN: 17 plant structures; EXPRESSED DURING: 11 growth stages; BEST Arabidopsis thaliana protein match is: unknown protein (TAIR:AT3G61920.1); Has 48 Blast hits to 47 proteins in 7 species: Archae - 0; Bacteria - 0; Metazoa - 0; Fungi - 0; Plants - 48; Viruses - 0; Other Eukaryotes - 0 (source: NCBI BLink).	2.992E-04

Table II-3. Genes with significantly increased expression in the aln-1 **mutant (continued).**

Affymetrix probe ID	AGI[a]	Fold change[b]	Gene symbol and description[c]	P-value[d]
245275_at	At4g15210	3.04	AT-BETA-AMY, ATBETA-AMY, BAM5, BMY1, RAM1, beta-amylase 5	3.408E-20
248311_at	At5g52570	3.03	B2, BCH2, BETA-OHASE 2, CHY2, beta-carotene hydroxylase 2	1.603E-12
266532_at	At2g16890	3.03	UDP-Glycosyltransferase superfamily protein	6.148E-06
263972_at	At2g42760	3.02	unknown protein; CONTAINS InterPro DOMAIN/s: Protein of unknown function DUF1685 (InterPro:IPR012881); Has 170 Blast hits to 164 proteins in 34 species: Archae - 0; Bacteria - 1; Metazoa - 26; Fungi - 10; Plants - 107; Viruses - 0; Other Eukaryotes - 26 (source: NCBI BLink).	2.829E-18
259653_at	At1g55240	3.01	Family of unknown function (DUF716)	3.973E-13
255484_at	At4g02540	3.01	Cysteine/Histidine-rich C1 domain family protein	6.119E-12
253074_at	At4g36140	3.01	disease resistance protein (TIR-NBS-LRR class), putative	4.445E-07
248395_at	At5g52120	3.00	AtPP2-A14, PP2-A14, phloem protein 2-A14	2.040E-11

Table II-4. Genes with significantly reduced expression in the *aln-1* mutant.

Listed are those whose changes in transcript levels decreased by equal to or greater than 3-fold with the statistical significance level of 0.001 by a two-way analysis of variance (ANOVA). These genes were selected from the revised microarray data (Gene Expression Omnibus accession number GSE73841) that had been parametrically renormalized using the SuperNORM data service (Skylight Biotech Inc, Akita, Japan), according to the three-parameter lognormal distribution method (Konishi 2004).

Affymetrix probe ID	AGI[a]	Fold change[b]	Gene symbol and description[c]	P-value[d]
263174_at	At1g54040	-35.12	ESP, ESR, TASTY, epithiospecifier protein	6.444E-22
253707_at	At4g29200	-34.79	Beta-galactosidase related protein	1.139E-08
266385_at	At2g14610	-32.83	ATPR1, PR 1, PR1, pathogenesis-related gene 1	4.620E-08
266070_at	At2g18660	-28.28	PNP-A, plant natriuretic peptide A	3.414E-07
255437_at	At4g03060	-24.18	AOP2, AOP2 (ALKENYL HYDROXALKYL PRODUCING 2); oxidoreductase, acting on paired donors, with incorporation or reduction of molecular oxygen, 2-oxoglutarate as one donor, and incorporation of one atom each of oxygen into both donors	4.062E-22
261449_at	At1g21120	-18.58	O-methyltransferase family protein	4.834E-06
252345_at	At3g48640	-15.34	unknown protein; FUNCTIONS IN: molecular_function unknown; INVOLVED IN: biological_process unknown; LOCATED IN: endomembrane system; EXPRESSED IN: 10 plant structures; EXPRESSED DURING: 10 growth stages; CONTAINS InterPro DOMAIN/s: Protein of unknown function DUF677 (InterPro:IPR007749); BEST Arabidopsis thaliana protein match is: Protein of unknown function (DUF677) (TAIR:AT5G66670.2); Has 42 Blast hits to 42 proteins in 3 species: Archae - 0; Bacteria - 0; Metazoa - 0; Fungi - 0; Plants - 42; Viruses - 0; Other Eukaryotes - 0 (source: NCBI BLink).	1.603E-04
249082_at	At5g44120	-15.06	ATCRA1, CRA1, CRU1, RmlC-like cupins superfamily protein	6.134E-07
259925_at	At1g75040	-13.69	PR-5, PR5, pathogenesis-related gene 5	3.250E-10
250445_at	At5g10760	-13.55	Eukaryotic aspartyl protease family protein	3.299E-11
253767_at	At4g28520	-13.53	CRC, CRU3, cruciferin 3	5.723E-08
265837_at	At2g14560	-13.32	LURP1, Protein of unknown function (DUF567)	3.411E-10
250476_at	At5g10140	-12.50	AGL25, FLC, FLC, FLF, K-box region and MADS-box transcription factor family protein	3.044E-19
262421_at	At1g50290	-10.78	unknown protein; Has 2 Blast hits to 2 proteins in 1 species: Archae - 0; Bacteria - 0; Metazoa - 0; Fungi - 0; Plants - 2; Viruses - 0; Other Eukaryotes - 0 (source: NCBI BLink).	2.203E-22
246642_s_at	At5g34920	-10.76	transposable element gene	2.470E-06
251344_at	At3g60920	-9.34	CONTAINS InterPro DOMAIN/s: Beige/BEACH (InterPro:IPR000409); BEST Arabidopsis thaliana protein match is: WD-40 repeat family protein / beige-related (TAIR:AT2G45540.1); Has 1795 Blast hits to 1563 proteins in 214 species: Archae - 2; Bacteria - 29; Metazoa - 830; Fungi - 160; Plants - 230; Viruses - 0; Other Eukaryotes - 544 (source: NCBI BLink).	2.455E-08
254574_at	At4g19430	-8.70	unknown protein; FUNCTIONS IN: molecular_function unknown; INVOLVED IN: biological_process unknown; LOCATED IN: chloroplast; EXPRESSED IN: 17 plant structures; EXPRESSED DURING: 13 growth stages; Has 30201 Blast hits to 17322 proteins in 780 species: Archae - 12; Bacteria - 1396; Metazoa - 17338; Fungi - 3422; Plants - 5037; Viruses - 0; Other Eukaryotes - 2996 (source: NCBI BLink).	1.484E-12
251625_at	At3g57260	-8.43	BG2, BGL2, PR-2, PR2, beta-1,3-glucanase 2	2.338E-11
248062_at	At5g55450	-8.29	Bifunctional inhibitor/lipid-transfer protein/seed storage 2S albumin superfamily protein	5.891E-16
263133_at	At1g78450	-8.12	SOUL heme-binding family protein	2.275E-17
257365_x_at	At2g26020	-7.51	PDF1.2b, plant defensin 1.2b	1.537E-06
267546_at	At2g32680	-7.45	AtRLP23, RLP23, receptor like protein 23	5.887E-07
248683_at	At5g48490	-7.27	Bifunctional inhibitor/lipid-transfer protein/seed storage 2S albumin superfamily protein	2.875E-17

[a] Arabidopsis thaliana gene identifier code assigned by the Arabidopsis Genome Initiatives (AGI; https://www.arabidopsis.org/portals/nomenclature/).

[b] Mean of two independent biological experiments (aln-1 versus wild-type).

[c] Gene symbol and description as provided by The Arabidopsis Information Resource (TAIR; release 10; https://www.arabidopsis.org/).

[d] P-value determined by a two-way ANOVA.

Table II-4. Genes with significantly reduced expression in the aln-1 **mutant (continued).**

Affymetrix probe ID	AGI[a]	Fold change[b]	Gene symbol and description[c]	P-value[d]
252549_at	At3g45860	-7.09	CRK4, cysteine-rich RLK (RECEPTOR-like protein kinase) 4	4.908E-11
265893_at	At2g15040	-7.01	AtRLP18, RLP18, pseudogene, disease resistance protein-related, low similarity to disease resistance protein Cf-2.1 (Lycopersicon pimpinellifolium) GI:1184075; contains Pfam profile PF00560: Leucine Rich Repeat; blastp match of 38% identity and 4.4e-96 P-value to GP|1184075|gb|AAC15779.1||U42444 Cf-2.1 {Lycopersicon pimpinellifolium}	1.419E-12
249777_at	At5g24210	-6.69	alpha/beta-Hydrolases superfamily protein	1.831E-10
247684_at	At5g59670	-6.59	Leucine-rich repeat protein kinase family protein	4.733E-05
264513_at	At1g09420	-5.96	G6PD4, glucose-6-phosphate dehydrogenase 4	9.646E-26
256603_at	At3g28270	-5.94	Protein of unknown function (DUF677)	6.281E-22
258016_at	At3g19350	-5.92	MPC, maternally expressed pab C-terminal	7.141E-09
255653_at	At4g00960	-5.81	Protein kinase superfamily protein	2.461E-05
259385_at	At1g13470	-5.77	Protein of unknown function (DUF1262)	2.084E-05
255879_at	At1g67000	-5.70	Protein kinase superfamily protein	2.648E-06
249890_at	At5g22570	-5.67	ATWRKY38, WRKY38, WRKY DNA-binding protein 38	1.900E-07
263947_at	At2g35820	-5.66	ureidoglycolate hydrolases	2.486E-14
254265_s_at	At4g23140	-5.64	CRK6, cysteine-rich RLK (RECEPTOR-like protein kinase) 6	1.302E-13
267253_at	At2g22960	-5.60	alpha/beta-Hydrolases superfamily protein	6.679E-06
262382_at	At1g72920	-5.52	Toll-Interleukin-Resistance (TIR) domain family protein	9.049E-10
263584_at	At2g17040	-5.43	anac036, NAC036, NAC domain containing protein 36	2.872E-06
258028_at	At3g27473	-5.42	Cysteine/Histidine-rich C1 domain family protein	7.227E-11
248169_at	At5g54610	-5.22	ANK, ankyrin	6.468E-10
256631_at	At3g28320	-4.85	Protein of unknown function (DUF677)	5.048E-07
260568_at	At2g43570	-4.76	CHI, chitinase, putative	1.539E-07
249780_at	At5g24240	-4.67	Phosphatidylinositol 3- and 4-kinase ;Ubiquitin family protein	8.731E-11
249867_at	At5g23020	-4.65	IMS2, MAM-L, MAM3, 2-isopropylmalate synthase 2	6.950E-18
262651_at	At1g14100	-4.60	FUT8, fucosyltransferase 8	1.031E-12
265109_s_at	At1g62630	-4.56	Disease resistance protein (CC-NBS-LRR class) family	1.868E-17
260904_at	At1g02450	-4.52	NIMIN-1, NIMIN1, NIM1-interacting 1	7.944E-07
257139_at	At3g28890	-4.49	AtRLP43, RLP43, receptor like protein 43	1.892E-06
245038_at	At2g26560	-4.45	PLA IIA, PLA2A, PLP2, PLP2, phospholipase A 2A	1.557E-16
267084_at	At2g41180	-4.42	VQ motif-containing protein	9.787E-13
267569_at	At2g30790	-4.38	PSBP-2, photosystem II subunit P-2	1.660E-15
257382_at	At2g40750	-4.36	ATWRKY54, WRKY54, WRKY DNA-binding protein 54	2.989E-15

Table II-4. Genes with significantly reduced expression in the aln-1 **mutant (continued).**

Affymetrix probe ID	AGI[a]	Fold change[b]	Gene symbol and description[c]	P-value[d]
254253_at	At4g23320	-4.28	CRK24, cysteine-rich RLK (RECEPTOR-like protein kinase) 24	2.008E-07
265063_at	At1g61500	-4.23	S-locus lectin protein kinase family protein	8.497E-14
249645_at	At5g36910	-4.22	THI2.2, thionin 2.2	1.596E-18
245349_at	At4g16690	-4.15	ATMES16, MES16, methyl esterase 16	6.321E-11
265993_at	At2g24160	-4.12	pseudogene, leucine rich repeat protein family, contains leucine rich-repeat domains Pfam:PF00560, INTERPRO:IPR001611; contains some similarity to Cf-4 (Lycopersicon hirsutum) gi|2808683|emb|CAA05268; blastp match of 37% identity and 8.4e-98 P-value to GP|2808683|emb|CAA05268.1||AJ002235 Cf-4 {Lycopersicon hirsutum}	3.359E-10
254805_at	At4g12480	-4.09	pEARLI 1, Bifunctional inhibitor/lipid-transfer protein/seed storage 2S albumin superfamily protein	1.725E-10
246821_at	At5g26920	-4.04	CBP60G, Cam-binding protein 60-like G	3.237E-11
250063_at	At5g17880	-4.00	CSA1, disease resistance protein (TIR-NBS-LRR class)	5.581E-18
266071_at	At2g18680	-3.99	unknown protein; FUNCTIONS IN: molecular_function unknown; INVOLVED IN: biological_process unknown; LOCATED IN: endomembrane system; EXPRESSED IN: male gametophyte, pollen tube; EXPRESSED DURING: L mature pollen stage, M germinated pollen stage; BEST Arabidopsis thaliana protein match is: unknown protein (TAIR:AT2G18690.1); Has 30201 Blast hits to 17322 proteins in 780 species: Archae - 12; Bacteria - 1396; Metazoa - 17338; Fungi - 3422; Plants - 5037; Viruses - 0; Other Eukaryotes - 2996 (source: NCBI BLink).	3.373E-07
266286_at	At2g29170	-3.99	NAD(P)-binding Rossmann-fold superfamily protein	7.009E-12
246603_at	At1g31690	-3.98	Copper amine oxidase family protein	7.832E-21
261221_at	At1g19960	-3.97	BEST Arabidopsis thaliana protein match is: transmembrane receptors (TAIR:AT2G32140.1); Has 41 Blast hits to 41 proteins in 17 species: Archae - 0; Bacteria - 2; Metazoa - 23; Fungi - 0; Plants - 11; Viruses - 0; Other Eukaryotes - 5 (source: NCBI BLink).	2.356E-13
245052_at	At2g26440	-3.97	Plant invertase/pectin methylesterase inhibitor superfamily	4.413E-19
250135_at	At5g15360	-3.94	unknown protein; Has 4 Blast hits to 4 proteins in 2 species: Archae - 0; Bacteria - 0; Metazoa - 0; Fungi - 0; Plants - 4; Viruses - 0; Other Eukaryotes - 0 (source: NCBI BLink).	2.920E-10
257625_at	At3g26230	-3.91	CYP71B24, cytochrome P450, family 71, subfamily B, polypeptide 24	5.710E-09
248327_at	At5g52750	-3.88	Heavy metal transport/detoxification superfamily protein	3.025E-16
248848_at	At5g46520	-3.86	Disease resistance protein (TIR-NBS-LRR class) family	1.433E-08
256336_at	At1g72030	-3.86	Acyl-CoA N-acyltransferases (NAT) superfamily protein	1.160E-15
245690_at	At5g04230	-3.81	ATPAL3, PAL3, phenyl alanine ammonia-lyase 3	2.579E-06
253945_at	At4g27050	-3.80	F-box/RNI-like superfamily protein	1.136E-19
257623_at	At3g26210	-3.78	CYP71B23, cytochrome P450, family 71, subfamily B, polypeptide 23	8.243E-17
251705_at	At3g56400	-3.75	ATWRKY70, WRKY70, WRKY DNA-binding protein 70	7.516E-11
253414_at	At4g33050	-3.75	EDA39, calmodulin-binding family protein	1.033E-13
258537_at	At3g04210	-3.67	Disease resistance protein (TIR-NBS class)	1.045E-14
266395_at	At2g43100	-3.65	ATLEUD1, IPMI2, isopropylmalate isomerase 2	9.123E-11
259560_at	At1g21270	-3.63	WAK2, wall-associated kinase 2	1.400E-10
252712_at	At3g43800	-3.52	ATGSTU27, GSTU27, glutathione S-transferase tau 27	3.544E-22
253911_at	At4g27300	-3.49	S-locus lectin protein kinase family protein	2.237E-25
246099_at	At5g20230	-3.46	ATBCB, BCB, BCB, SAG14, blue-copper-binding protein	5.289E-06
252060_at	At3g52430	-3.36	ATPAD4, PAD4, alpha/beta-Hydrolases superfamily protein	7.033E-07

Table II-4. Genes with significantly reduced expression in the aln-1 **mutant (continued).**

Affymetrix probe ID	AGI[a]	Fold change[b]	Gene symbol and description[c]	P-value[d]
256376_s_at	At1g66690	-3.34	S-adenosyl-L-methionine-dependent methyltransferases superfamily protein	1.219E-06
249843_at	At5g23570	-3.34	ATSGS3, SGS3, XS domain-containing protein / XS zinc finger domain-containing protein-related	2.664E-14
258419_at	At3g16670	-3.33	Pollen Ole e 1 allergen and extensin family protein	4.390E-10
256382_at	At1g66860	-3.32	Class I glutamine amidotransferase-like superfamily protein	3.460E-14
256596_at	At3g28540	-3.28	P-loop containing nucleoside triphosphate hydrolases superfamily protein	4.838E-08
247602_at	At5g60900	-3.28	RLK1, receptor-like protein kinase 1	5.753E-12
260745_at	At1g78370	-3.27	ATGSTU20, GSTU20, glutathione S-transferase TAU 20	1.747E-10
246293_at	At3g56710	-3.27	SIB1, sigma factor binding protein 1	3.155E-11
258277_at	At3g26830	-3.26	CYP71B15, PAD3, Cytochrome P450 superfamily protein	3.761E-05
248975_at	At5g45040	-3.26	Cytochrome c	2.017E-20
249481_at	At5g38900	-3.21	Thioredoxin superfamily protein	2.793E-06
251524_at	At3g58990	-3.21	IPMI1, isopropylmalate isomerase 1	6.946E-13
260396_at	At1g69720	-3.20	HO3, heme oxygenase 3	2.576E-08
254231_at	At4g23810	-3.17	ATWRKY53, WRKY53, WRKY family transcription factor	1.288E-11
258147_at	At3g18070	-3.16	BGLU43, beta glucosidase 43	1.110E-07
245592_at	At4g14540	-3.15	NF-YB3, nuclear factor Y, subunit B3	9.618E-11
263126_at	At1g78460	-3.13	SOUL heme-binding family protein	6.918E-19
248970_at	At5g45380	-3.12	ATDUR3, DUR3, solute:sodium symporters;urea transmembrane transporters	1.316E-16
255184_at	At4g07730	-3.12	transposable element gene	2.513E-06
252977_at	At4g38560	-3.08	Arabidopsis phospholipase-like protein (PEARLI 4) family	1.235E-04
253046_at	At4g37370	-3.07	CYP81D8, cytochrome P450, family 81, subfamily D, polypeptide 8	5.829E-09
264635_at	At1g65500	-3.06	unknown protein; FUNCTIONS IN: molecular_function unknown; INVOLVED IN: biological_process unknown; LOCATED IN: endomembrane system; EXPRESSED IN: 14 plant structures; EXPRESSED DURING: 9 growth stages; BEST Arabidopsis thaliana protein match is: unknown protein (TAIR:AT1G65486.1); Has 23 Blast hits to 23 proteins in 2 species: Archae - 0; Bacteria - 0; Metazoa - 0; Fungi - 0; Plants - 23; Viruses - 0; Other Eukaryotes - 0 (source: NCBI BLink).	8.677E-12
253411_at	At4g32980	-3.06	ATH1, homeobox gene 1	2.344E-12
252411_at	At3g47430	-3.05	PEX11B, peroxin 11B	4.476E-13
258897_at	At3g05730	-3.05	Encodes a defensin-like (DEFL) family protein.	1.976E-07
262381_at	At1g72900	-3.04	Toll-Interleukin-Resistance (TIR) domain-containing protein	8.690E-11
247812_at	At5g58390	-3.04	Peroxidase superfamily protein	2.089E-10
255319_at	At4g04220	-3.01	AtRLP46, RLP46, receptor like protein 46	7.219E-12
245454_at	At4g16920	-3.00	Disease resistance protein (TIR-NBS-LRR class) family	1.522E-08
261782_at	At1g76110	-3.00	HMG (high mobility group) box protein with ARID/BRIGHT DNA-binding domain	1.965E-12

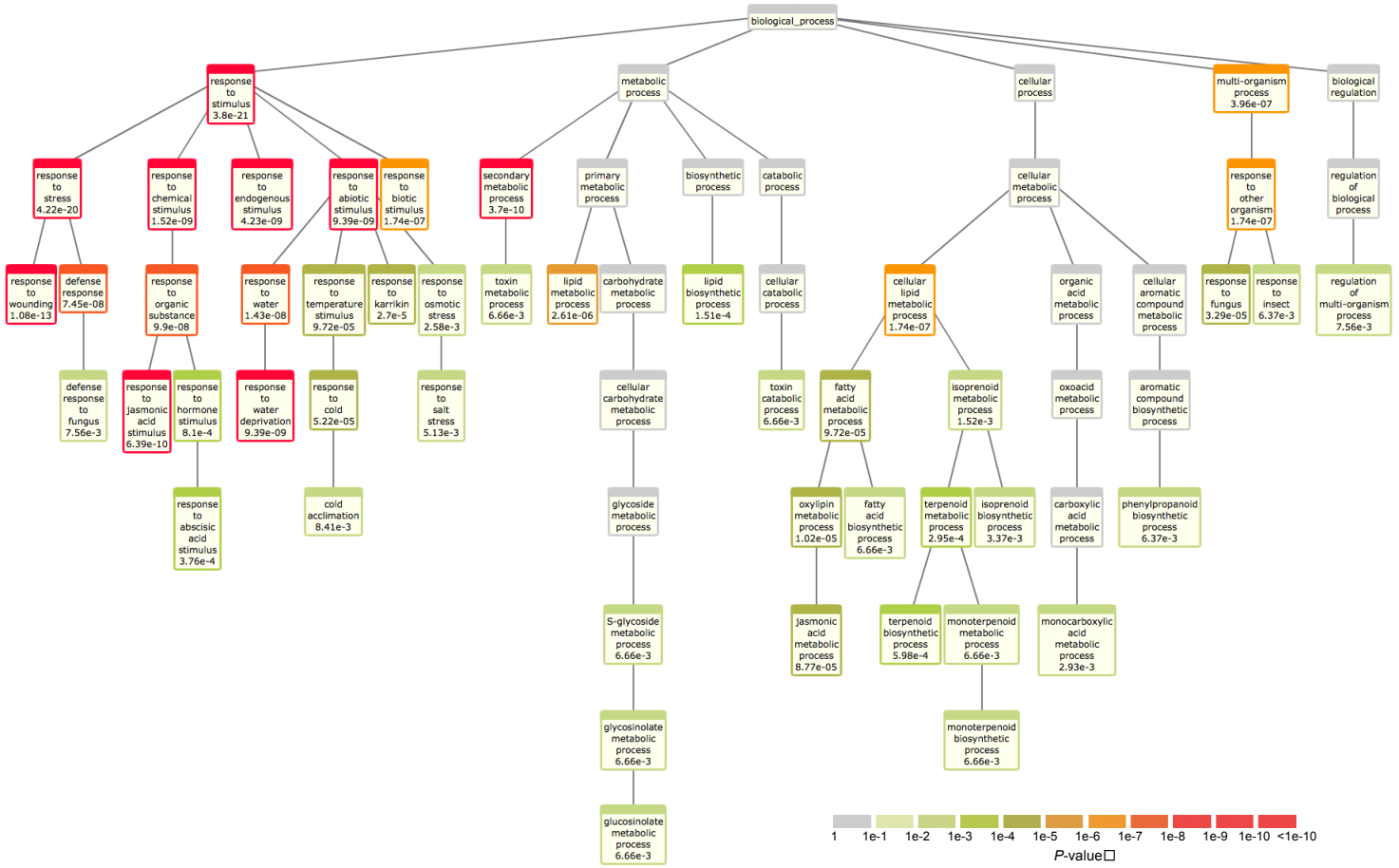

Figure II-1. Hierarchical tree graph of over-represented GO terms for genes with significantly increased expression in the *aln-1* mutant.

A total of 47 enriched GO terms under Biological Process were found for 211 genes with significantly increased expression (≥ 3-fold changes, Table II-3) using the BioMaps tool of VirtualPlant version 1.3 (Katari *et al*., 2010; http://virtualplant.bio.nyu.edu/cgi-bin/vpweb/) in the default-setting mode (Fisher's exact test with false discovery rate correction, $P < 0.01$). Each box shows the name of the GO term and, where appropriate, the P value (< 0.01) for the significance of enrichment. The P values are also indicated by the frame color of each box according to the gradient scale. The rank direction of the graph runs from top to bottom.

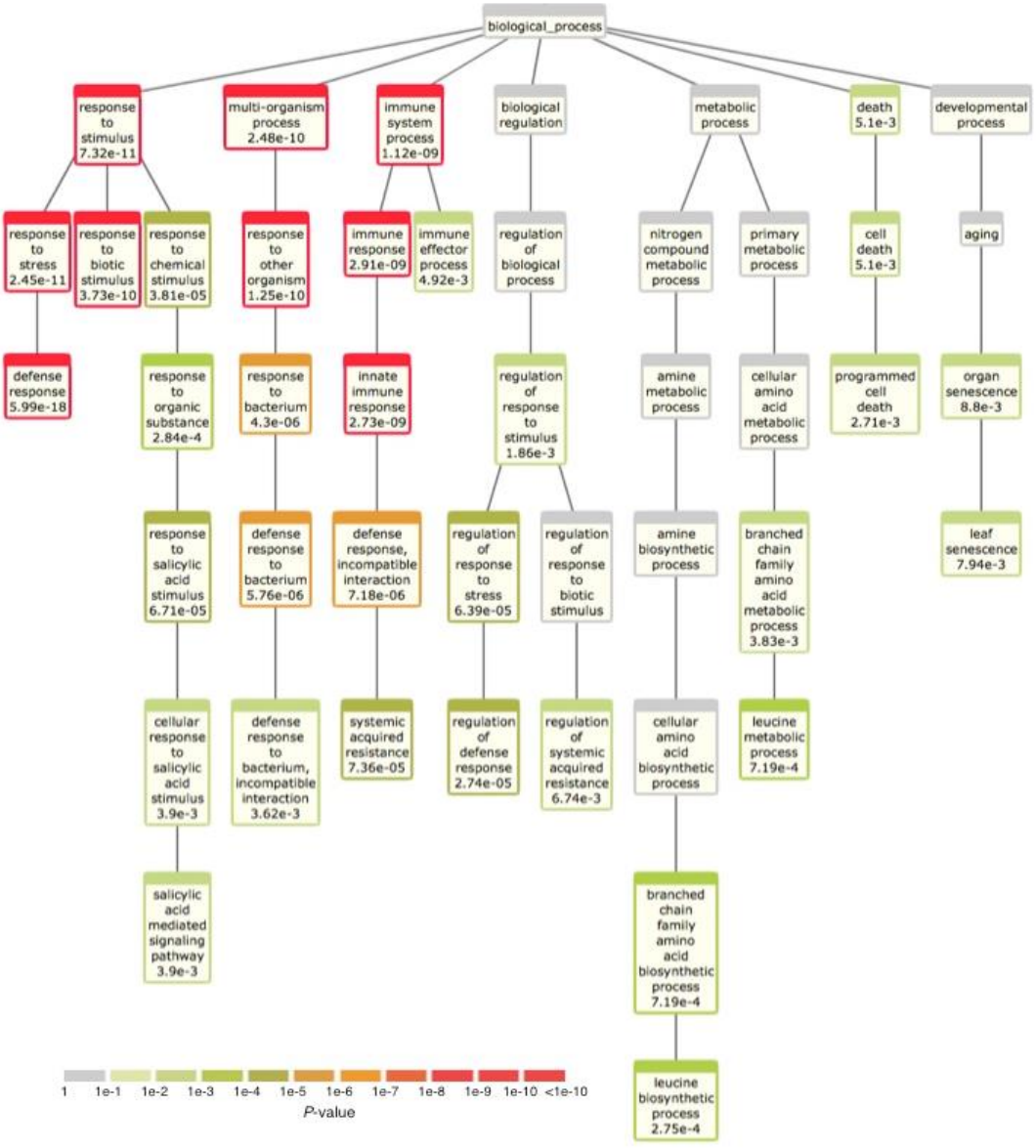

Figure II-2. Hierarchical tree graph of over-represented GO terms for genes with significantly reduced expression in the *aln-1* mutant.
A total of 33 enriched GO terms under Biological Process were found for 113 genes with significantly reduced expression (≥ 3-fold changes, Table II-4) using the BioMaps tool of VirtualPlant version 1.3 (Katari *et al*., 2010; http://virtualplant.bio.nyu.edu/cgi-bin/vpweb/) in the default-setting mode (Fisher's exact test with false discovery rate correction, $P < 0.01$). Each box shows the name of the GO term and, where appropriate, the *P* value (< 0.01) for the significance of enrichment. The *P* values are also indicated by the frame color of each box according to the gradient scale. The rank direction of the graph runs from top to bottom.

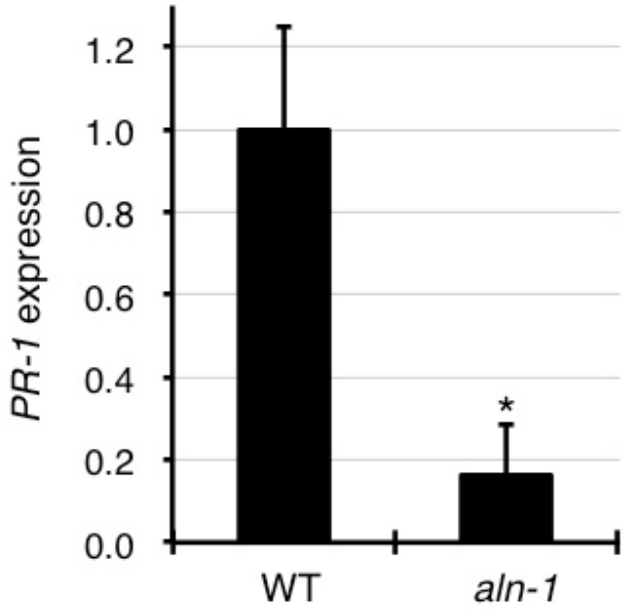

Figure II-3. Basal level expression of *PR-1* as a canonical SA marker. RNA was extracted from aerial parts of 2-week-old seedlings of WT and *aln-1* mutants grown under normal aseptic conditions. Relative mRNA levels were determined by real-time reverse transcription-quantitative PCR using *ACTIN2* expression as reference and presented as values relative to the WT level. The sequences of primers are listed in Supplementary Table S1. Data are means ± SEM from three independent experiments (*$P < 0.05$ by Student's *t*-test comparison to the WT level).

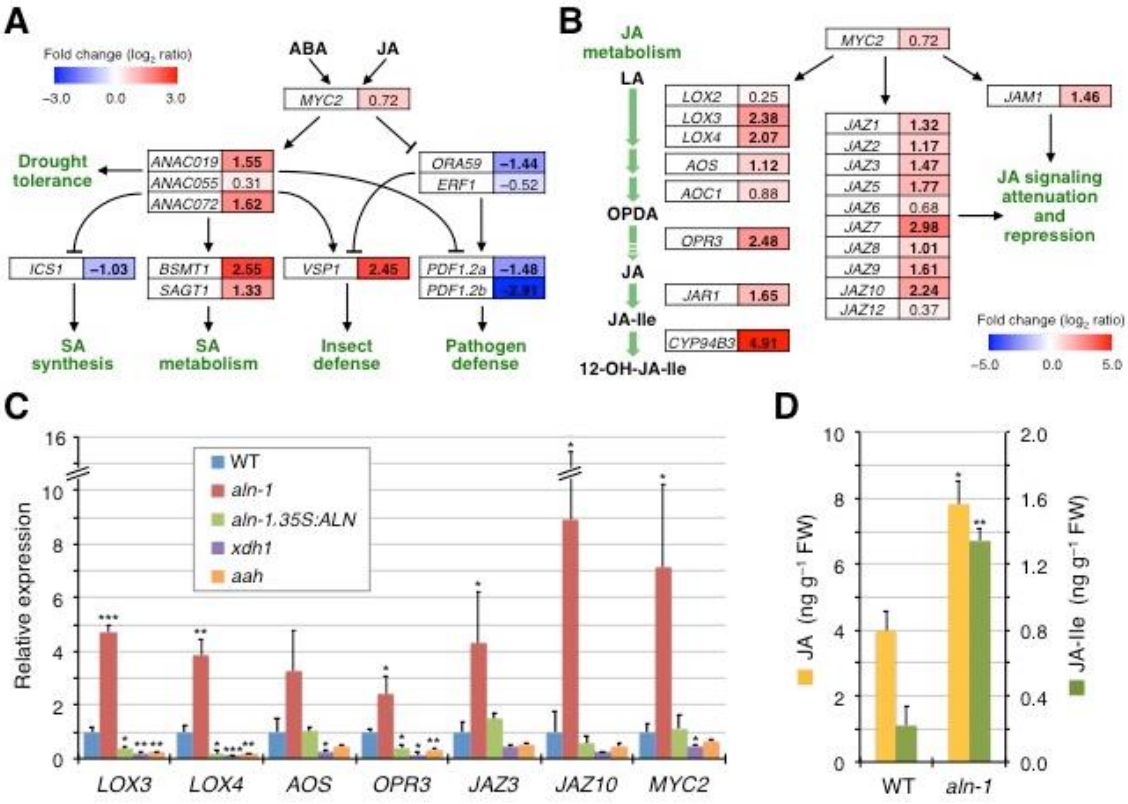

Figure II-4. The *aln-1* mutant shows altered levels of basal expression of MYC2-regulated JA-related genes and has enhanced JA and JA-Ile levels.
(A and B) Simplified schemes of MYC2-mediated signaling processes, with emphasis on JA–ABA and JA–SA crosstalk in abiotic and biotic responses (A; mostly based on Kazan and Manners, 2013) and MYC2-mediated transcriptional activation of genes for JA metabolic enzymes and those involved in JA signaling (B). Genes are indicated in open boxes, and their positive and negative actions are denoted by lines with an arrow and a bar end, respectively. For each gene, the microarray-based relative expression ratio (*aln-1* mutant versus the WT) is represented in $\log_2$ scale and by a boxed color on the blue-to-red gradient scale, with significant fold changes ($|\log_2(aln\text{-}1/\text{WT})| \geq 1$) in bold. Abbreviations not defined in the text are: LA, linolenic acid; OPDA, 12-oxo-phytodienoic acid; 12-OH-JA-Ile, 12-hydroxyjasmonoyl-l-isoleucine. (C) RT-qPCR for expression of the selected genes in the WT, three purine catabolic mutants (*aln-1*, *xdh1*, and *aah*), and the complemented mutant (*aln-1 35S:ALN*). RNA was extracted from the aerial parts of 2-week-old seedlings grown under normal aseptic conditions. Relative mRNA levels for each gene were determined using *ACTIN2* expression as reference and are presented as values relative to those of the WT. (D) Endogenous jasmonate levels of WT and *aln-1* mutants were quantified by LC-ESI-MS/MS in 2-week-old seedlings grown under normal aseptic conditions. In (C) and (D), data are means ±SE from three independent experiments, and asterisks denote significant differences between WT and mutant plants (*$P < 0.05$; **$P < 0.01$; ***$P < 0.001$ by Student's *t*-test).

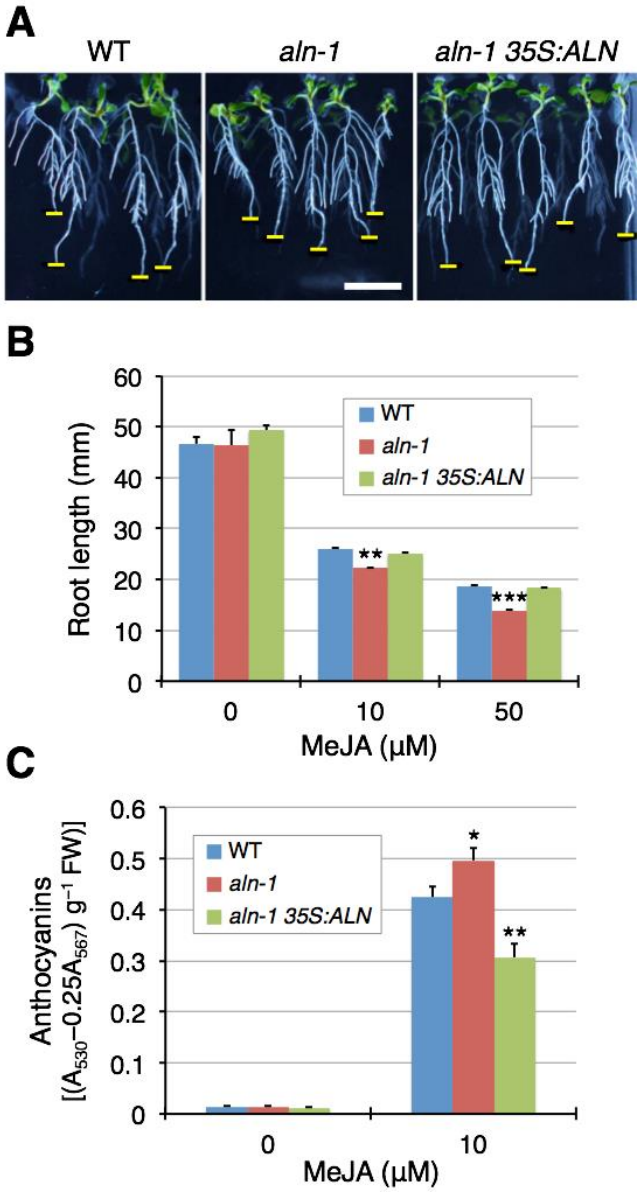

Figure II-5. The *aln-1* mutant exhibits increased sensitivity to exogenous MeJA.
Sterile seedlings of the WT, *aln-1* mutant, and the complemented mutant (*aln-1 35S:ALN*) were grown for 8 d on standard medium supplemented with MeJA and examined for root growth and anthocyanin accumulation. (A) Typical root growth in the presence of 10 µM MeJA. Horizontal bars indicate a scale of 10mm in length (thick) and the position of a primary root tip (thin). (B) Primary root length in the presence of 10 µM and 50 µM MeJA. Data are means ±SE ($n \geq 16$). (C) Anthocyanin levels in the presence of 10 µM MeJA. Data are means ±SE (n=8). Asterisks denote significant differences between WT and mutant plants (*$P < 0.05$; **$P < 0.01$; ***$P < 0.001$ by Student's t-test).

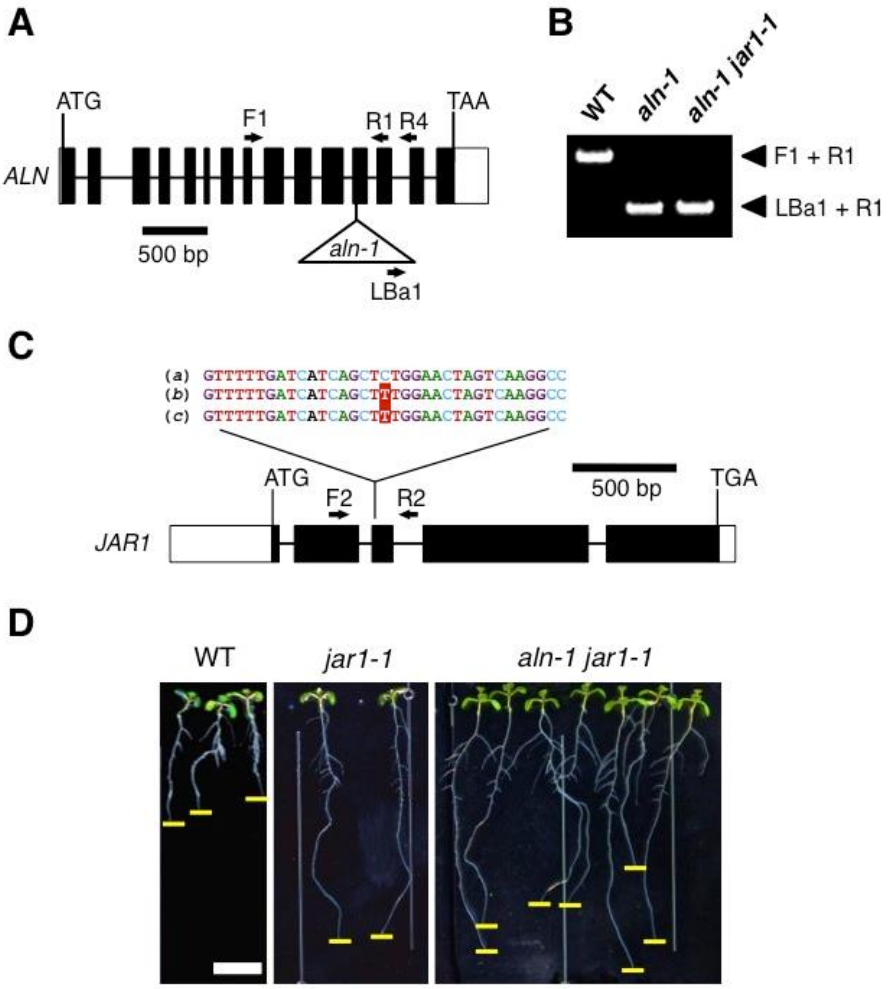

Figure II-6. Characterization of the *aln-1 jar1-1* double mutant.
The homozygous mutants of *aln-1* (SALK_000325; Yang and Han, 2004; Watanabe *et al.*, 2014) and *jar1-1* (CS8072; Staswick *et al.*, 1992) were crossed to obtain the double mutant *aln-1 jar1-1*. (A) Diagram of the T-DNA insertion in the *ALN* gene in the *aln-1* mutant. Arrows denote PCR primers. (B) PCR-based genotyping of the double mutant using primers specific to *ALN* (F1 and R1) and the left border sequence of T-DNA (LBa1). (C) Diagram of the *JAR1* gene structure and the confirmation of the *jar1-1* mutation in the double mutant. The nucleotide sequence of the wild-type *JAR1* allele (*a*) from TAIR (At2g46370; https://www.arabidopsis.org/) was compared to that of the double mutant, as determined by dideoxy sequencing with primers F2 (*b*) and R2 (*c*), to confirm the single nucleotide missense mutation that occurs in exon 3 (Staswick *et al.*, 2002). The sequences of primers are listed in Table II-1. (D) Typical root growth of 8-day-old seedlings of WT, *jar1-1*, and *aln-1 jar1-1* genotypes in the presence of 10 μM methyl jasmonate (MeJA). Note that the root growth of the *jar1-1* mutant is moderately insensitive to MeJA (Staswick *et al.*, 1992, 2002). Horizontal bars indicate a scale of 10 mm in length (white) and the position of a primary root tip (yellow).

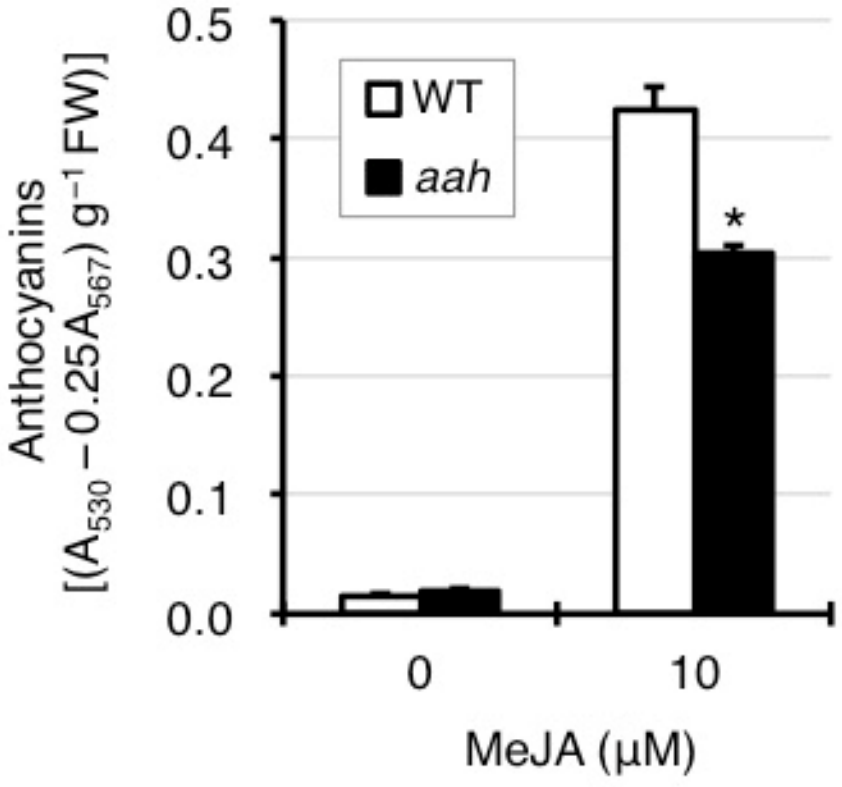

Figure II-7. Reduced response to MeJA of anthocyanin accumulation in the *aah* mutant.
Sterile seedlings of WT and the *aah* mutant were grown for 8 days on standard medium supplemented with 10 μM MeJA and examined for anthocyanin accumulation as described in the main text. FW, fresh weight. Data are means ± SEM ($n = 8$; *$P < 0.001$ by Student's *t*-test comparison to the WT levels).

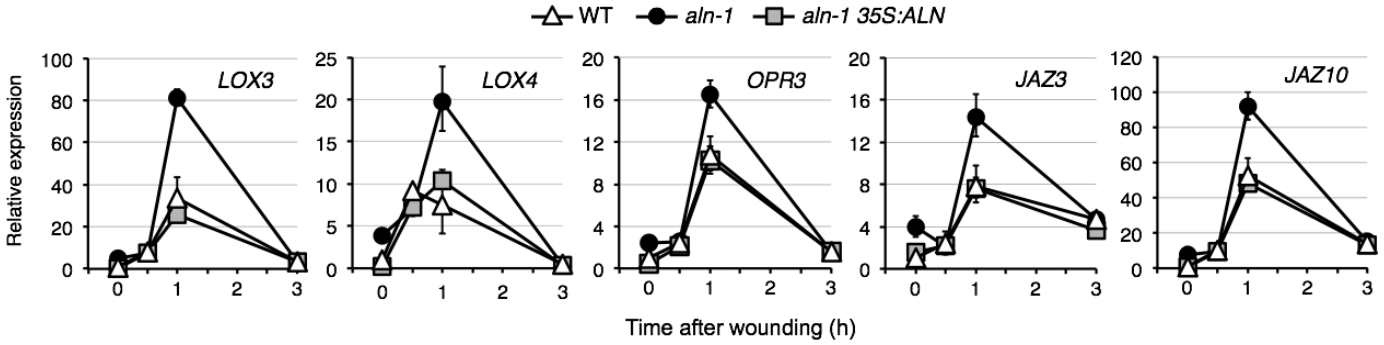

Figure II-8. The *aln-1* mutant enhances wounding-inducible expression of genes involved in JA biosynthesis and signaling.
RNA was extracted from aerial parts of 2-week-old seedlings of the WT, *aln-1* mutant, and the complemented mutant (*aln-1 35S:ALN*) at the indicated time points after wounding of rosette leaves. Relative mRNA levels were determined as described in Fig. 1C and are presented as values relative to those of the WT at zero time. Data are means ±SE from three independent experiments.

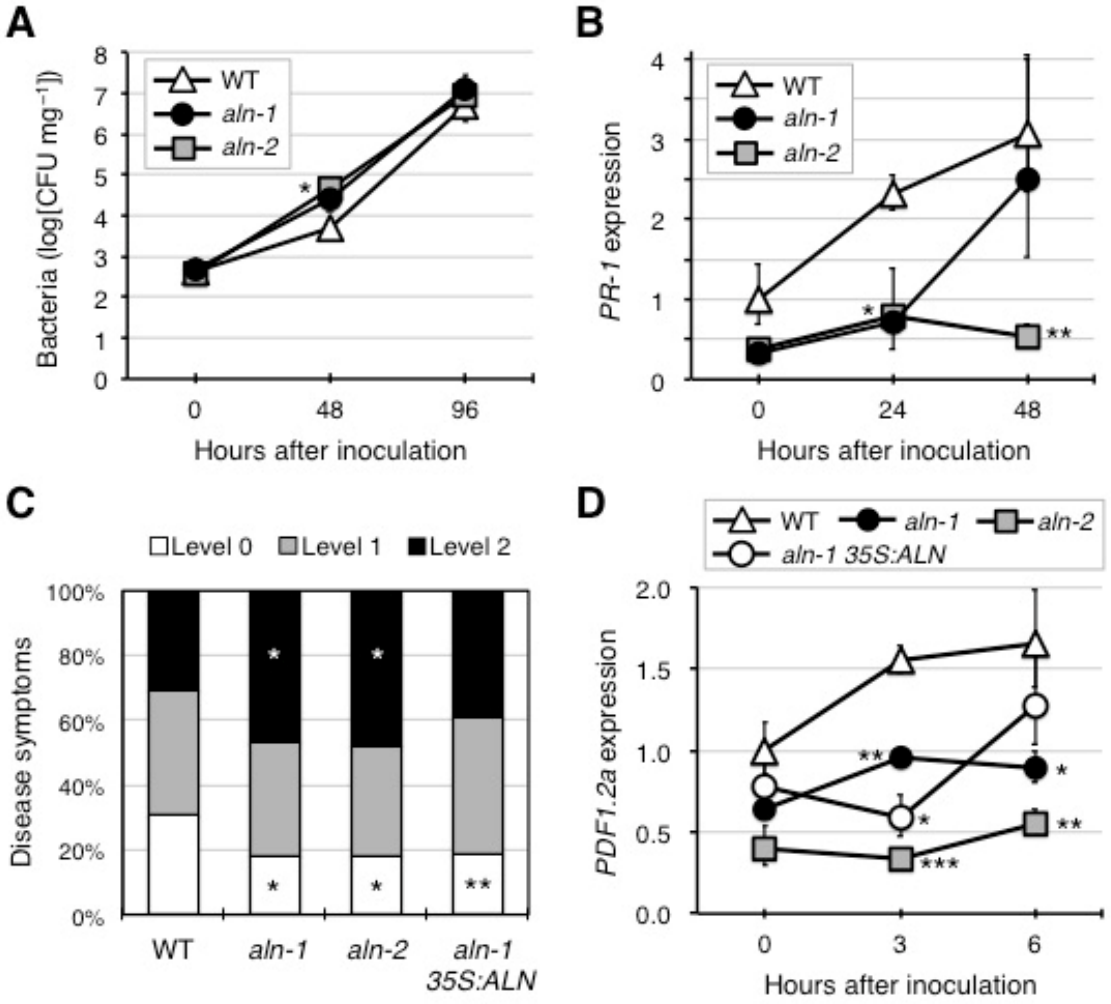

Figure II-9. Effect of *aln* mutations on resistance to bacterial pathogens.
(A) Resistance to *Pst* DC3000 was evaluated for 2-week-old seedlings of the WT and two allelic *aln* mutants (*aln-1* and *aln-2*). At 48 and 96 hpi, internal bacterial populations were determined as mg^{-1} FW of whole rosettes (n = 4). (B) Time-course expression of the SA marker *PR-1* in leaves inoculated with *Pst* DC3000. Relative mRNA levels were determined as described in Fig. 1C and are presented as values relative to those of the WT at zero time. Data are means ±SE from three independent experiments. (C) Resistance to *Pcc* EC1 was evaluated for leaves from 2-week-old seedlings of the WT, two allelic *aln* mutants, and the complemented mutant (*aln-1 35S:ALN*). Disease symptoms were scored at 24 hpi according to three criteria: level 0, no symptoms; level 1, symptoms restricted within the inoculated region; level 2, symptoms extended over the inoculated region ($n \geq 169$). (D) Time-course expression of the ERF branch marker *PDF1.2a* in leaves inoculated with *Pcc* EC1 was determined as described in (B). Asterisks denote significant differences between WT and mutant plants [*$P < 0.05$; **$P < 0.01$; ***$P < 0.001$ by Student's t-test, except in (C), where Fisher's exact test was used].

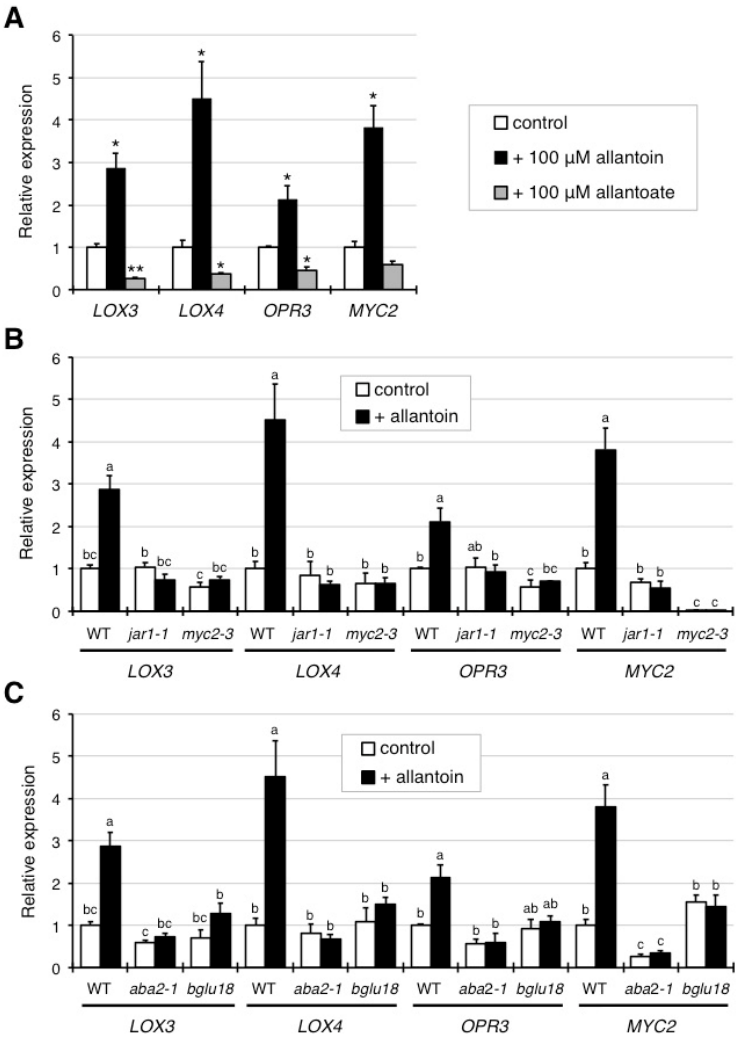

Figure II-10. Exogenous allantoin induces JA-responsive gene expression in an ABA-dependent manner.
(A) Effects of exogenous allantoin and allantoate on JA-responsive gene expression in the WT. RNA was extracted from aerial parts of sterile seedlings that had been grown for 2 weeks on standard medium containing allantoin or allantoate at 100 µM, and relative mRNA levels for each gene were determined as described in Fig. 1C. Data are means ±SE from three independent experiments, and asterisks denote significant differences between control and treated seedlings (*$P < 0.01$; **$P < 0.001$ by Student's *t*-test). (B and C) Effect of exogenous allantoin on JA-responsive gene expression in bioactive JA-deficient *jar1-1* and JA-insensitive *myc2-3* mutants (B), and in ABA-deficient *aba2-1* and *bglu18* mutants (C). WT data are the same as presented in (A) and are shown for comparison. Data are means ±SE from three independent experiments, and different letters indicate significant differences ($P < 0.05$ by Tukey's test).

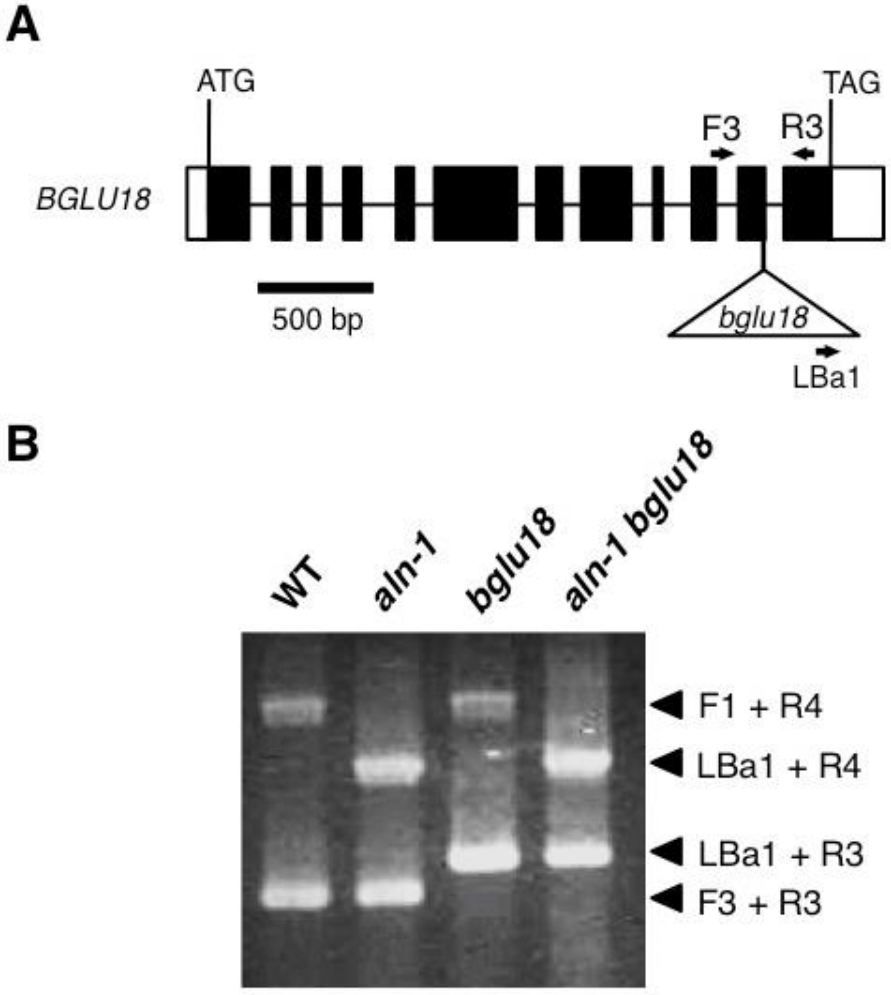

Figure II-11. Characterization of the *aln-1 bglu18* double mutant.
The homozygous mutants of *aln-1* (SALK_000325; Yang and Han, 2004; Watanabe *et al.*, 2014) and *bglu18* (SALK_075731C; Ogasawara *et al.*, 2009) were crossed to obtain the double mutant *aln-1 bglu18*. (A) Diagram of the T-DNA insertion in the *BGLU18* gene in the *bglu18* mutant. Arrows denote PCR primers. (B) PCR-based genotyping of the double mutant using primers specific to *ALN* (F1 and R4; see Supplementary Fig. S5), *BGLU18* (F3 and R3), and the left border sequence of T-DNA (LBa1). The sequences of primers are listed in Table II-1.

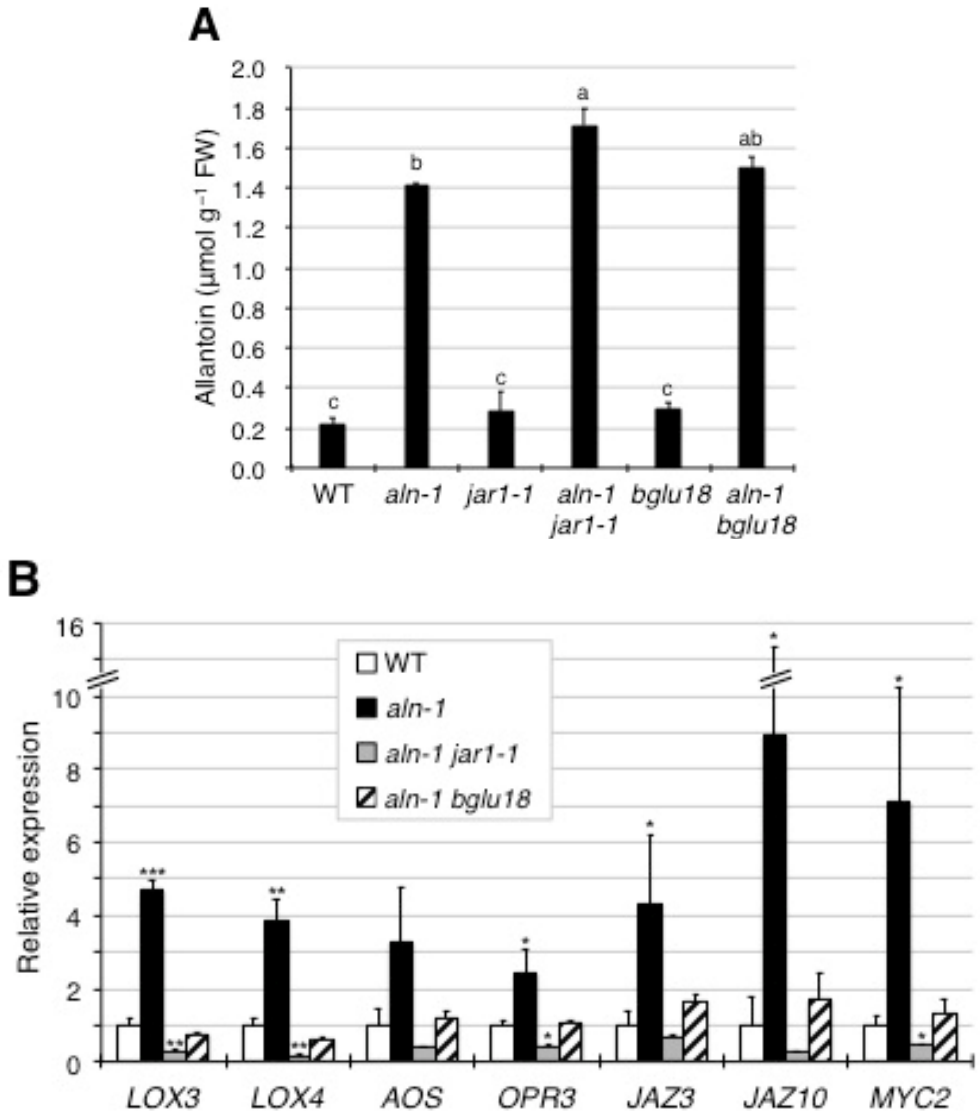

Figure II-12. The *aln* mutation activates JA-responsive gene expression in an ABA-dependent manner.
(A) Endogenous allantoin levels in aseptically grown 2-week-old seedlings of JA- and ABA-related single and double mutants. Data are means ±SE from three independent experiments, and different letters indicate significant differences ($P < 0.05$ by Tukey's test). (B) RT-qPCR was performed for RNA samples extracted from the aerial parts of 2-week-old sterile seedlings of *aln-1 jar1-1* or *aln-1 bglu18* double mutants. Relative mRNA levels for each gene were determined and are presented as values relative to WT data that are taken from Fig. II-4C, to simplify comparison. Data are means ±SE from three independent experiments, and asterisks denote significant differences between WT and mutant plants (*$P < 0.05$; **$P < 0.01$; ***$P < 0.001$ by Student's *t*-test).

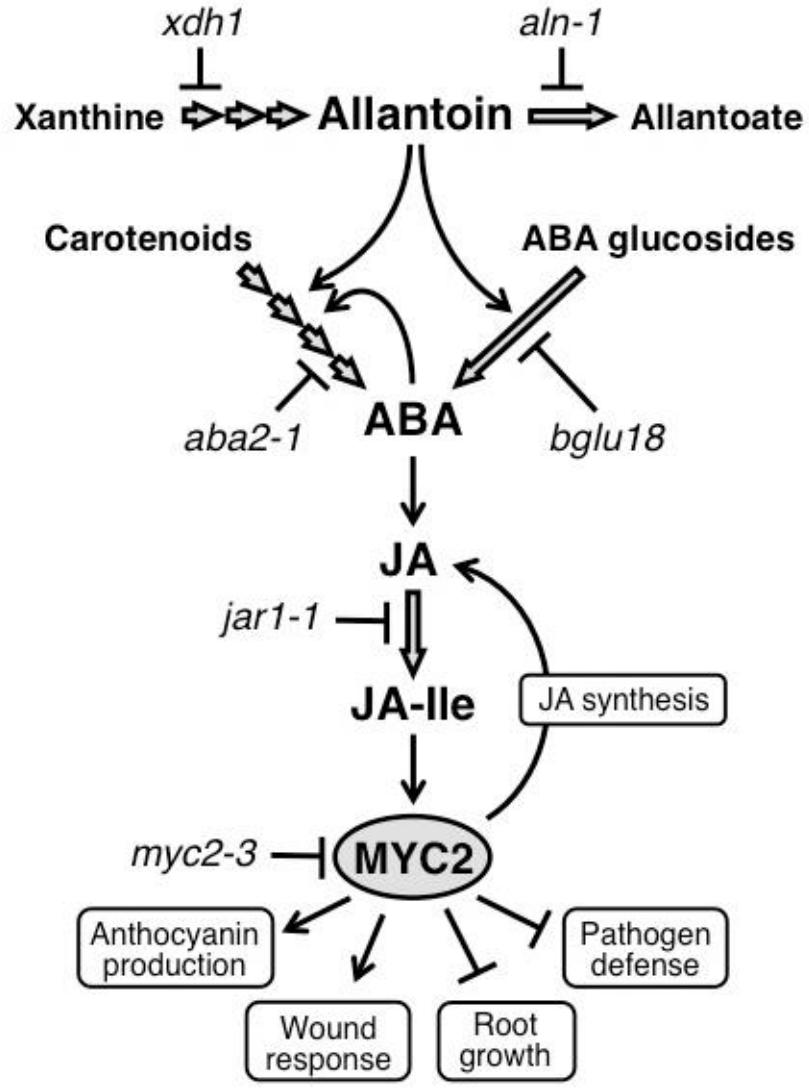

Figure II-13. Schematic model for how allantoin activates JA responses in Arabidopsis. Accumulation of allantoin causes enhanced ABA levels through *de novo* synthesis from carotenoids and/or hydrolytic conversion from inactive ABA glucosides, thereby activating ABA-dependent JA responses mediated by MYC2. The effect of allantoin on *de novo* synthesis may be indirect due to positive feedback of ABA released from the inactive pool (Watanabe *et al.*, 2014*b*). The open arrows indicate metabolic routes, and lines with arrows and bar ends represent positive and negative causal relationships, respectively.

GENERAL CONCLUSIONS

Plants are rich in diverse metabolic pathways compared with other organisms (Keurentjes *et al.*, 2006). Thanks to great wealth of metabolic diversity, plants are able to adapt to constantly changing environments; however, physiological functions and significance of many metabolic pathways remain yet to be elucidated.

Purine catabolism is regarded as a housekeeping metabolic pathway that is widely conserved in plants. Although recent efforts have identified genes for enzymes involved in this catabolism, the general role of this pathway is still obscure. The main function of purine catabolism has been thought as N recycling and remobilization, since it releases four molar equivalents of ammonia after complete oxidation of a purine ring. It has not been experimentally shown that, however, purine catabolism substantially contributes to efficient N utilization (Werner and Witte, 2011). Apart from N recycling and remobilization, the evidence for the stress-physiological roles of purine catabolism recently emerged. The mode of action of purine catabolism in stress adaptation, however, also remains largely unexplored. These research backgrounds suggested that purine catabolism might play two different parts in plants: growth maintenance and stress responses. To address this, I conducted the detailed analyses on both N-recycling and stress-physiological roles of purine catabolism.

In CHPTER I, using Arabidopsis knockout mutants defective in ureide degradation and transport, I evaluated the physiological importance of purine catabolism in efficient N utilization. Arabidopsis mutants defective in ALN and AAH (*aln-1*, *aln-2* and *aah*) exhibited N deficiency-like symptoms

such as early flowering and senescence, and impaired plant growth and fertility. The growth reduction tended to be more severe under N-deficient conditions. Moreover, N-use efficiency was significantly decreased in these ureide degradation mutants compared with WT plants, suggesting that purine catabolism substantially contributes to efficient N utilization. To test the possibility that ureides are involved in sink–source N remobilization, I examined ureide contents in various organs of WT and degradation mutants. Results showed that allantoate accumulated in upper parts (inflorescence stem and silique) with the progression of senescence. Interestingly, the mutants defective in ureide transporters (*ups1* and *ups2*) significantly decreased allantoate levels in upper parts, and showed early flowering and growth impairment like the degradation mutants, implying that allantoate is the main vehicle for N remobilization derived from purine catabolism in Arabidopsis. Consistent with this, gene expression study revealed that Arabidopsis upregulated genes involved in allantoate biosynthesis (*XDH1* and *ALN*) and ureide transport (*UPS1* and *UPS2*) during natural senescence. Taken together, these lines of evidence obtained through this study suggest that ureide degradation and transport contribute to efficient N utilization in Arabidopsis.

In CHAPTER II, I investigated the effect of allantoin accumulation in plant hormone responses, since allantoin is a metabolic intermediate that often accumulates in stressed plants, and it was recently shown in Arabidopsis that allantoin activates ABA production, thereby stimulating stress-related gene expression and enhancing the seedling tolerance to abiotic stress. A detailed re-examination of the microarray data of an allantoin-accumulating *aln-1* confirmed the increased expression of

ABA-related genes and also revealed altered expression of genes involved in JA responses, probably under the control of MYC2, a master switch in the JA signaling pathway. Consistent with the transcriptome profiles, the *aln-1* mutant displayed increased JA levels and enhanced responses to mechanical wounding and exogenous JA. Moreover, *aln* mutants demonstrated modestly increased susceptibility to *Pst* DC3000 and *Pcc* EC1, probably reflecting the antagonistic action of MYC2 on the defense against these bacterial phytopathogens. Exogenously administered allantoin elicited the expression of JA-responsive genes, including *MYC2*, in WT plants, supporting the idea that allantoin might be responsible for the observed JA-related phenotypes of *aln* mutants. However, mutants deficient in bioactive JA (*jar1-1*), insensitive to JA (*myc2-3*), or deficient in ABA (*aba2-1* and *bglu18*) suppressed the effect of exogenous allantoin. The suppression was further confirmed in *aln-1 jar1-1* and *aln-1 bglu18* double mutants. These results indicate that allantoin can activate the MYC2-regulated JA signaling pathway through ABA production. Overall, this study suggests a possible connection of purine catabolism with stress hormone homeostasis and signaling, and highlights the potential importance of allantoin in these interactions.

To summarize, this study demonstrated that purine catabolism might be involved in both efficient N utilization and stress hormone responses (Fig. 4). In Arabidopsis plants exposed to environmental stresses, allantoin is accumulated and then leads to enhanced ABA and JA responses. Synergetic interactions of ABA and JA enhance MYC2 activity, which generally results in contrasting effects on biotic stress responses: increased resistance to insect herbivores and suppression of pathogen defenses. Probably, allantoin

is involved in the fine-tuning of hormone responses to optimize plant fitness in environmental adversity. On the other hand, in plants grown on normal growth conditions or those released from stress conditions, degradation of purine compounds might provides substantial amounts of N nutrition that is required for plant growth and reproduction. Such a dual function of purine catabolism may enable sessile plants to efficiently adapt to constantly changing environment and nutrient availability.

Finally, this study has pointed out the possible importance of the multifunctionality of plant metabolism for the survival in nature. I hope that this concept contributes to better understanding of plant surviving strategy in the future.

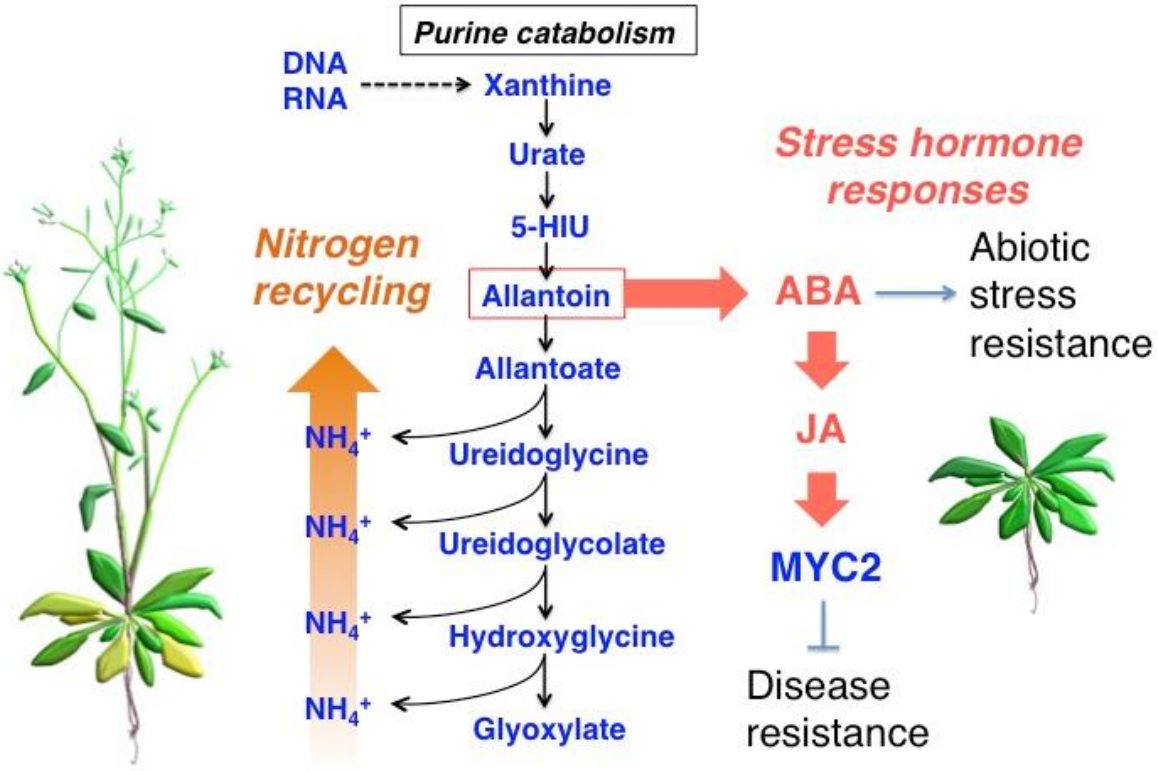

Figure 4. Possible model for the dual role of purine catabolism. Allantoin is accumulated in stress conditions and enhances ABA and JA responses. ABA contributes to abiotic stress resistance, and JA activates MYC2 activity and suppresses disease resistance. In plants grown under normal conditions or those released from stress conditions, purine catabolism provides N nutrition for sustaining healthy growth.

Acknowledgements

I would like to express my sincere thanks to my academic adviser, Professor Atsushi Sakamoto, Hiroshima University, for giving me a chance to perform research in his laboratory. Thanks to his repeated encouragement and support, I could continue my research without inconvenience. I greatly appreciate his critical thinking and writing skills that helped me to become an independent researcher.

I thank Dr. Hiroshi Shimada for not only his academic advices but also his great efforts to provide lab members a pleasant working environment. He always took lead in solving problems in the laboratory such as instrument faults.

I want to offer my appreciation to all my collaborators in other universities. Dr. Yasuhiro Ishiga, University of Tsukuba, helped me for bacterial infection tests, which provided me a breakthrough in this research. Without his experimental technics, I could not have done this work. Further thanks must be given to Dr. Takashi Hirayama, Dr. Izumi C. Mori and Takazu Matsuura, Okayama University, for supporting me for phytohormone measurements. They also hosted me in a great training course held in Okayama University. Thanks to this, I could see many great scientists including Dr. Ishiga. I wish to also thank Dr. Hironori Kaminaka and Dr. Mayumi Egusa, Tottori University, for bacterial infection tests and their kind advices. I also thank Dr. Tomokazu Konishi, Akita Prefectural University, for professional microarray analysis, which prompted me to start the study about JA. Dr. Masaru Nakata , NARO Agricultural Research Center, gave me kind advices on the experimental procedures for exogenous MeJA

treatments.

I would like to thanks current and former lab members for helping me, especially Dr. Shunsuke Watanabe, RIKEN Center for Sustainable Resource Science, who made a base of this work. He also taught me a lot of experimental methods.

Thank you, all of my family members. They are always best supporters of mine.

This study was supported by Japanese Society for Promotion of Science (JSPS) Fellowship for Young Scientists (DC1, 26-5367) and Graduate Student Research Grant of Hiroshima University Alumni Association.

References

Abe H, Yamaguchi-Shinozaki K, Urao T, Iwasaki T, Hosokawa D, Shinozaki K (1997) Role of Arabidopsis MYC and MYB homologs in drought- and abscisic acid-regulated gene expression. *The Plant Cell* **9:** 1859–1868.

Adie BAT, Pérez-Pérez J, Pérez-Peréz MM, Godoy M, Sánchez-Serrano J-J, Schmelz EA, Solano R (2007) ABA is an essential signal for plant resistance to pathogens affecting JA biosynthesis and the activation of defenses in Arabidopsis. *The Plant Cell* **19:** 1665–1681.

Alamillo JM, Díaz-Leal JL, Sánchez-Moran MV, Pineda M (2010) Molecular analysis of ureide accumulation under drought stress in *Phaseolus vulgaris* L. Plant, Cell & Environment **33:** 1828–1837.

Anderson JP, Badruzsaufari E, Schenk PM, Manners JM, Desmond OJ, Ehlert C, Maclean DJ, Ebert PR, Kazan K (2004) Antagonistic interaction between abscisic acid and jasmonate-ethylene signaling pathways modulates defense gene expression and disease resistance in Arabidopsis. *The Plant Cell* **16:** 3460–3479.

Brychkova G, Alikulov Z, Fluhr R, Sagi M (2008) A critical role for ureides in dark and senescence-induced purine remobilization is unmasked in the *Atxdh1* Arabidopsis mutant. *The Plant Journal* **54:** 496–509.

Bu Q, Jiang H, Li C, Zhai Q, Zhang J, Wu X, Sun J (2008) Role of the *Arabidopsis thaliana* NAC transcription factors ANAC019 and ANAC055 in regulating jasmonic acid-signaled defense responses. *Cell Research* **18:** 756–767.

Buchanan-Wollaston V (1997) The molecular biology of leaf senescence. *Journal of Experimental Botany* **48:** 181–199.

Carrión CA, Costa ML, Martínez DE, Mohr C, Humbeck K, Guiamet JJ (2013) *In vivo* inhibition of cysteine proteases provides evidence for the involvement of "senescence-associated vacuoles" in chloroplast protein degradation during dark-induced senescence of tobacco leaves. *Journal of Experimental Botany* **64:** 4967–4980.

Chaffei C, Pageau K, Suzuki A, Gouia H, Ghorbel MH, Masclaux-Daubresse C (2004) Cadmium toxicity induced changes in nitrogen management in *Lycopersicon esculentum* leading to a metabolic safeguard through an amino acid storage strategy. *Plant and Cell Physiology* **45:** 1681–1693.

Chen THH, Murata N (2002) Enhancement of tolerance of abiotic stress by metabolic engineering of betaines and other compatible solutes. *Current Opinion in Plant Biology* **5:** 250–257.

Chini A, Fonseca S, Fernández G, Adie B, Chico JM, Lorenzo O, García-Casado, López-Vidriedo I, Lozano FM, Ponce MR, Micol PJL,

Solano R (2007) The JAZ family of repressors is the missing link in jasmonate signalling. *Nature* **448:** 666–671.

Chung HS, Koo AJK, Gao X, Jayanty S, Thines B, Jones AD, Howe GA (2008) Regulation and function of Arabidopsis *JASMONATE ZIM*-Domain genes in response to wounding and herbivory. *Plant Physiology* **146:** 952–964.

Collier R, Tegeder M (2012) Soybean ureide transporters play a critical role in nodule development, function and nitrogen export. *The Plant Journal* **72:** 355–367.

Coneva V, Simopoulos C, Casaretto JA, El-keremy A, Guevara DR, Cohn J, Zhu T, Guo L, Alexander DC, Bi Y-M, McNicholas PD Rothstein SJ (2014) Metabolic and co-expression network-based analyses associated with nitrate response in rice. *BMC Genomics* **15:** 1056.

Dahncke K, Witte C-P (2013) Plant purine nucleoside catabolism employs a guanosine deaminase required for the generation of aanthosine in *Arabidopsis*. *The Plant Cell* **25:** 4101–4109.

Datta DB, Triplett EW, Newcomb EH (1991) Localization of xanthine dehydrogenase in cowpea root nodules: implications for the interaction between cellular compartments during ureide biogenesis. *Proceedings of the National Academy of Sciences of the United States of America* **88:** 4700–4702.

Desimone M, Catoni E, Ludewig U, Hilpert M, Schneider A, Kunze R, Tegeder M, Frommer WB, Schumacher K (2002) A novel superfamily of transporters for allantoin and other oxo derivatives of nitrogen heterocyclic compounds in Arabidopsis. *The Plant Cell* **14:** 847–856.

Díaz-Leal JL, Gálvez-Valdivieso G, Fernández J, Pineda M, Alamillo JM (2012) Developmental effects on ureide levels are mediated by tissue-specific regulation of allantoinase in *Phaseolus vulgaris* L. *Journal of Experimental Botany* **63:** 4095–4106.

Dombrecht B, Xue GP, Sprague SJ, Kirkegaard JA, Ross JJ, Reid JB, Fitt GP, Sewelam N, Schenk PM, Manners JM, Kazan K (2007) MYC2 differentially modulates diverse jasmonate-dependent functions in Arabidopsis. *The Plant Cell* **19:** 2225–2245.

Evans JR, Seemann JR (1989) The allocation of protein nitrogen in the photosynthetic apparatus: costs, consequences, and control. In B WR, ed, Photosynthesis. Alan R Liss, Inc, New York, pp 183-205.

Fan J, Hill L, Crooks C, Doerner P, Lamb C (2009) Abscisic acid has a key role in modulating diverse plant-pathogen interactions. *Plant Physiology* **150:** 1750–1761.

Fernández-Calvo P, Chini A, Fernández-Barbero G, *et al*. (2011) The Arabidopsis bHLH transcription factors MYC3 and MYC4 are targets of JAZ repressors and act additively with MYC2 in the activation of

jasmonate responses. *The Plant Cell* **23:** 701–715.

García-Andrade J, Ramírez, V, Flors V, Vera P (2011) Arabidopsis *ocp3* mutant reveals a mechanism linking ABA and JA to pathogen-induced callose deposition. *The Plant Journal* **67:** 783–794.

Glantzounis GK, Tsimoyiannis EC, Kappas AM, Galaris DA (2005) Uric acid and oxidative stress. *Current Pharmaceutical Design* **11:** 4145–4151.

Gojon A, Krouk G, Perrine-Walker F, Laugier E (2011) Nitrate transceptor(s) in plants. *Journal of Experimental Botany* **62:** 2299–2308.

Good AG, Shrawat AK, Muench DG (2004) Can less yield more ? Is reducing nutrient input into the environment compatible with maintaining crop production? *Trends in Plant Science* **9:** 597–605.

Hauck OK, Scharnberg J, Escobar NM, Wanner G, Giavalisco P, Witte CP (2014) Uric acid accumulation in an Arabidopsis urate oxidase mutant impairs seedling establishment by blocking peroxisome maintenance. *The Plant Cell* **26:** 3090– 3100.

Hesberg C, Hänsch R, Mendel RR, Bittner F (2004) Tandem orientation of duplicated xanthine dehydrogenase genes from Arabidopsis thaliana: Differential gene expression and enzyme activities. *Journal of Biological Chemistry* **279:** 13547–13554.

Higashi K, Ishiga Y, Inagaki Y, Toyoda K, Shiraishi T, Ichinose Y (2008)

Modulation of defense signal transduction by flagellin-induced WRKY41 transcription factor in *Arabidopsis thaliana*. *Molecular Genetics and Genomics* **279:** 303–312.

Hirel B, Bertin P, Quilleré I, Bourdoncle W, Attagnant C, Dellay C, Gouy A, Cadiou S, Retailliau C, Falque M, Gallais A (2001) Towards a better understanding of the genetic and physiological basis for nitrogen use efficiency in maize. *Plant physiology* **125:** 1258–1270.

Hiruma K, Nishiuchi T, Kato T, Bednarek P, Okuno T, Schulze-Lefert P, Takano Y (2011) *Arabidopsis ENHANCED DISEASE RESISTANCE 1* is required for pathogen-induced expression of plant defensins in nonhost resistance, and acts through interference of *MYC2*-mediated repressor function. *The Plant Journal* **67:** 980–992.

Hu Y, Jiang L, Wang F, Yu D (2013) Jasmonate regulates the INDUCER OF CBF EXPRESSION-C-REPEAT BINDING FACTOR/DRE BINDING FACTOR1 cascade and freezing tolerance in *Arabidopsis*. *The Plant Cell* **25:** 2907–2924.

Huang D, Wu W, Abrams SR, Cutler AJ (2008) The relationship of drought-related gene expression in *Arabidopsis thaliana* to hormonal and environmental factors. *Journal of Experimental Botany* **59:** 2991–3007.

Hussain SS, Ali M, Ahmad M, Siddique KH (2011) Polyamines: natural and engineered abiotic and biotic stress tolerance in plants. *Biotechnology Advances* **29:** 300–311.

Irani S, Todd CD (2016) Ureide metabolism under abiotic stress in *Arabidopsis thaliana*. *Journal of Plant Physiology* **199:** 87–95.

Ishida H, Yoshimoto K, Izumi M, Reisen D, Yano Y, Makino A, Ohsumi Y, Hanson MR, Mae T (2008) Mobilization of rubisco and stroma-localized fluorescent proteins of chloroplasts to the vacuole by an *ATG* gene-dependent autophagic process. *Plant Physiology* **148:** 142–155.

Ishiga Y, Ishiga T, Uppalapati SR, Mysore KS (2011) *Arabidopsis* seedling flood-inoculation technique: a rapid and reliable assay for studying plant-bacterial interactions. *Plant Methods* **7:** 32.

Kadota Y, Sklenar J, Derbyshire P, Stransfeld L, Asai S, Ntoukakis V, Jones JDG, Shirasu K, Menke F, Jones A, Zipfel C (2014) Direct regulation of NADPH oxidase RBOHD by the PRR-associated kinase BIK1 during plant immunity. *Molecular Cell* **54:** 43–55.

Kanani H, Dutta B, Klapa MI (2010) Individual vs. combinatorial effect of elevated CO_2 conditions and salinity stress on *Arabidopsis thaliana* liquid cultures: comparing the early molecular response using time-series transcriptomic and metabolomic analyses. *BMC Systems Biology* **4:** 177.

Kaplan F, Kopka J, Haskell DW, Zhao W, Schiller KC, Gatzke N, Sung DY, Guy CL (2004) Exploring the temperature-stress metabolome of Arabidopsis. *Plant Physiology* **136:** 4159–4168.

Katari MS, Nowicki SD, Aceituno FF, Nero D, Kelfer J, Thompson LP, Cabello JM, Davidson RS, Goldberg AP, Shasha DE, Coruzzi GM, Gutiérrez RA (2010) VirtualPlant: a software platform to support systems biology research. *Plant Physiology* **152:** 500–515.

Kato Y, Murakami S, Yamamoto Y, Chatani H, Kondo Y, Nakano T, Yokota A, Sato F (2004) The DNA-binding protease, CND41, and the degradation of ribulose-1,5-bisphosphate carboxylase/oxygenase in senescent leaves of tobacco. *Planta* **220:** 97–104.

Kazan K, Manners JM (2013) MYC2: the master in action. *Molecular Plant* **6:** 686–703.

Keurentjes JJB, Fu J, de Vos CHR, Lommen A, Hall RD, Bino RJ, van der Plas LHW, Jansen RC, Vreugdenhil D, Koornneef M (2006) The genetics of plant metabolism. *Nature genetics* **38:** 842–849.

Konishi T (2004) Three-parameter lognormal distribution ubiquitously found in cDNA microarray data and its application to parametric data treatment. *BMC Bioinformatics* **5:** 5.

Konishi T (2011) Microarray test results should not be compensated for multiplicity of gene contents. *BMC Systems Biology* **5:** S6.

Krouk G, Lacombe B, Bielach A, Perrine-Walker F, Malinska K, Mounier E, Hoyerova K, Tillard P, Leon S, Ljung K, Zazimalova E, Benkova E, Nancy P, Gojon A (2010) Nitrate-regulated auxin transport

by NRT1.1 defines a mechanism for nutrient sensing in plants. *Developmental Cell* **18:** 927–937.

Lamberto I, Percudani R, Gatti R, Folli C, Petrucco S (2010) Conserved alternative splicing of Arabidopsis transthyretin-like determines protein localization and *S*-allantoin synthesis in peroxisomes. *The Plant Cell* **22:** 1564–1574.

Laurie-Berry N, Joardar V, Street IH, Kunkel BN (2006) The *Arabidopsis thaliana JASMONATE INSENSITIVE 1* gene is required for suppression of salicylic acid-dependent defenses during infection by *Pseudomonas syringae*. *Molecular Plant-Microbe Interactions* **19:** 789–800.

Lee KH, Piao HL, Kim HY, Choi SM, Jiang F, Hartung W, Hwang I, Kwak JM, Lee IJ, Hwang I (2006) Activation of glucosidase via stress-induced polymerization rapidly increases active pools of abscisic acid. *Cell* **126:** 1109–1120.

Lee TA, Vande Wetering SW, Brusslan JA (2013) Stromal protein degradation is incomplete in *Arabidopsis thaliana* autophagy mutants undergoing natural senescence. *BMC Res Notes* **6:** 17.

Léon-Kloosterziel KM, Gil MA, Ruijs GJ, Jacobsen SE, Olszewski NE, Schwartz SH, Zeevaart JAD, Koornneef M (1996) Isolation and characterization of abscisic acid-deficient *Arabidopsis* mutants at two new loci. *The Plant Journal* **10:** 655–661.

Lescano CI, Martini C, Gonzáles CA, Desimone M (2016) Allantoin accumulation mediated by allantoinase downregulation and transport by Ureide Permease 5 confers salt stress tolerance to *Arabidopsis* plants. *Plant Molecular Biology* **91:** 581–595.

Livak KJ, Schmittgen TD (2001) Analysis of relative gene expression data using real-time quantitative PCR and the $2^{-\Delta\Delta Ct}$ Method. *Methods* **25:** 402–408.

Lorenzo O, Chico JM, Sánchez-Serrano JJ, Solano R (2004) *JASMONATE-INSENSITIVE1* encodes a MYC transcription factor essential to discriminate between different jasmonate-regulated defense responses in Arabidopsis. *The Plant Cell* **16:** 1938–1950.

Lunn JE, Delorge I, Figueroa CM, Van Dijck P, Stitt M (2014) Trehalose metabolism in plants. *The Plant Journal* **79:** 544–567.

Lysøe E, Seong K-Y, Kistler HC (2011) The transcriptome of *Fusarium graminearum* during the infection of wheat. *Molecular Plant-Microbe Interactions* **24:** 995–1000.

Ma X, Wang W–M, Bittner F, Schmidt N, Berkey R, Zhang L, King H, Zhang Y, Feng J, Wen Y, Tan L, Li Y, Zhang Q, Deng Z, Xiong X, Xiao S (2016) Dual and opposing roles of xanthine dehydrogenase in defense-associated reactive oxygen species metabolism in Arabidopsis. *The Plant Cell* **28:** tpc.00880.2015.

Mae T, Ohira K (1981) The remobilization of nitrogen related to leaf growth and senescence in rice plants (*Oryza sativa* L.). *Plant and Cell Physiology* **22:** 1067–1074.

Mae T, Makino A, Ohira K (1983) Changes in the amounts of ribulose biphosphate carboxylase synthesized and degraded during the life span of rice leaf (*Oryza sativa* L.). *Plant and Cell Physiology*. **24:** 1079–1086.

Marchive C, Roudier F, Castaings L, Bréhaut V, Blondet E, Colot V, Meyer C, Krapp A (2013) Nuclear retention of the transcription factor NLP7 orchestrates the early response to nitrate in plants. *Nature communications* **4:** 1713.

Martin A, Lee J, Kichey T, Geretes D, Zivy M, Tatout C, Dubois F, Balliau T, Valot B, Davanture M, Tercé-Laforgue T, Quilleré I, Coque M, Gallais A, Gonzalez-Moro M-B, Bethencourt L, Habash DZ, Lea PJ, Charcosset A, Perez P, Murigebeux A, Sakakibara H, Edwards KJ, Hirel B (2006) Two cytosolic glutamine synthetase isoforms of maize are specifically involved in the control of grain production. *The Plant Cell* **18:** 3252–3274.

Martínez DE, Costa ML, Gomez FM, Otegui MS, Guiamet JJ (2008) "Senescence-associated vacuoles" are involved in the degradation of chloroplast proteins in tobacco leaves. *The Plant Journal* **56:** 196–206.

Masclaux-Daubresse C, Daniel-Vedele F, Dechorgnat J, Chardon F, Gaufichon L, Suzuki A (2010) Nitrogen uptake, assimilation and

remobilization in plants: challenges for sustainable and productive agriculture. *Annals of Botany* **105:** 1141–1157.

Millet YA, Danna CH, Clay NK, Songnuan W, Simon MD, Werck-Reichhart D, Ausubel FM (2010) Innate immune responses activated in *Arabidopsis* roots by microbe-associated molecular patterns. *The Plant Cell* **22:** 973–990.

Montalbini P (1991) Effect of rust infection on levels of uricase, allantoinase and ureides in susceptible and hypersensitive bean leaves. *Physiological and Molecular Plant Pathology* **39:** 173–188.

Montalbini P (1992*a*) Inhibition of hypersensitive response by allopurinol applied to the host in the incompatible relationship between *Phaseolus vulgaris* and *Uromyces phaseoli*. *Journal of Phytopathology* **134:** 218–228.

Montalbini P (1992*b*) Ureides and enzymes of ureide synthesis in wheat seeds and leaves and effect of allopurinol on *Puccinia recondita* f. sp. *tritici* infection. *Plant Science* **87:** 225–231.

Montalbini P (1995) Effect of rust infection on purine catabolism enzyme levels in wheat leaves. *Physiological and Molecular Plant Pathology* **46:** 275–292.

Montalbini P, Torre Della G (1996) Evidence of a two-fold mechanism responsible for the inhibition by allopurinol of the hypersensitive

response induced in tobacco by tobacco necrosis virus. *Physiological and Molecular Plant Pathology* **48:** 273–287.

Nakagawa A, Sakamoto S, Takahashi T, Morikawa H, Sakamoto A (2007) The RNAi-mediated silencing of xanthine dehydrogenase impairs growth and fertility and accelerates leaf senescence in transgenic *Arabidopsis* plants. *Plant and Cell Physiology* **48:** 1484–1495.

Nakata M, Mitsuda N, Herde M, Koo AJK, Moreno JE, Suzuki K, Howe GA, Ohme-Takagi M (2013) A bHLH-type transcription factor, ABA-INDUCIBLE BHLH-TYPE TRANSCRIPTION FACTOR/JA-ASSOCIATED MYC2-LIKE1, acts as a repressor to negatively regulate jasmonate signaling in *Arabidopsis*. *The Plant Cell* **25:** 1641–1656.

Nickstadt A, Thomma BPHJ, Feussner I, Kangasjärvi J, Zeier J, Loeffler C, Scheel D, Berger S (2004) The jasmonate-insensitive mutant *jin1* shows increased resistance to biotrophic as well as necrotrophic pathogens. *Molecular Plant Pathology* **5:** 425–434.

Nikiforova VJ, Kopka J, Tolstikov V, Fiehn O, Hopkins L, Hawkesford MJ, Hesse H, Hoefgen R (2005) Systems rebalancing of metabolism in response to sulfur deprivation, as revealed by metabolome analysis of Arabidopsis plants. *Plant Physiology* **138:** 304–318.

Niu Y, Figueroa P, Browse J (2011) Characterization of JAZ-interacting bHLH transcription factors that regulate jasmonate responses in

Arabidopsis. *Journal of Experimental Botany* **62:** 2143–2154.

Norman-Setterblad C, Vidal S, Palva ET (2000) Interacting signal pathways control defense gene expression in Arabidopsis in response to cell wall-degrading enzymes from *Erwinia carotovora*. *Molecular Plant-Microbe Interactions* **13:** 430–438.

Nourimand M, Todd C (2016) Allantoin increases cadmium tolerance in Arabidopsis via activation of antioxidant mechanisms. *Plant and Cell Physiology* **57:** 2485–2496.

Nozoa P, Vidmar JJ, Tranbarger TJ, Mouline K, Damiani I, Tillard P, Zhuo D, Glass ADM, Touraine B (2007) Regulation of the nitrate transporter gene *AtNRT2.1* in *Arabidopsis thaliana*: responses to nitrate, amino acids and developmental stage. *Plant Molecular Biology* **52:** 689–703.

Ogasawara K, Yamada K, Christeller JT, Kondo M, Hatsugai N, Hara-Nishimura I, Nishimura M (2009) Constitutive and inducible ER bodies of *Arabidopsis thaliana* accumulate distinct ß-glucosidases. *Plant and Cell Physiology* **50:** 480–488.

Olea F, Pérez-García A, Cantón FR, Rivera ME, Cañas R, Ávila C, Cazorla FM, Cánovas FM, De Vicente A (2004) Up-regulation and localization of asparagine synthetase in tomato leaves infected by the bacterial pathogen *Pseudomonas syringae*. *Plant and Cell Physiology* **45:** 770–780.

Oliver MJ, Guo L, Alexander DC, Ryals JA, Wone BW, Cushman JC **(**2011) A sister group contrast using untargeted global metabolomic analysis delineates the biochemical regulation underlying desiccation tolerance in *Sporobolus stapfianus*. *The Plant Cell* **23:** 1231–1248.

Ono Y, Wada S, Izumi M, Makino A, Ishida H (2013) Evidence for contribution of autophagy to Rubisco degradation during leaf senescence in *Arabidopsis thaliana*. *Plant, Cell & Environment* **36:** 1147–1159.

Pageau K, Reisdorf-Cren M, Morot-Gaudry JF, Masclaux-Daubresse C (2006) The two senescence-related markers, *GS1* (cytosolic glutamine synthetase) and *GDH* (glutamate dehydrogenase), involved in nitrogen mobilization, are differentially regulated during pathogen attack and by stress hormones and reactive oxygen species in Nicotiana tabacum L. leaves. *Journal of Experimental Botany* **57:** 547–557.

Pan X, Welti R, Wang X (2010) Quantitative analysis of major plant hormones in crude plant extracts by high-performance liquid chromatography-mass spectrometry. *Nature Protocols* **5:** 986–992.

Pélissier HC, Frerich A, Desimone M, Schumacher K, Tegeder M (2004) PvUPS1, an allantoin transporter in nodulated roots of French bean. *Plant physiology* **134:** 664–675.

Pélissier HC, Tegeder M (2007) PvUPS1 plays a role in source–sink transport of allantoin in French bean (*Phaseolus vulgaris*). *Functional Plant Biology* **34:** 282–291.

Peña-Cortés H, Sánchez-Serrano JJ, Mertens R, Willmitzer L, Prat S (1989) Abscisic acid is involved in the wound-induced expression of the proteinase inhibitor II gene in potato and tomato. *Proceedings of the National Academy of Sciences of the United States of America* **86:** 9851–9855.

Peña-Cortés H, Fisahn J, Willmitzer L (1995) Signals involved in wound-induced proteinase inhibitor II gene expression in tomato and potato plants. *Proceedings of the National Academy of Sciences of the United States of America* **92:** 4106–4113.

Penninckx IAMA, Thomma BPHJ, Buchala A, Métraux J-P, Broekaert WF (1998) Concomitant activation of jasmonate and ethylene response pathways is required for induction of a plant defensin gene in Arabidopsis. *The Plant Cell* **10:** 2103–2113.

Pérez-García A, Pereira S, Pissarra J, García Gutiérrez A, Cazorla FM, Salema R, de Vicente A, Cánovas FM (1998*a*) Cytosolic localization in tomato mesophyll cells of a novel glutamine synthetase induced in response to bacterial infection or phosphinothricin treatment. *Planta* **206:** 426–434.

Pérez-García A, de Vicente A, Cantón FR, Cazorla FM, Codina JC, García-Gutiérrez A, Cánovas FM (1998*b*) Light-dependent changes of tomato glutamine synthetase in response to *Pseudomonas syringae* infection or phosphinothricin treatment. *Physiologia Plantarum* **102:**

377–384.

Pré M, Atallah M, Champion A, De Vos M, Pieterse CMJ, Memelink J (2008) The AP2/ERF domain transcription factor ORA59 integrates jasmonic acid and ethylene signals in plant defense. *Plant Physiology* **147:** 1347–1357.

Preston J, Tatematsu K, Kanno Y, Hobo T, Kimura M, Jikumaru Y, Yano R, Kamiya Y, Nambara E (2009) Temporal expression patterns of hormone metabolism genes during imbibition of *Arabidopsis thaliana* seeds: A comparative study on dormant and non-dormant accessions. *Plant and Cell Physiology* **50:** 1786–1800.

Pessoa J, Sárkány Z, Ferreira-da-Silca F, Martins S, Almeida MR, Li J, Damas AM (2010) Functional characterization of *Arabidopsis* thaliana transthyretin-like protein. *BMC Plant Biology* **10:** 30.

Raya-Gonzalez J., Pelagio-Flores R., Lopez-Bucio J (2012) The jasmonate receptor COI1 plays a role in jasmonate-induced lateral root formation and lateral root positioning in *Arabidopsis thaliana*. *Journal of Plant Physiology* **169:** 1348–1358.

Reymond P, Weber H, Damond M, Farmer EE (2000) Differential gene expression in response to mechanical wounding and insect feeding in Arabidopsis. *The Plant Cell* **12:** 707–719.

Rose MT, Rose TJ, Pariasca-Tanaka J, Yoshihashi T, Neuweger H,

Goesmann A, Frei M, Wissuwa M (2012) Root metabolic response of rice (*Oryza sativa* L.) genotypes with contrasting tolerance to zinc deficiency and bicarbonate excess. *Planta* **236:** 959–973.

Rubin G, Tohge T, Matsuda F, Saito K, Scheible W-R (2009) Members of the LBD family of transcription factors repress anthocyanin synthesis and affect additional nitrogen responses in *Arabidopsis*. *The Plant cell* **21:** 3567–3584.

Sagi M, Omarov RT, Lips SH (1998) The Mo-hydroxylase xanthine dehydrogenase and aldehyde oxidase in ryegrass as affected by nitrogen and salinity. *Plant Science* **135:** 125–135.

Sasaki-Sekimoto Y, Jikumaru Y, Obayashi T, Saito H, Masuda S, Kamiya Y, Ohta, H, Shirasu K (2013) Basic helix-loop-helix transcription factors JASMONATE-ASSOCIATED MYC2-LIKE1 (JAM1), JAM2, and JAM3 are negative regulators of jasmonate responses in Arabidopsis. *Plant Physiology* **163:** 291–304.

Schubert KR (1986) Products of biological nitrogen-fixation in higher plants: synthesis, transport, and metabolism. *Annual Review of Plant Physiology* **37:** 539–574.

Schmidt A, Su Y-H, Kunze R, Warner S, Hewitt M, Slocum RD, Ludewig U, Frommer WB, Desimone M (2004) UPS1 and UPS2 from Arabidopsis mediate high affinity transport of uracil and 5-fluorouracil. *Journal of Biological Chemistry* **279:** 44817–44824.

Schmidt A, Baumann N, Schwarzkopf A, Frommer WB, Desimone M (2006) Comparative studies on Ureide Permeases in *Arabidopsis thaliana* and analysis of two alternative splice variants of *AtUPS5*. *Planta* **224:** 1329–1340.

Serraj R, Vadez V, Denison RF, Sinclair TR (1999) Involvement of ureides in nitrogen fixation inhibition in Soybean. *Plant Physiology* **119:** 289–296.

Serventi F, Ramazzina I, Lamberto I, Puggioni V, Gatti R, Percudani R (2010) Chemical basis of nitrogen recovery through the ureide pathway: formation and hydrolysis of S-ureidoglycine in plants and bacteria. *ACS Chemical Biology* **5:** 203–214.

Silvente SS, Sobolev APA, Lara MM (2012) Metabolite adjustments in drought tolerant and sensitive soybean genotypes in response to water stress. *PLoS One* **7:** e38554.

Silvestri SS, Murphy AMA, Buonaurio RR, Carr JPJ (2008) Allopurinol, an inhibitor of purine catabolism, enhances susceptibility of tobacco to *Tobacco mosaic virus*. *Virus Research* **137:** 257–260.

Smith PMC, Atkins CA (2002) Purine biosynthesis. Big in cell division, even bigger in nitrogen assimilation. *Plant Physiology* **128:** 793–802.

Stasolla C, Katahira R, Thorpe TA, Ashihara H (2003) Purine and

pyrimidine nucleotide metabolism in higher plants. *Journal of Plant Physiology* **160:** 1271–1295.

Staswick PE, Su W, Howell SH (1992) Methyl jasmonate inhibition of root growth and induction of a leaf protein are decreased in an *Arabidopsis thaliana* mutant. *Proceedings of the National Academy of Sciences of the United States of America* **89:** 6837–6840.

Suhita D, Raghavendra AS, Kwak JM, Vavasseur A (2004) Cytoplasmic alkalization precedes reactive oxygen species production during methyl jasmonate- and abscisic acid-induced stomatal closure. *Plant Physiology* **134:** 1536–1545.

Sun J, Bankston JR, Payandeh J, Hinds TR, Zagotta WN, Zheng N (2014) Crystal structure of the plant dual-affinity nitrate transporter NRT1.1. *Nature* **507:** 73–77.

Szabados L, Savouré A (2010) Proline: a multifunctional amino acid. *Trends in Plant Science* **15:** 89–97.

Tabuchi M, Sugiyama K, Ishiyama K, Inoue E, Sato T, Takahashi H, Yamaya T (2005) Severe reduction in growth rate and grain filling of rice mutants lacking OsGS1;1, a cytosolic glutamine synthetase1;1. *The Plant Journal* **42:** 641–651.

Tegeder M (2014) Transporters involved in source to sink partitioning of amino acids and ureides: opportunities for crop improvement. *Journal of*

Experimental Botany **65:** 1865–1878.

Teng S, Keurentjes J, Bentsink L, Koornneef M, Smeekens S (2005) Sucrose-specific induction of anthocyanin biosynthesis in Arabidopsis requires the MYB75/PAP1 gene. *Plant Physiology* **139:** 1840–1852.

Tholl D, Aharoni A (2014) Small molecules: from structural diversity to signalling and regulatory roles. *The Plant Journal* **79:** 541–543.

Todd CD, Polacco JC (2006) *AtAAH* encodes a protein with allantoate amidohydrolase activity from *Arabidopsis thaliana*. *Planta* **223:** 1108–1113.

Tsukahara K, Sawada H, Kohno Y, Matsuura T, Mori IC, Terao T, Ioki M, Tamaoki M (2015) Ozone-induced rice grain yield loss is triggered via a change in panicle morphology that is controlled by *ABERRANT PANICLE ORGANIZATION 1* gene. *PLoS One* **10:** e0123308.

Vogels GD, Van der Drift C (1976) Degradation of purines and pyrimidines by microorganisms. *Bacteriological Reviews* **40:** 403–468.

Vos IA, Verhage A, Schuurink RC, Watt LG, Pieterse CMJ, Van Wees SCM (2013) Onset of herbivore-induced resistance in systemic tissue primed for jasmonate-dependent defenses is activated by abscisic acid. *Frontiers in Plant Science* **4:** 539.

Wang P, Kong C-H, Sun B, Xu X-H (2012) Distribution and function of

allantoin (5-ureidohydantoin) in rice grains. *Journal of Agricultural and Food Chemistry* **60:** 2793–2798.

Wang R, Xing X, Wang Y, Tran A, Crawford NM (2009) A genetic screen for nitrate regulatory mutants captures the nitrate transporter gene *NRT1.1*. *Plant Physiology* **151:** 472–478.

Wang W-S, Zhao X-Q, Li M, Huang L-Y, Xu J-L, Zhang F, Cui Y-R, Fu B-Y, Li Z-K (2016) Complex molecular mechanisms underlying seedling salt tolerance in rice revealed by comparative transcriptome and metabolomic profiling. *Journal of Experimental Botany* **67:** 405–419.

Wasternack C, Hause B (2013) Jasmonates: biosynthesis, perception, signal transduction and action in plant stress response, growth and development. *Annals of Botany* **111:** 1021–1058.

Watanabe S, Nakagawa A, Izumi S, Shimada, H, Sakamoto A (2010) RNA interference-mediated suppression of *xanthine dehydrogenase* reveals the role of purine metabolism in drought tolerance in Arabidopsis. *FEBS Letters* **584:** 1181–1186.

Watanabe S, Kounosu Y, Shimada H, Sakamoto A (2014*a*) Arabidopsis *xanthine dehydrogenase* mutants defective in purine degradation show a compromised protective response to drought and oxidative stress. *Plant Biotechnology* **31:** 173–178.

Watanabe S, Matsumoto M, Hakomori Y, Takagi H, Shimada H,

Sakamoto A (2014*b*) The purine metabolite allantoin enhances abiotic stress tolerance through synergistic activation of abscisic acid metabolism. *Plant, Cell & Environment* **37:** 1022–1036.

Werner AK, Sparkes IA, Romeis T, Witte C-P (2008) Identification, biochemical characterization, and subcellular localization of allantoate amidohydrolases from Arabidopsis and soybean. *Plant physiology* **146:** 418–430.

Werner AK, Romeis T, Witte C-P (2010) Ureide catabolism in *Arabidopsis thaliana* and *Escherichia coli*. *Nature Chemical Biology* **6:** 19–21.

Werner AK, Witte C-P (2011) The biochemistry of nitrogen mobilization: purine ring catabolism. *Trends in Plant Science* **16:** 381–387.

Werner AK, Medina-Escobar N, Zulawski M, Sparkes IA, Cao F-Q, Witte C-P (2013) The ureide-degrading reactions of purine ring catabolism employ three amidohydrolases and one aminohydrolase in Arabidopsis, Soybean, and Rice. *Plant Physiology* **163:** 672–681.

Wind J, Smeekens S, Hanson J (2010) Sucrose: metabolite and signaling molecule. *Phytochemistry* **71:** 1610–1614.

Wu H, Liu X, You L, Zhang L, Zhou D, Feng J, Zhao J, Yu J (2012) Effects of salinity on metabolic profiles, gene expressions, and antioxidant enzymes in Halophyte *Suaeda salsa*. *Journal of Plant Growth Regulation* **31:** 332–341.

Xiong L, Lee H, Ishitani M, Zhu J-K (2001) Regulation of osmotic stress-responsive gene expression by the *LOS6/ABA1* locus in *Arabidopsis*. *Journal of Biological Chemistry* **277:** 8588–8596.

Yamaya T, Kusano M (2014) Evidence supporting distinct functions of three cytosolic glutamine synthetases and two NADH-glutamate synthases in rice. *Journal of Experimental Botany* **65:** 5519-5525.

Yang J, Han K-H (2004) Functional characterization of allantoinase genes from Arabidopsis and a nonureide-type legume black locust. *Plant Physiology* **134:** 1039–1049.

Yasuda M, Ishikawa A, Jikumaru Y, Seki M, Umezawa T, Asami T, Maruyama-Nakashita A, Kudo T, Shinozaki K, Yoshida S, Nakashita H (2008) Antagonistic interaction between systemic acquired resistance and the abscisic acid-mediated abiotic stress response in *Arabidopsis*. *The Plant Cell* **20:** 1678–1692.

Yesbergenova Z, Yang G, Oron E, Soffer D, Fluhr R, Sagi M (2005) The plant Mo-hydroxylases aldehyde oxidase and xanthine dehydrogenase have distinct reactive oxygen species signatures and are induced by drought and abscisic acid. *The Plant Journal* **42:** 862–876.

Yobi A, Wone BW, Xu W, Alexander DC, Guo L, Ryals JA, Oliver MJ, Cushman JC (2013) Metabolomic profiling in *Selaginella lepidophylla* at various hydration states provides new insights into the mechanistic

basis of desiccation tolerance. *Molecular Plant* **6:** 369–385.

Yuan L, Loqué D, Ye F, Frommer WB, von Wirén N (2007) Nitrogen-dependent posttranscriptional regulation of the ammonium transporter AtAMT1;1. *Plant Physiology* **143:** 732–744.

Zrenner R, Stitt M, Sonnewald U, Boldt R (2006) Pyrimidine and purine biosynthesis and degradation in plants. *Annual Review of Plant Biology* **57:** 805–836.